# INFORMATION TO USERS

The most advanced technology has been used to photograph and reproduce this manuscript from the microfilm master. UMI films the text directly from the original or copy submitted. Thus, some thesis and dissertation copies are in typewriter face, while others may be from any type of computer printer.

**The quality of this reproduction is dependent upon the quality of the copy submitted.** Broken or indistinct print, colored or poor quality illustrations and photographs, print bleedthrough, substandard margins, and improper alignment can adversely affect reproduction.

In the unlikely event that the author did not send UMI a complete manuscript and there are missing pages, these will be noted. Also, if unauthorized copyright material had to be removed, a note will indicate the deletion.

Oversize materials (e.g., maps, drawings, charts) are reproduced by sectioning the original, beginning at the upper left-hand corner and continuing from left to right in equal sections with small overlaps. Each original is also photographed in one exposure and is included in reduced form at the back of the book.

Photographs included in the original manuscript have been reproduced xerographically in this copy. Higher quality 6" x 9" black and white photographic prints are available for any photographs or illustrations appearing in this copy for an additional charge. Contact UMI directly to order.

U·M·I

University Microfilms International
A Bell & Howell Information Company
300 North Zeeb Road, Ann Arbor, MI 48106-1346 USA
313/761-4700 800/521-0600

Order Number 9119666

# Spatial and temporal expression of neuronal protein NP185 in developing avian cerebellum

Perry, Douglas Gentz, Ph.D.

City University of New York, 1991



U·M·I
300 N. Zeeb Rd.
Ann Arbor, MI 48106

A

# SPATIAL AND TEMPORAL EXPRESSION OF NEURONAL PROTEIN NP185 IN DEVELOPING AVIAN CEREBELLUM

by

DOUGLAS G. PERRY

A dissertation submitted to
the Graduate Faculty in Biomedical Sciences
in partial fulfillment of the requirements for
the degree of Doctor of Philosophy,
The City University of New York.

1991

This manuscript has been read and accepted for the Graduate Faculty in Biomedical Sciences in satisfaction of the dissertation requirement for the degree of Doctor of Philosophy.

1/7/91
Date

Dr. Saul Puszkin
Chair of Examining Committee

1/3/91
Date

Dr. Terry A. Krulwich
Executive Officer

Dr. John Durham

Dr. Reza Green

Dr. Ed Johnson

Dr. David Pumplin

Supervisory Committee

The City University of New York

# Abstract

**SPATIAL AND TEMPORAL EXPRESSION OF NEURONAL PROTEIN NP185 IN DEVELOPING AVIAN CEREBELLUM**

by

Douglas G. Perry

Adviser: Professor Saul Puszkin

NP185 is a protein found in nervous tissue (Kohtz and Puszkin, J Biol Chem **263**:7418). Biochemical results (Kohtz & Puszkin, J Neurochem **52**:285; Su *et al.*, J Neurosci Res [in press]) demonstrate that NP185 co-purifies with bovine brain clathrin-coated vesicles (CCVs), has a phosphorylation-sensitive binding affinity for tubulin, binds to sites in synaptic vesicles and nerve terminal membranes, and promotes clathrin cage assembly *in vitro*. These findings suggest a supportive role for NP185 in the function of neuronal CCVs. To further understand the nature of NP185, I followed its distribution in developing central nervous tissue by immunohistochemical light microscopy, compared this distribution to that of neuronal (NF68, synaptophysin) and nonneuronal (GFAP, vimentin) proteins, and demonstrated NP185 localization in the neuromuscular junction of skeletal muscle. **RESULTS:** 1) Glial cells, although strongly labelled for GFAP and vimentin, are never labelled for NP185. 2) The external granular and ventricular layers of the developing cerebel-

lum are negative for NP185. The mantle layer is labelled for NP185 from its inception. 3) Membranous labelling for NP185 is very strong in migrating neuroblasts. In the mantle layer, NP185 labelling follows a gradient consistent with the directional gradient of synaptic formation. 4) The distribution of NP185 is identical to that of synaptophysin. The labelling pattern of NF68 generates an intense cytoplasmic immunofluorescent stain in cerebellar Purkinje cells, but NP185 yields only membranous staining in these same cells. 5) In chick skeletal muscle, NP185 is co-distributed with acetylcholine receptors (AchRs). The AchR distribution pattern found in these experiments is consistent with previous studies (Buc-Caron *et al.*, Develop Biol **95**:378; Bender *et al.*, Neurol **26**:477) of the neuromuscular junction. **CONCLUSIONS**: 1) NP185 is strictly neuron-specific, but NP185 distribution is not limited to the central nervous system. 2) Developmental expression of NP185 follows a pattern consistent with synaptogenesis. 3) NP185 is concentrated in synaptic terminals of mature neurons. 4) NP185 is located in the neuromuscular junctions of skeletal muscle.

In view of these findings, the "docking protein" model may be appropriate for NP185 function in nerve endings.

# PREFACE

This research builds upon the work of former graduate students in Saul Puszkin's laboratory. Stave Kohtz developed the monoclonal antibodies that eventually led to his discovery of NP185 (Kohtz and Puszkin, 1988). It was no small matter to uncover a protein that electrophoretically co-migrates with clathrin heavy chain--hidden in the typically large clathrin band at 180 kD. Dr. Kohtz did much to characterize NP185, including identifying its specificity for brain and its affinity for tubulin (Kohtz and Puszkin, 1989). Borcherng Su purified NP185 and continued with the biochemical analysis. He worked out the relative affinities of NP185 for clathrin light chains (LCs), decoated clathrin-coated vesicles (CCVs), synaptic vesicles (SVs), and synaptosomal membranes (Su, 1989).

I came in at the next step with a developmental study of NP185. This involved a great deal of preliminary work, to establish antibody cross-reactivities, embryonic expression, and proper conditions for immunohistochemistry. From the start, Dr. Puszkin never failed to provide encouragement and help. His understanding of cell biology in general, and coated vesicle research in particular, was a source of guidance on many occasions. When conflicts arose, his patience and tolerance were exemplary. I can

only hope that I will be as good to my future students as he was to me.

I reserve special thanks to my friend and colleague, Dr. Veneta Hanson. She taught me every single technique and procedure that made this research possible. I could not summarize my indebtedness to her without sounding fulsome.

Finally, I dedicate this dissertation to my wife, Meg, who so patiently put up with the widowhood of being married to a graduate student. As always, her support was the foundation for everything else and the basis of my happiness.

# TABLE OF CONTENTS

Copyright Statement . . . . . ii

Approval Page . . . . . iii

Abstract . . . . . iv

PREFACE . . . . . vi

TABLE OF CONTENTS . . . . . viii

LIST OF TABLES . . . . . x

LIST OF FIGURES . . . . . xi

I. INTRODUCTION . . . . . 1
A. REVIEW OF COATED VESICLES AND COAT PROTEINS . . 2
1. History . . . . . 3
2. Purification . . . . . 4
3. Structure . . . . . 5
a. Overall coat structure . . . . . 5
b. Clathrin structure . . . . . 12
c. Heavy chains . . . . . 19
d. Light chains . . . . . 20
e. Adaptors . . . . . 25
4. Function . . . . . 27
5. Mechanism . . . . . 31
B. PRELIMINARY CONSIDERATIONS . . . . . 35
1. Choice of Animal . . . . . 35
2. Choice of tissue . . . . . 36

II. METHODS . . . . . 48
A. NOMENCLATURE . . . . . 48
B. WESTERN BLOT ANALYSIS . . . . . 48
1. Sample preparation . . . . . 48
2. Immunoblot technique . . . . . 50
C. IMMUNOLOCALIZATION . . . . . 50
1. Tissue preparation . . . . . 50
2. Controls . . . . . 52

III. RESULTS . . . . . 56
A. DEVELOPMENTAL EXPRESSION OF NP185 . . . . . 56
B. IMMUNOLOCALIZATION . . . . . 58
1. Ontogenic distribution of NP185 . . . . . 58
2. NP185 distribution in mature cerebellum . . 80
3. Comparative distributions of neuronal proteins 88
a. Synaptophysin . . . . . 89
b. Neurofilament NF68 . . . . . 93

4. Comparative distributions of nonneuronal proteins . . . . . 110
a. Glial fibrillary acidic protein . . . . 111
b. Vimentin . . . . . 113
5. Localization of NP185 in the neuromuscular junction . . . . . 116
a. Establishing NP185 localization . . . . 117
b. Double-labelling of NP185 and AchR . . 131

IV. DISCUSSION . . . . . 141

V. APPENDIX: Abbreviations used in text . . . . . 148

VI. BIBLIOGRAPHY . . . . . 149

# LIST OF TABLES

Table I. Cerebellar neurons. . . . . 41
Table II. Cerebellar glial cells. . . . . 44
Table III. Summary of embryo samples. . . . . 49
Table IV. Incidence of positive label of NP185 in the neuromuscular junction. . . . . 130
Table V. Incidence of double-labelling in the neuromuscular junction. . . . . 138

# LIST OF FIGURES

Figure 1. Electron micrograph of coated vesicle. . . 7
Figure 2. Nested shell diagram of coated vesicle. . . 9
Figure 3. Icosahedral barrel structure of coated vesicle. . . . . 11
Figure 4. Modular structure of the triskelion. . . . 13
Figure 5. "Tramline" appearance of polyhedral edge. . 16
Figure 6. Crossover packing of triskelions. . . . . 18
Figure 7. Scheme of endocytosis and membrane recycling. 29
Figure 8. Model of clathrin lattice formation. . . . 33
Figure 9. Midsagittal section of cerebellum. . . . . 37
Figure 10. Stained section through the cerebellar cortex. . . . . 39
Figure 11. Excitatory pathways. . . . . 42
Figure 12. Inhibitory interneurons in the cerebellar cortex. . . . . 43
Figure 13. Rostrocaudal direction of central nervous system development. . . . . 46
Figure 14. Control, chick embryo. . . . . 53
Figure 15. Control, chicken skeletal muscle. . . . . 54
Figure 16. Western blot of chick embryo samples. . . 57
Figure 17. Typical NP185 label in early embryo. . . . 60
Figure 18. Reticular immunoreactivity surrounding cell bodies. . . . . 62
Figure 19. Distribution of NP185 at E14. . . . . 64
Figure 20. Early neuropil labelling for NP185. . . . 67
Figure 21. NP185 distribution at E15. . . . . 69
Figure 22. Labelling of young Purkinje cells for NP185. 71
Figure 23. Apical cone of Purkinje cell, labelled for NP185. . . . . 73
Figure 24. NP185 distribution in embryonic cerebellar cortex. . . . . 75
Figure 25. Migrating granule cell, labelled for NP185. 79
Figure 26. NP185 distribution in mature cerebellar cortex. . . . . 81
Figure 27. Perimembranous labelling of Purkinje cells for NP185. . . . . 84
Figure 28. Glomerular distribution of NP185. . . . . 87
Figure 29. Synaptophysin distribution in murine cerebellum. . . . . 90
Figure 30. Differential distribution of synaptophysin. 92
Figure 31. Earliest expression of NF68. . . . . 95
Figure 32. Distribution of NF68 in E7 embryo. . . . . 97
Figure 33. Labelling of Purkinje cells for NF68. . . 99
Figure 34. Perikaryal labelling of NF68. . . . . 101
Figure 35. NF68 distribution in mature cerebellum. 104
Figure 36. NF68 distribution in the mature Purkinje layer. . . . . 106
Figure 37. NF68 confinement to Basket cell pinceau. 108
Figure 38. Immunolabelling for GFAP. . . . . 112

Figure 39. Localization of vimentin in Bergmann glial fibers. . . . . 115
Figure 40. Presence of NP185 in chicken skeletal muscle. . . . . 118
Figure 41. Gross morphology of neuromuscular junction. 120
Figure 42. Localization of NP185 in chick skeletal muscle. . . . . 122
Figure 43. Close-up of NP185 localization. . . . . 124
Figure 44. NP185 distribution in muscle cross-section. 126
Figure 45. Linear labelling for NP185 in neuromuscular junction. . . . . 128
Figure 46. Double label of AchR and NP185. . . . . 132
Figure 47. Codistribution of AchR and NP185. . . . 134
Figure 48. Co-localization of AchR and NP185 in a neuromuscular junction. . . . . 136

# I. INTRODUCTION

Coated vesicles are found in many different types of cells (Cheng *et al.*, 1980). Undoubtedly many of these coated vesicle populations share the same functions. Yet the adaptins, proteins associated with coated vesicles, exhibit heterogeneity even within a single cell (Glickman *et al.*, 1989). This suggests that coated vesicles have specialized functions depending on their location, and that coated vesicle-associated proteins impart these functions.

The central aim of this study is to establish the spatial and temporal expression of neuronal protein NP185 in the avian cerebellum. Previous studies (Su, 1989; Kohtz and Puszkin, 1988) showed that this protein is detected only in brain tissue and can be isolated from brain clathrin-coated vesicles. Biochemical experiments (Kohtz and Puszkin, 1989) revealed that NP185 has binding affinity for tubulin. This binding is affected by casein kinase II-mediated phosphorylation of tubulin. Recently, NP185 was found to bind to clathrin light chain, and to sites present in decoated vesicles, synaptic vesicles and nerve ending membranes (Su *et al.*, 1991). These studies suggest a role for NP185 in neuronal function.

This laboratory possesses a well characterized monoclonal antibody to NP185 (Kohtz and Puszkin, 1988) that

can be used for immunolocalization in tissue sections. Correlating the developmental expression of NP185 with cerebellar neurogenesis--including synaptogenesis--can yield insights into the function this protein. Studying the comparative distribution of NP185 with other neuronal and glial proteins can provide additional information on its cellular distribution within the nervous system. Finally, localizing NP185 in peripheral nervous tissue can give evidence of this protein's general role in the brain.

## A. REVIEW OF COATED VESICLES AND COAT PROTEINS

Coated membranes are directly involved in endocytosis (Friend and Farquhar, 1967), intracellular transport (Pearse, 1987; Rothman, 1986), membrane retrieval, including retrieval of synaptic membranes (Heuser and Reese, 1973), selective membrane transport (Pearse and Bretscher, 1981) and placental transport (Ockleford, 1976), secretion (Benson *et al.*, 1985; Franke *et al.*, 1976), and concentration of membrane receptors (Pearse, 1985; Bretscher *et al.*, 1980).

Since the first characterization of "bristled" pits and associated vesicles in 1964 (Roth and Porter), investigators quickly realized that coated vesicles and pits play an essential role in cellular survival, as evidenced by the universal distribution of these elements in eukaryotic cells (Ungewickell and Branton, 1982). Indeed, cells lacking expression of clathrin, the major coat protein

(Pearse, 1976), have received only limited attention (Pearse, 1987). Payne and Schekman (1985) examined yeast cells in which one of the alleles of the clathrin heavy chain gene CHC1 was rendered nonfunctional, resulting in second-generation cells deficient in coated membranes. Some cells died; surviving cells were able to secrete invertase, albeit incompletely, suggesting a secretory pathway independent of coated vesicles. "Life without clathrin" has been discussed (Fine, 1989; Orci *et al.*, 1986; Rothman, 1986), but the basic necessity of coated vesicles in eukaryotic cells is regarded as a truism.

**1. History**

"Vesicles in a basket" were first described by Kanaseki and Kadota in 1969, using purified vesicle preparations from guinea pig brain and liver. Using electron micrography techniques, the authors made detailed observations of coated vesicles and "empty baskets." The general accuracy of their descriptions, which included the polygonal structure of the baskets and the structural changes associated with endocytosis, has survived to the present. Based on the endurance of intact coated vesicles after exposure to stress forces of 100,000 g, the authors even postulated the existence of a connector substance linking the outer basket to the inner vesicle membrane. Adaptors, as the connector substances have come to be called, were not biochemically isolated for another 13 years (Blitz *et al.*,

1977), and not formally identified as such until 1984 (Pearse and Robinson). The *basket* term has since been dropped. In current parlance *coat* refers to the entire structure surrounding a vesicle and *cage* refers to the empty baskets made from purified clathrin (Crowther and Pearse, 1981).

Following the discovery of coated vesicles, Pearse isolated, characterized, and named the major coat protein, clathrin (1975). Three years later, she identified other related coat proteins having $M_r$ 33 and 36 kD (Pearse, 1978). These were later termed clathrin light chains β and α, respectively (Kirchhausen and Harrison, 1981; Ungewickell and Branton, 1981). In 1982, Ungewickell and Branton proposed that the term *clathrin* refer to the entire 8S coat subunit obtained from sedimentation. This subunit consists of three heavy chains (180 kD each; to which Pearse originally applied the term *clathrin*) and three light chains, α (36 kD) and β (33 kD). These light chains occur in the ratio of 1:2.

**2. Purification**

Bovine brain is the usual source for coated vesicles and coat proteins. Fresh brains are stripped of their meninges and the grey matter collected by aspiration. The buffer used for most of the purification process is 100 mM MES, 1 mM EGTA, 0.1 mM $MgCl_2$, and 0.02% $NaN_3$ (Ungewickell *et al.*, 1981). The grey matter is homogenized, then

centrifuged first at 20,000 X *g*, followed by 100,000 X *g* (Schook *et al.*, 1979). Coated vesicles are purified by subjection to discontinuous sucrose gradients (Blitz *et al.*, 1977). These vesicles can be stripped of their coats by incubation for 1 hr in 10 mM Tris, pH 8.5, with an efficiency of 80 to 85% (Unanue *et al.*, 1981). The coat proteins at this point consist of clathrin and the adaptors. These can be separated from each other by dissolving the coat protein extract in a buffer of high ionic strength and lower pH. This buffer contains 1 M Tris-Cl (pH 7.0), 1 mM EDTA, 0.1% 2-mercaptoethanol, 0.02% $NaN_3$ and 0.2 mM PMSF ("extraction buffer"; Pearse, 1989). The protein solution is then dialyzed against 20 mM ethanolamine (pH 8.9), 2 mM EDTA and 1 mM dithiothreitol. The dialyzate is then resolved by FPLC (applying a salt gradient to a Mono Q column) into two populations, clathrin and the adaptors (Ahle *et al.*, 1988). The main point of the last extraction step is that clathrin can be separated and purified under high salt conditions. Varying the extraction buffer in this step by using either 0.5 M Tris-Cl or 2 M urea produces triskelions that have the same appearance (Ungewickell *et al.*, 1981).

**3. Structure**

a. Overall coat structure

The striking appearance of the coat has been extensively commented upon (Pearse, 1989; Pearse, 1987; Pearse and

Crowther, 1987; Larkin *et al.*, 1986; Vigers *et al.*, 1986; Ungewickell and Branton, 1982; Crowther and Pearse, 1981; Pearse, 1976; Kanaseki and Kadota, 1969; Roth and Porter, 1964). Using electron microscopy, the earliest observers noted areas of membrane, including intracellular vesicles, that had unusually high electron density (Heuser and Reese, 1973). A typical example is seen in Figure 1 (adapted from Pearse, 1987).

**Figure 1.** Electron micrograph of coated vesicle.

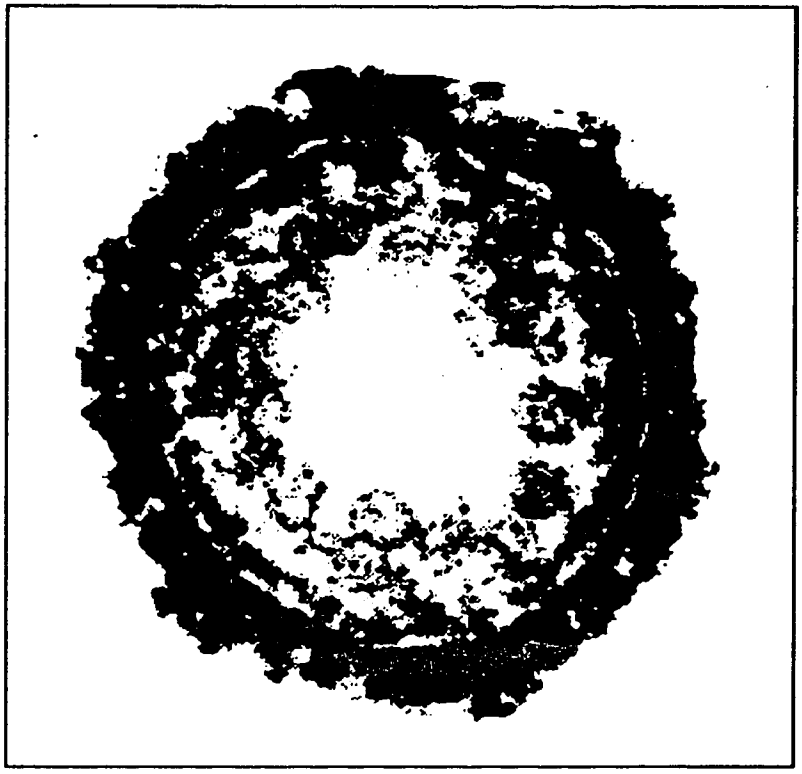

Vesicles with high density regions surrounding them were described as wheels, bristles, baskets, and even coronets (Kanaseki and Kadota, 1969; Roth and Porter, 1964). These graphic descriptions all arose from the highly organized polyhedral structure of the coat, the edges of which being detected in such a variety of aspects. Although coated vesicles can vary in diameter from 500 to 2500 Å (Pearse and Crowther, 1981), their morphology is similar in different cells (Bloom *et al.*, 1980a), which attests to the functional significance of their structure.

The coat consists of three consecutive shells: an outer clathrin cage (Pearse, 1976), heavy chain terminal domains ("inner fingers," Vigers *et al.*, 1986), and adaptors, which provide a link between the outer coat and the inner vesicle membrane (Pearse, 1989). Pearse provided a schematic representation of this nested shell arrangement, shown in Figure 2 (adapted from Pearse, 1987).

**Figure 2**. Nested shell diagram of coated vesicle.

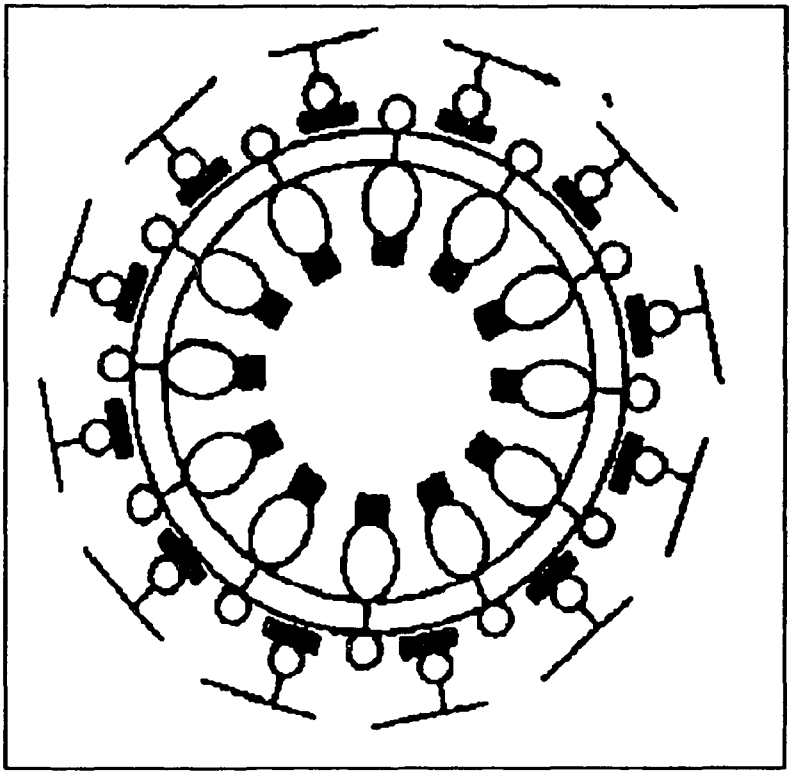

The inner ovals represent the external surface receptors with tails that extend through the membrane to the cytoplasmic surface studded with coat proteins.

Vigers *et al.* (1986) made a tilt series of electron micrographs to reconstruct the three dimensional structure of clathrin cages embedded in vitreous ice. The cages consist of icosahedral barrels: 8 hexagons (2 on top and bottom and 6 around the equator) and 12 pentagons (6 arrayed in 2 encircling rows). Their findings defend the model proposed by Pearse in 1976 (Figure 3).

**Figure 3.** Icosahedral barrel structure of coated vesicle.

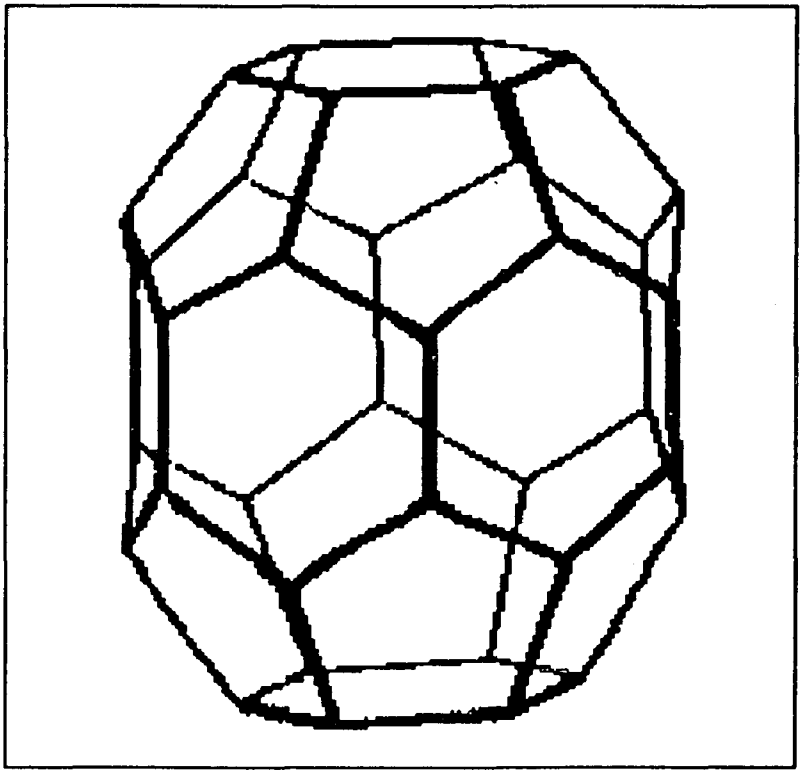

In addition, they were able to visualize the heavy chain terminal domains not accounted for by the length of the polyhedral edges (Pearse and Crowther, 1981). These "inner fingers of density" form an inner shell that resides between the outer polyhedron and the inner adaptors. In a coated vesicle, the vesicle membrane is innermost, with the cytoplasmic side exposed. The cytoplasmic tails of the appropriate membrane receptors are bound to the adaptors.

b. Clathrin structure

The clathrin product discussed in Section A sediments at 8S (Ungewickell and Branton, 1982), and therefore is called the 8S subunit. A remarkable feature of this subunit is its trimeric bent-leg appearance, appropriately termed *triskelion* by Pearse (1975; Figure 4).

**Figure 4**. Modular structure of the triskelion.

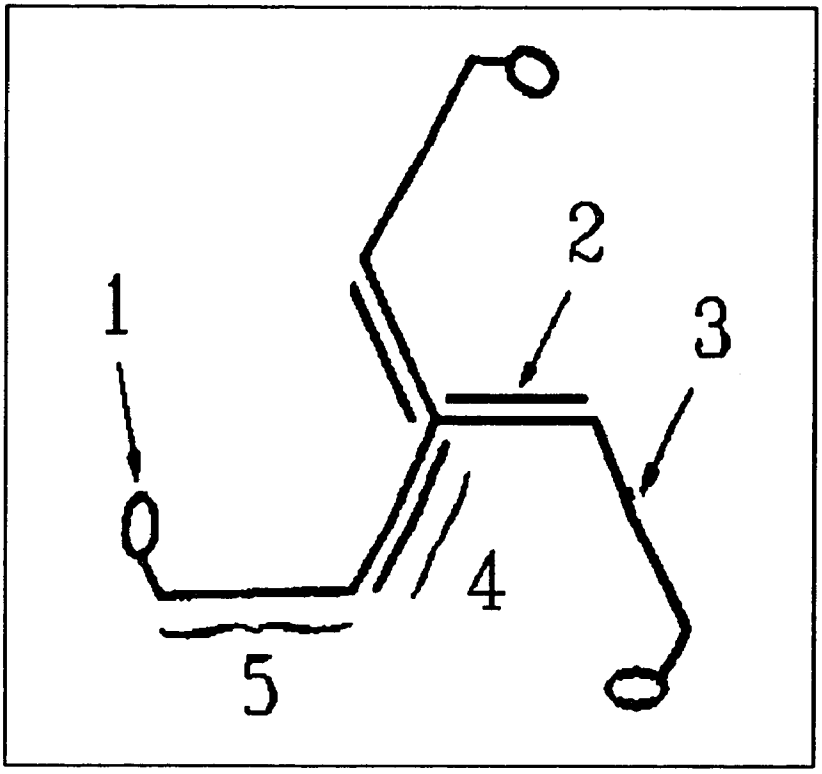


**1**: terminal domain; **2**: light chain; **3**: heavy chain; **4**: proximal arm; **5**: distal arm.

The molecular weight of a triskelion was estimated by sedimentation equilibrium to be 627+/-55 kD (Ungewickell and Branton, 1981). 8S subunits are composed of 3 clathrin heavy chains ($M_r$ = 180 kD each) and 3 clathrin light chains (33 kD, $LC_\beta$, or 36 kD, $LC_\alpha$) (Kirchhausen and Harrison, 1981). The three heavy chains are joined at their proximal ends to form a 3-fold axis of symmetry, with each heavy chain leg separated by a 120 degree angle. Each leg has a kink in the middle, dividing the proximal and distal segments. A semispiralled bend occurs towards the end of each leg, providing a demarcation between the distal and terminal segments. The proximal and distal segments form the polyhedral edges (discussed below). The terminal segments bend inward to form the "inner fingers of density" (Vigers *et al.*, 1986). A typical clathrin cage contains around 30 triskelions (Pearse and Crowther, 1981).

Since their presence was first detected it was noted that coats associated with membrane pits or vesicles assumed a polyhedral lattice (Kanaseki and Kadota, 1969). The functional significance of this polyhedral structure is related to the curvature changes that occur as a coated membrane buds off to form a coated vesicle. This was recognized early on (Heuser and Reese, 1973). The actual packing arrangement was worked out by Crowther & Pearse (1981). They speculated that triskelions must be both firm and flexible; firm to supply a framework for membrane

invagination, flexible to allow plane-to-dome transition. This could be done if a triskelion were positioned at each vertex of the cage lattice, allowing a point of flexion, as is indeed the case. In this configuration, a pentagon can be formed by removing one triskelion and a heptagon formed by adding one (Pearse and Crowther, 1981). Each edge of a polyhedron has the proximal halves of two neighboring triskelions and distal halves of two adjoining triskelions running parallel, which gives a "double tramline" appearance in electron micrographs (Figure 5).

**Figure 5**. "Tramline" appearance of polyhedral edge.

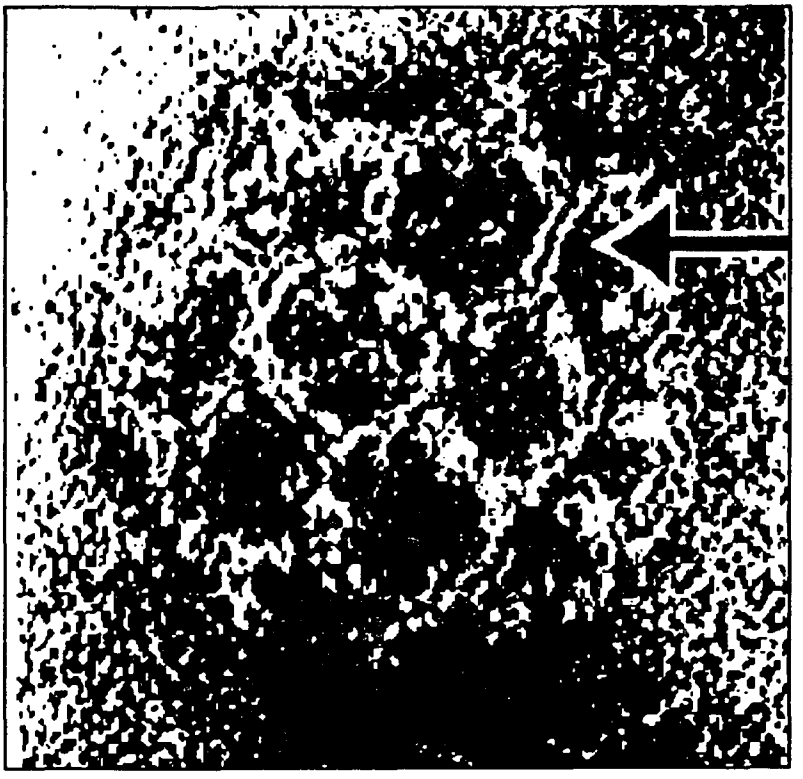

Electron micrograph of single coated vesicle. Arrow indicates area of interest.

The double tramline effect is caused by the packing of the triskelions in a crossover arrangement, shown in Figure 6.

**Figure 6.** Crossover packing of triskelions.

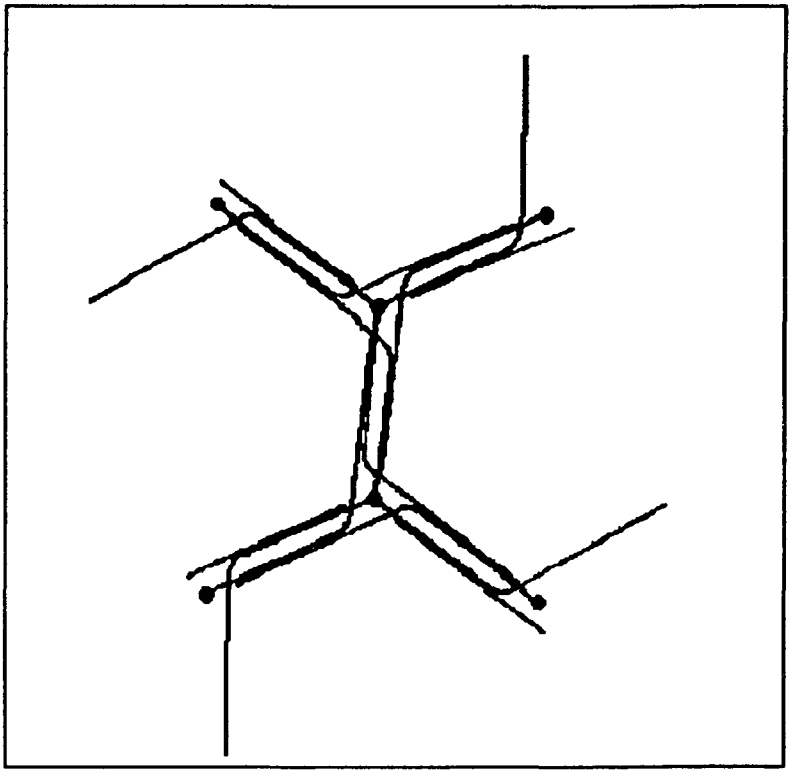

The vertices of six triskelions are included, but only two complete triskelions are shown; one leg participates in the packing of four triskelions.

"Crossover" packing refers to two triskelions with proximal legs running parallel and distal ends crossing over this parallel axis at the point of the kink between the proximal and distal ends. This crossover is complementary, with the distal ends running along opposite polyhedral edges (Crowther and Pearse, 1981).

Electron microscopy has allowed triskelion dimensions to be measured (Pearse and Crowther, 1981). In the individual triskelion dissociated from a cage, the length of a single leg is 430 Å, with the proximal segment comprising 160 Å. The polyhedral edge of a cage is 180 Å. A triskelion leg runs along two edges, accounting for approximately 360 Å. This leaves the 70 Å distal tip unaccounted for. This distal tip corresponds with the "inner finger of density" visualized by Vigers *et al.* (1986).

c. Heavy chains

The clathrin heavy chain, forming the backbone of the triskelion, imparts the polyhedral organization to coats and cages. Because of their configuration constraints, heavy chains are likely to have a role that is more structural than dynamic (Jackson *et al.*, 1987). This does not mean that the molecules are rigid. Ungewickell and Branton (1982) pointed out that heavy chains are 50% α-helical. These regions possibly are flexible globular domains (Pretorius *et al.*, 1981). Changes in the polyhedral geometry associated with endocytosis must require some

degree of heavy chain junctional flexibility (Lisanti *et al.*, 1984; Pearse and Crowther, 1981).

d. Light chains

In her first report on her isolation of clathrin, Pearse (1978) commented on the appearance of a 36 and 33 kD doublet species which copurified with clathrin. These have been termed clathrin associated proteins ($CAP_1/CAP_2$; Puszkin *et al.*, 1983; Lisanti *et al.*, 1982) and clathrin light chains (LCA/LCB, Kirchhausen *et al.*, 1987; $LC_\alpha/LC_\beta$, Bar-Zvi, 1985). The molar ratio of clathrin triskelion to total light chain is 1:1; the ratio of $\alpha$ to $\beta$ light chains on each triskelion is 1:2 (Ungewickell and Branton, 1982).

Four clathrin light chain isoforms have so far been characterized (Hill *et al.*, 1988): brain and nonbrain light chains $\alpha$ and $\beta$. Using bovine adrenal glands as nonbrain tissue, Holmes *et al.* (1984) discovered that nonbrain isoforms are present to a small degree in brain, but not the other way around. Kirchhausen *et al.* (1987) and Jackson *et al.* (1987) determined the primary structures of these isoforms, generated oligonucleotides based on those sequences, and cloned the complementary DNA fragments. $LC_\alpha$ & $LC_\beta$ are made from two different but closely related genes. The transcriptional products of these genes are subjected to differential splicing, yielding the brain and nonbrain isoforms. Bovine brain $LC_\alpha$ has 243 amino acids, $LC_\beta$ 231 amino acids; adrenal $LC_\alpha$ has 213 and

adrenal $LC_\beta$ 210. The molecular weights were calculated to be 26.7 kD for brain $LC_\alpha$, 25.1 kD for brain $LC_\beta$, 23.3 kD for nonbrain $LC_\alpha$, and 23.1 for nonbrain $LC_\beta$ (Jackson *et al.*, 1987). As a comparison of calculated versus apparent molecular weights, on SDS-PAGE the apparent molecular weights are 38, 35, 34, and 32 kD, respectively. The existence of at least these four isoforms may be related to a necessary diversity of coated vesicles.

The brain light chains have extra amino acid sequences, primarily hydrophobic, inserted at position 158 (Jackson *et al.*, 1987). This is two thirds of the way down the polypeptide chain. Brain $LC_\alpha$ has 30 amino acids inserted and brain $LC_\beta$ has 18 amino acids inserted. These insertions give brain light chains a slightly higher molecular weight than the nonbrain species. The shorter $LC_\beta$ brain insertion sequence is homologous with the amino-terminal end of the larger $LC_\alpha$ sequence. These sequences, exposed in coated vesicles, are well conserved in different mammalian species.

Indeed, the gene products in general show strong homology across three mammalian species (Jackson and Parham, 1988). The differences between $LC_\alpha$ and $LC_\beta$ within the same tissue, based on percent homology, is much greater than the differences of the related chains across tissues. This pattern holds for the three orders of mammals studied, and implies the divergence of a single gene. Yeast

has only one type of clathrin light chain, supporting this implication.

The sequences flanking the brain light chain insertions are homologous with the sequences in nonbrain light chains. It is likely that the genes are the same, based on the observation that encoding sequences are conserved even in nonallelic genes. The extra sequences in brain light chains probably are produced by a posttranscriptional modification of the mRNA. This modification may be the result of differential splicing.

Light chains have two functional regions, a heavy chain binding region (amino acids 93-157) and a "vesicle diversity" region (amino acids 158-208) containing the brain insertion sequences (Brodsky *et al.*, 1987). This latter region could also have other tissue-specific sequences that allow differential clathrin activity (for example, a diversity of coated vesicle size & shape). It may also provide a recognition site for adaptors.

The existence of light chain isoforms in higher vertebrates, ubiquitous and well-conserved, suggests that light chains have a major functional role in coated membranes. This role is probably regulatory in nature (Hanson *et al.*, 1990; Schook and Puszkin, 1985; Lisanti *et al.*, 1982). However, the specific function of clathrin light chains is not known (Jackson and Parham, 1988; Ungewickell *et al.*, 1981). Two approaches can be taken to fill this gap. One

can begin by studying heavy and light chain interaction. One can also correlate changes in light chain properties with intracellular events.

A major starting point towards understanding the interaction of heavy and light chains is to ascertain the actual binding sites. Brodsky *et al.* (1987) determined that the heavy chain binding domain resides between residues 95 through 157. Investigation of the mechanism by which this domain binds to the heavy chain involves the work of two laboratories (Jackson and Parham, 1988; Kirchhausen *et al.*, 1987). Studying the primary light chain structure, Kirchhausen *et al.* identified ten groups of seven amino acids (heptads) which could form α-helices. Through van der Waals forces of attraction these heptads could impart a coiled-coil supersecondary structure (Crick, 1983). This could serve as a heavy chain binding mechanism.

At about the same time, Jackson *et al.* observed homology between the binding region, predicted to be α-helical, and an α-helical region of intermediate filaments (1987). They implicated a light chain α-helix as being functional in heavy chain binding, but did not recognize any heptads based on their analysis of the primary structure, and concluded that light chains did not have any coiled-coil α-helices. In a later paper (1988), Jackson and Parham agreed that light chain heptads do indeed exist, and that

the "conserved side" of these heptads are likely to be the heavy chain binding sites.

Identification of the light chain binding sites does not immediately explain the functional interaction of light chains with heavy chains. It is noteworthy that light chains are found wherever heavy chains are located, even in yeast (Jackson and Parham, 1988), yet clathrin triskelions can self-assemble into cages without light chains being present (Puszkin *et al.*, 1982; Ungewickell and Branton, 1982). Their functional importance must be more regulatory than structural, although this is not to say that light chains have no structural significance.

By its *raison d'être*, a regulatory protein is dynamic and able to change its biochemical or biophysical properties in response to specific conditions. Phosphorylation and dephosphorylation cascades triggered by second messengers are good examples of this (Krebs and Beavo, 1979). $LC_{\beta}$ is phosphorylated by casein kinase II (Schook and Puszkin, 1985; Usami *et al.*, 1985) on serine residues 11 and 13 (Hill *et al.*, 1988). This phosphorylation sequence is conserved between species (Jackson *et al.*, 1987; Kirchhausen *et al.*, 1987). $LC_{\alpha}$ is not phosphorylated by casein kinase II because it does not have serine in the polypeptide sequence 9 - 13.

Although light chains are not directly involved with clathrin-vesicle interaction (Ungewickell *et al.*, 1981),

they might be involved in the conversion between coated vesicles and coated pits. Since it serves as a phosphorylation substrate, $LC_\beta$ is a good possible candidate as a regulator or modulator of clathrin assembly.

A step in this direction has been taken by Hanson *et al.* (1990), who discovered that phosphorylated $LC_\beta$ inhibits phosphorylation by a cyclic nucleotide/$Ca^{++}$-independent kinase of a 50 kD assembly polypeptide associated with coat proteins (pp50; Pauloin *et al.*, 1982). pp50 in turn could possibly participate in a control step in coat assembly-disassembly (Pauloin and Jollès, 1986).

e. Adaptors

Adaptors, also called assembly polypeptides (Zaremba & Keen, 1983), form the inner shell of the three-layered vesicle coat. The middle layer of this coat is created by the inner projection of the 60 kD terminal domain of the clathrin heavy chains. The outer layer consists of the clathrin lattice formed by the polygonal array of heavy chain triskelions and associated light chains. The adaptors presumably serve as the link between the coat proteins and the receptors associated with the vesicle membrane itself, residing innermost to the entire coat assembly. The adaptors are divided into two categories, based on their affinity properties in hydroxylapatite columns (Robinson and Pearse, 1986): HA-I and HA-II. The HA-I adaptor has a heterodimer of 100 kD polypeptides,

γ-adaptin and β-adaptin, and two associated polypeptides of 47 and 19 kD. The HA-II adaptor also has a heterodimer of 100 kD polypeptides, α-adaptin and β-adaptin, and two other associated polypeptides of 50 and 16 kD. HA-I adaptors are found in the coated vesicles of the Golgi apparatus; HA-II adaptors are associated with the plasma membrane coated vesicles.

These adaptors have different binding specificities for membrane receptors, even for the same membrane receptor, as shown in the pioneering work of Glickman *et al.* (1989). The mannose-6-phosphate (M6P) receptor reportedly is found on both Golgi and plasma membranes. HA-I and HA-II adaptors can both bind to the cytoplasmic tail of M6P receptors, but at different locations, as demonstrated by binding competition experiments. Using site-directed mutagenesis, the cytoplasmic portion of the receptor was modified to replace two tyrosine residues with alanine and valine. This modification did not affect HA-I/M6P receptor interaction, but abolished HA-II affinity for this receptor. Thus a "tyrosine signal" must play a part in the recognition of plasma membrane coated pits, where HA-II is naturally found. This suggests that the adaptors participate in the intracellular trafficking of membrane receptors.

Robinson has done extensive work on the α-adaptins of HA-II (Robinson, 1989). α-adaptin has two bands on SDS-

PAGE, A & C (band B is β-adaptin). Adaptins $\alpha_A$ and $\alpha_C$ are closely related to each other. Adaptin $\alpha_C$ is found in all tissues (including brain), and $\alpha_A$ is primarily expressed in brain (Robinson, 1987). Robinson cloned the cDNAs for these adaptins. She determined that each is encoded by separate but related genes. Screening a mouse brain cDNA library, she surmised that no other related genes are present. Robinson also carried out *in situ* hybridization in mouse brain sections using antisense DNA to determine where $\alpha_A$ is expressed. Both $\alpha_A$ and $\alpha_C$ were present in brain, as expected, but $\alpha_A$ was found highly concentrated in an area corresponding to the dentate gyrus of the hippocampus. In contrast, $\alpha_C$ was concentrated in both this structure and the habenular nucleus of the thalamus. Both areas consist of high concentrations of neuronal cell bodies. Further resolution of the hippocampus revealed that $\alpha_A$ was distributed evenly between granule cell and pyramidal cell layers. $\alpha_C$ was much more concentrated in the pyramidal cell layer. From these results Robinson deduced that $\alpha_A$ and $\alpha_C$ are most abundant in neuronal cell bodies, and both adaptins are produced by the same cells but in differential amounts. She speculated that the intracellular differences in α-adaptin abundance may be associated with subpopulations of coated vesicles, such as synaptic versus nonsynaptic vesicles.

**4. Function**

As seen in Figure 7, adapted from Pearse and Crowther (1987), the involvement of coated pits and vesicles in membrane recycling is at once complex and elegantly simple.

**Figure 7**. Scheme of endocytosis and membrane recycling.

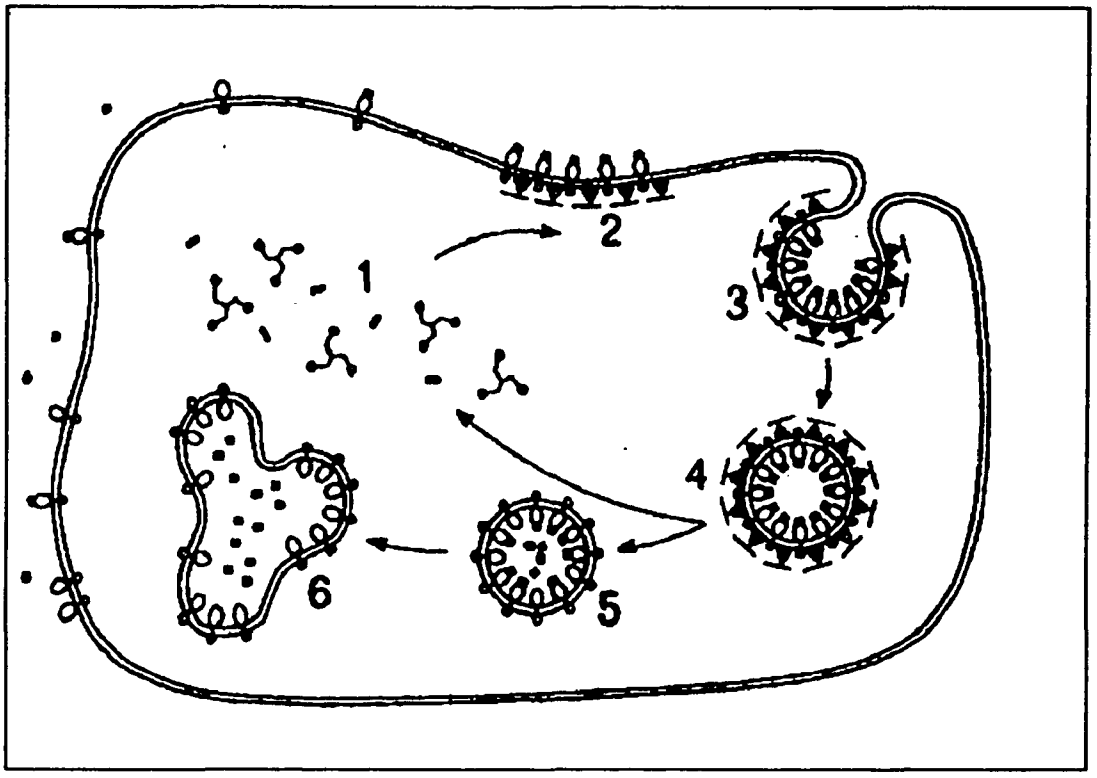


**1**: Free clathrin and adaptors; **2**: coated pit; **3**: budding invagination; **4**: coated vesicle; **5**: decoated vesicle; **6**: endosome.

Free clathrin triskelions (1) assemble into clathrin rafts (2). These rafts are bound to membrane receptors by accessory proteins collectively called adaptins and concentrated in particular regions as coated pits. On a simple morphologic basis, electron microscopic observation of newly formed coated pits did not show any preferred sites of assembly, nor did the membrane itself appear to have any morphologically distinct areas associated with coated pit formation. However, it is known that these regions serve as diffusion sinks for laterally diffusible integral membrane receptors (Bleil and Bretscher, 1982; Helenius *et al.*, 1980; Wall *et al.*, 1980; Haigler *et al.*, 1979; Willingham *et al.*, 1979; Gorden *et al.*, 1978; Schlessinger *et al.*, 1978). Presumably, these receptors are anchored by their cytoplasmic tails to adaptors (functional complexes of adaptins). Coated pits occupy approximately 2% of a cell surface, yet they can contain as much as 70% of the cell surface receptors. Once the receptors come in contact with the coated pit, their high binding affinity effectively excludes other unrelated membrane proteins. On the cytoplasmic side, soluble clathrin triskelions and adaptins come in contact with the existing clathrin rafts of the coated pit and bind with high affinity. Thus coated pit growth involves coassembly of membrane receptors and coat proteins into a transmembrane superstructure. Nascent coated pits are first visualized as 2 or 3

polygons, and grow by border addition. Once a critical size is reached, invagination commences. The planar arrangement of the clathrin hexagonal array gives way to a polyhedral dome, possibly to relieve any stress caused by the crossover packing of the triskelions. The concavity of the forming polyhedron causes invagination of the plasma membrane, seen from the cytoplasmic side as budding of an incipient coated vesicle. The final apposition of the bud base is followed by a pinching off of the coated vesicle (4). This final pinching off, a seemingly trivial process, involves considerable molecular rearrangement of highly complex and heterogeneous components--the membrane phospholipid bilayer, coat proteins, receptors and perhaps other integral proteins--and the biophysical mechanism of this coordinated transition is still a mystery. Once formed, the coated vesicle quickly uncoats (5), leaving the vesicle free to fuse with other vesicles to form an endosome (6), and the solubilized coat proteins free to participate once again in the endocytic process (1). This uncoating process is mediated by an uncoating ATPase (Schlossman *et al.*, 1984), later identified as the heat shock protein HSP70 (Chappell *et al.*, 1986).

**5. Mechanism**

Ungewickell and Branton (1982) assert that hexagonal facets of clathrin are transformed into pentagons during coated pit invagination. A pertinent question is whether

this geometrical change actually causes the invagination, or merely accompanies it. Pearse and Crowther (1987) suggested that the budding process is driven by the binding of membrane receptors with the accessory coat proteins. This induces a curvature in the membrane due to the energetically favored state. The binding of free clathrin to the perimeter of the growing coated membrane raft may enhance and contribute to the growing curvature of the coat.

The theoretical considerations of Lisanti *et al.* (1984) illuminate the role of lattice transformation in forming a dome structure. The conversion of a planar hexagonal array into a dome is accomplished by introducing functionally important pentagons and heptagons, as shown in Figure 8.

**Figure 8**. Model of clathrin lattice formation.

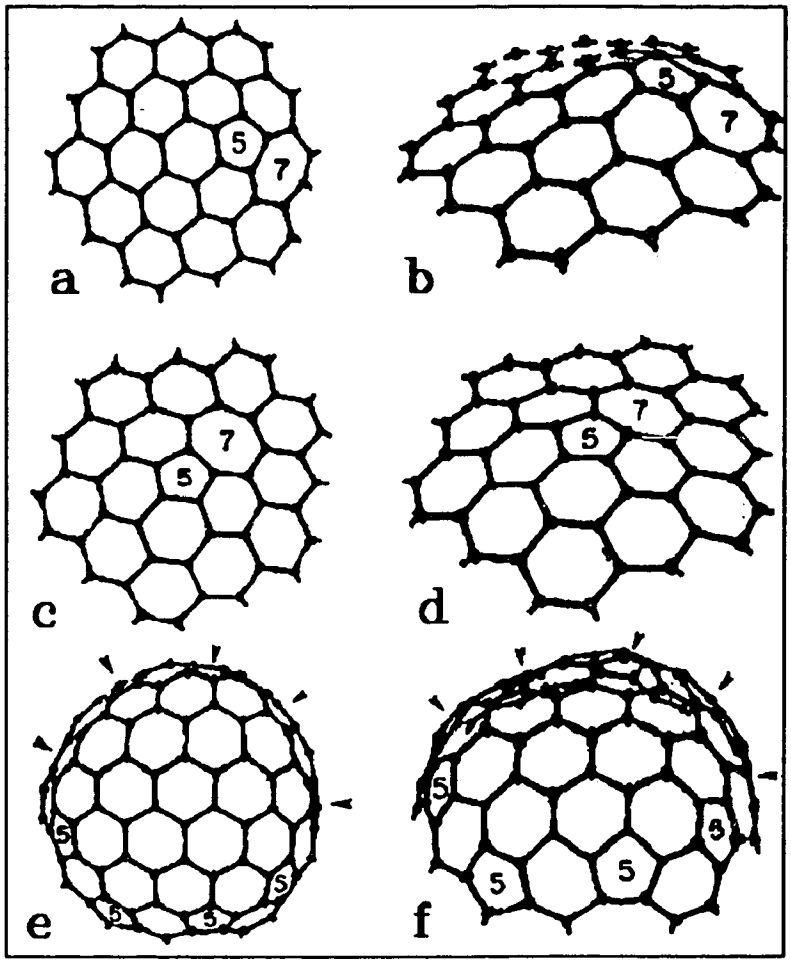


**a, c, e**: superior view; **b, d, f**: oblique view. Transformation of hexagons into pentagons and heptagons causes more convex deformation at the periphery (a, b) than at the center (c, d) of a coated pit. Consequently, the budding vesicle has more pentagons at its base (e, f).

In *a* through *d*, two hexagons are transformed into a pentagon and a heptagon, creating a "bubble" on the otherwise planar surface; this bubble could form either in the middle of the lattice (*c* and *d*) or at the edge (*a* and *b*). The bubble acts as a seed for stress on the neighboring hexagons, which in turn undergo polygonal conversion, with heptagons giving way to pentagons. Pentagons relieve triskelion stress at the expense of high angularity between the adjacent facets, adding to the curvature of the lattice and creating the vesicle bud. This model is corroborated by the stunning electron microscopic evidence of Heuser (1980). He quantitated the population of pentagons as a function of coat curvature, and found the highest proportion in the most mature buds.

Dislocation of the triskelions comprising the coat lattice induces these polygonal transformations. The mechanism of this dislocation may involve some other regulatory protein, perhaps uncoating ATPase (Lisanti *et al.*, 1984). The driving force behind increased coat curvature is the attenuation of torsional stress on the triskelions. In effect, a domed scaffold is built, and the attached membrane is passively pulled along with it.

In summary, a major function of coated vesicles is internalization of extracellular compounds by receptor-mediated endocytosis (Goldstein *et al.*, 1979), through the process described above. This process serves a fundamen-

tal role in cell life, including cellular growth and development.

## B. PRELIMINARY CONSIDERATIONS

### 1. Choice of Animal

Since NP185 is nervous tissue-specific and co-purifies with coated vesicles, it is reasonable to suspect that this protein is in some way functionally associated with the vesicular activities of neurons. Such activities include membrane uptake in the terminal bouton, axonal transport from perinuclear structures, growth cone formation and synaptogenesis. Correlating NP185 localization with underlying events in nervous tissue development has the potential to yield useful information on the function of this protein. This approach is well established and has given fruitful results to others (Leclerc *et al.*, 1989; Bannerman *et al.*, 1986; Bignami *et al.*, 1985; Fults *et al.*, 1985; McComb and Bigner, 1985; Wiedenmann and Franke, 1985; Obata and Fujita, 1984; Hantaï *et al.*, 1983; Duband and Thiery, 1982).

Based on these considerations, the animal of choice is *Gallus domesticus*, the white leghorn chicken. The embryo is of course thoroughly accessible, and the stages of embryological development are well characterized (Hamburger and Hamilton, 1951). The major reservation of this choice is that the class is Aves, not Mammalia, giving rise to questions of antibody cross-reactivity and phy-

letic differences. Immunoblot analysis established the suitability of chicken tissue for use in this study.

**2. Choice of tissue**

I chose the cerebellum as the object of study for the following reasons: 1) The gross anatomy of the cerebellum is readily identifiable, thanks to landmark features, such as folia, that remain in lineament even in sections mounted on slides (Larsell, 1967; Figure 9).

**Figure 9**. Midsagittal section of cerebellum.

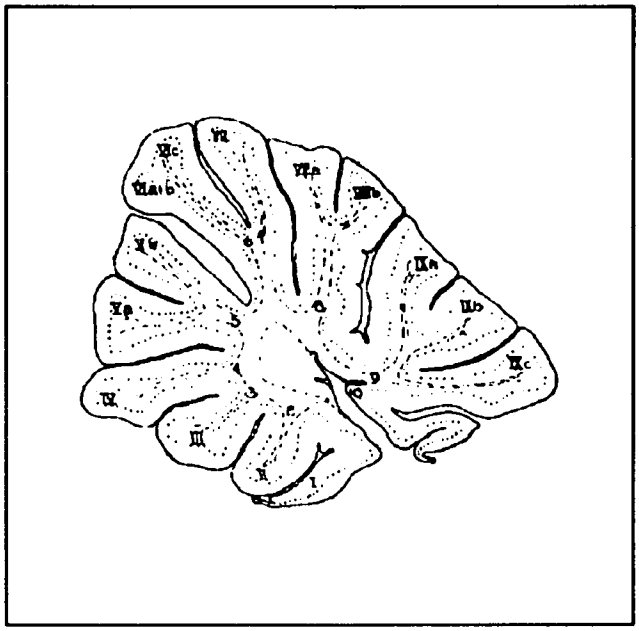

Cerebellum of young adult bantam chicken.

2) The histology of the cerebellum is clearly delimited by distinct regions, such as the cortical layers, which have their own characteristic appearance (Martin, 1989; Figure 10).

**Figure 10.** Stained section through the cerebellar cortex.

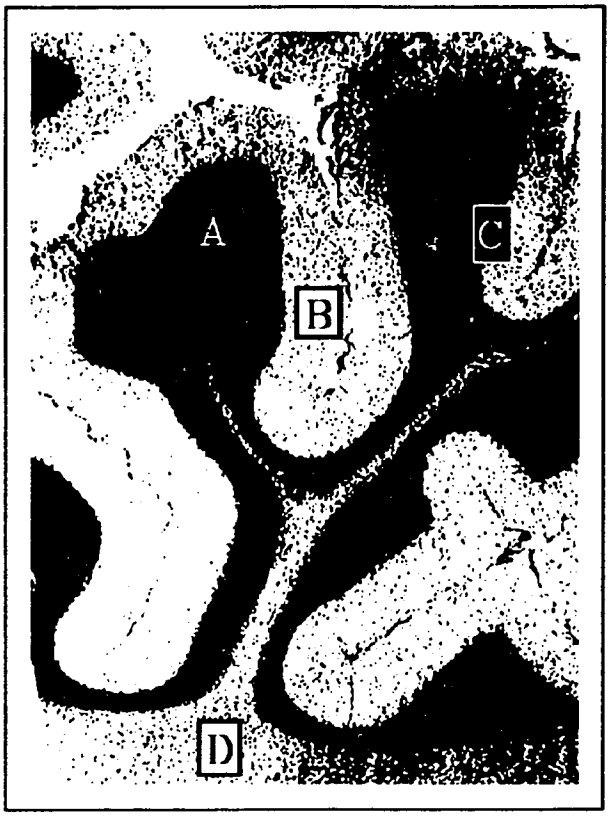


**A**: granular layer; **B**: molecular layer; **C**: Purkinje layer (border between granular and molecular layers); **D**: white matter.

3) The cellular population of the cerebellum is of limited diversity, consisting of 5 types of neurons (Martin, 1989; Table I, p. 41; Figure 11, p. 42; Figure 12, p. 43) and 4 types of glial cells (Table II, p. 44).

**Table I.** Cerebellar neurons.

| CEREBELLAR NEURONS | | | |
|---|---|---|---|
| **Projection neuron** | | | |
| Cell type | Distribution | Action | Target |
| Purkinje cell | Purkinje layer | Inhibitory | Deep nuclei<br>Vestibular nuclei |
| **Interneurons** | | | |
| Cell type | Distribution | Action | Target |
| Granule cell | Granular layer | Excitatory | Purkinje cells<br>Stellate cells<br>Basket cells<br>Golgi cells |
| Basket cell | Molecular layer | Inhibitory | Purkinje cells |
| Stellate cell | Molecular layer | Inhibitory | Purkinje cells |
| Golgi cell | Granular layer | Inhibitory | Granule cells |

1: Martin, 1989.

**Figure 11.** Excitatory pathways.

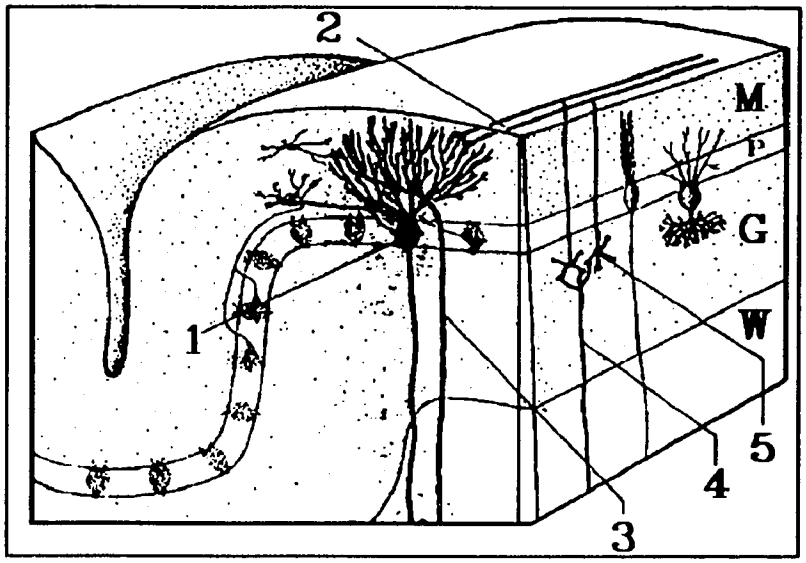


**1**: Purkinje cell; **2,3,4**: parallel, climbing, mossy fibers; **5**: granule cell. **M,P,G**: molecular, Purkinje, granular layers; **W**: white matter.

**Figure 12.** Inhibitory interneurons in the cerebellar cortex.

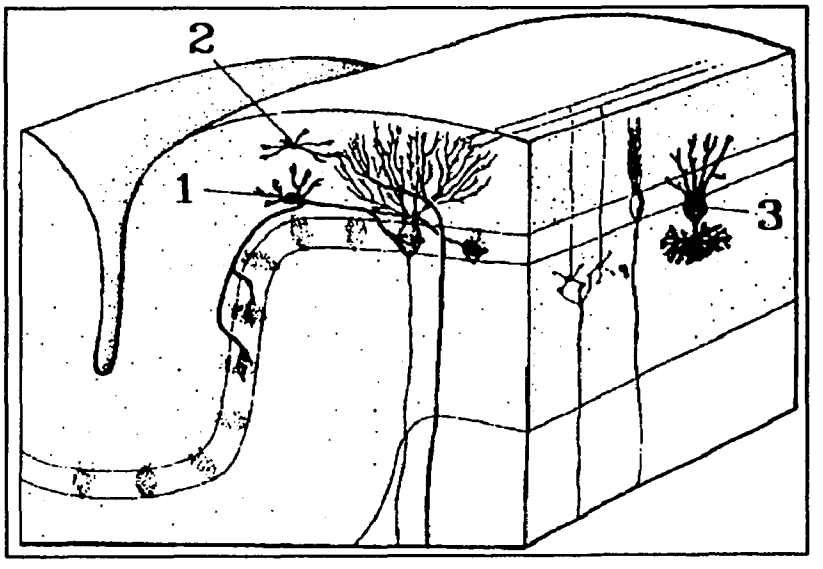


**1**: basket cell; **2**: stellate cell; **3**: Golgi cell.

**Table II**. Cerebellar glial cells.

| CEREBELLAR GLIAL CELLS | | | |
|---|---|---|---|
| **Neuroglia** | | | |
| Cell type | Origin | Primary Distribution | Function |
| Protoplasmic astrocyte | Glioepithelium | Granular layer | Blood-brain barrier<br>Nutrient delivery<br>Waste removal |
| Bergmann glial cells | Glioepithelium | Molecular layer | Migratory cell guidance<br>Neuronal scaffolding |
| Fibrous astrocyte | Glioepithelium | White matter | Neuronal scaffolding |
| Oligodendrocytes | Glioepithelium | Satellite cells<br>Nerve fibers | Myelination |
| **Mesoglia** | | | |
| Cell type | Origin | Primary Distribution | Function |
| Microglia | Pia mater<br>Blood vessels | Scattered | Immunosurveillance |

1: Lowe *et al.*, 1989; Wilkin and Levi, 1986; Sotelo, 1967; Polak, 1965.

4) The direction of central nervous system development is rostrocaudal (Patten, 1951), and therefore the cerebellum emerges from the metencephalon relatively late (embryonic day E4). This allows the use of larger embryos, which are easier to manipulate and dissect (Figure 13, p. 46).

**Figure 13**. Rostrocaudal direction of central nervous system development.

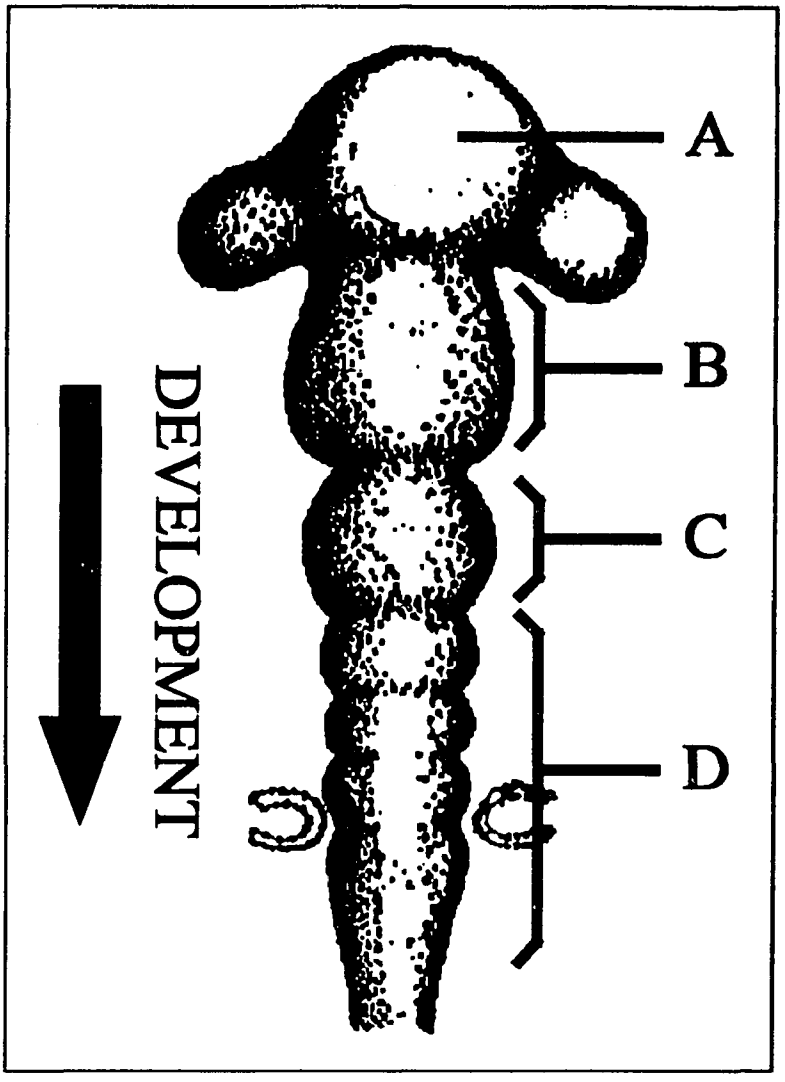


**A**: prosencephalon; **B**: mesencephalon; **C**: metencephalon; **D**: myelencephalon.

In general, cerebellar neurogenesis faithfully reflects the major features of neurogenesis throughout the central nervous system (Mugnaini, 1969), and serves as an excellent model for study.

# II. METHODS

## A. NOMENCLATURE

Chick embryos are staged both chronologically and developmentally. Chronological staging begins the day of egg laying (embryonic day zero: E0) and continues for 21 days to hatching (E21). Hatching day is termed posthatching day zero (P0); subsequent days are termed P1, P2, etc. Developmental staging follows the system of Hamburger and Hamilton (1951), based on carefully defined morphological criteria. Each developmental stage is termed S1, S2, etc., up to S46, hatching.

## B. WESTERN BLOT ANALYSIS

### 1. Sample preparation

Certified pathogen-free fertilized eggs were obtained from a commercial supplier (SPAFAS) and placed in a rocking egg incubator (Lyon Electric). Within 12 hr, and every day thereafter, embryos were harvested, weighed, and staged by the method of Hamburger and Hamilton (1951). For stage E1 to E5, whole embryos at each stage were pooled to obtain sufficient amounts of protein. On E6 and E7, embryonic heads were pooled, and on E8 and E10 individual heads were used; individual brains were used thereafter. A summary of this sample collection is given in Table III.

**Table III.** Summary of embryo samples.

| EMBRYO SAMPLES | | | |
|---|---|---|---|
| day[1] | samples[2] | weight[3] (mg) | stage[4] |
| E1 | 13 embryos | 426 | ~5 |
| E2 | 17 embryos | 307 | ~6 |
| E3 | 16 embryos | 276 | ~13 |
| E4 | 14 embryos | 474 | ~18 |
| E5 | 5 embryos | 591 | ~24 |
| E6 | 2 heads | 365 | ~26 |
| E7 | 2 heads | 434 | ~31 |
| E8 | 1 head, no eyes | 314 | 35 |
| E10 | 1 head, no eyes or beak | 549 | 36 |
| E11 | 1 brain | 189 | 36 |
| E12 | 1 brain | 219 | 37 |
| E13 | 1 brain | 259 | 38 |
| E14 | 1 brain | 319 | 39 |
| E15 | 1 brain | 397 | 41 |
| E16 | 1 brain | 464 | 42 |
| E17 | 1 brain | 589 | 43 |

**1**: embryonic day; **2**: samples pooled where indicated; **3**: in the case of pooled samples, refers to total weight; **4**: developmental stage (Hamburger and Hamilton, 1951).

Assuming tissue density to be near to that of water, equal volumes of PBS were added to each tissue and the contents homogenized in a small glass grinder at 4 °C. The homogenate was diluted 1:1 with 50 mM Tris, 1% SDS, 5% 2-mercaptoethanol, 0.02% phenol red, 30% glycerin ("sample buffer").

**2. Immunoblot technique**

Sodium dodecyl sulfate-polyacrylamide gel electrophoresis (SDS-PAGE) was performed generally following the method of Laemmli (1970). Sample preparations were loaded onto one-dimensional gels consisting of 10% acrylamide. For immunoblotting, gels with migrated proteins were electrophoretically transferred to nitrocellulose sheets using a Hoefer apparatus, following the procedure described by the manufacturer. Nitrocellulose filters were fixed, then saturated with 0.1% bovine serum albumin (BSA) and 0.05% Tween 20 in Tris-buffered saline (TBS), pH 7.5. Filters were incubated at 4 °C overnight with the primary antibody in 0.1% BSA, 0.05% Tween 20, and TBS. The next morning they were washed three times with 0.05% Tween 20 and TBS, then incubated for 1 h at 4 °C with phosphatase-conjugated goat anti-mouse IgG (Boehringer).

## C. IMMUNOLOCALIZATION[1]

**1. Tissue preparation**

Chicken embryos were harvested and staged as in section II.B.1, page 48, then fixed in 0.2% picric acid, 4% form-

aldehyde, and phosphate-buffered saline (PBS), for 30 min, according to the method of Zamboni and de Martino (1967). Healthy adult Balb/c mice and white leghorn chickens were sacrificed by cervical dislocation. Excised cerebella were fixed in the picric acid/formaldehyde (PAF) solution for 5 hr at 4 °C. Pectoral muscles from chicks were excised and fixed in 4% formaldehyde/PBS for 3 hr at room temperature (RT). In all cases the fixed tissue was then soaked in 15% sucrose in PBS overnight at 4 °C. The following morning, the tissue was immersed in OCT medium, frozen in liquid nitrogen, and sagittally sectioned at 8 µm in a Harris cryostat. The sections were mounted on slides and rinsed in PBS. The tissue sections were permeabilized with 0.5% Triton in PBS for 5 min, rinsed, and blocked with goat anti-mouse IgG 1/100 for 30 min at 4 °C. After rinsing, the sections were incubated overnight at 4 °C with primary antibody diluted 1/100 with 1% BSA in PBS pH 7.4 (BSA/PBS), washed, and then incubated with goat anti-mouse IgG-FITC for 45 min at room temperature. Primary monoclonal antibodies (mAbs) consisted of 8G8, raised against NP185 in this laboratory (Kohtz and Puszkin, 1988); obtained from Boehringer Mannheim were SY38, NR4, G-A-5, and 3B4, recognizing synaptophysin, neurofilament NF68, glial fibrillary acidic protein (GFAP), and vimentin, respectively. Control tissue sections were incubated with either the second antibody only,

or with mouse control ascites and second antibody. The sections were given a last rinse in PBS. To minimize photobleaching of the fluorescein label, the final sections were covered with a mixture of 1% *p*-phenylenediamine in 90% v/v glycerol buffered with PBS (Johnson and de C Nogueira Araujo, 1981). The slides were then sealed with coverslips and nail polish. Epifluorescence was observed on a Zeiss Axiomat inverted microscope. Fluorescein excitation was accomplished with a 450-490 nm band pass filter; emission was measured with a 520 nm long wave filter. Rhodamine excitation was accomplished with a 510-560 nm band pass filter; emission was measured with a 590 nm long wave filter.

**2. Controls**

False positive and false negative reactions were possible, and rigorous controls were applied in all the experiments. To test for false positive results, every experiment included sections which were treated identically to the other sections with the exclusion of the first antibody. Examples of these controls are shown in Figure 14 and Figure 15 (page 54).

**Figure 14.** Control, chick embryo.

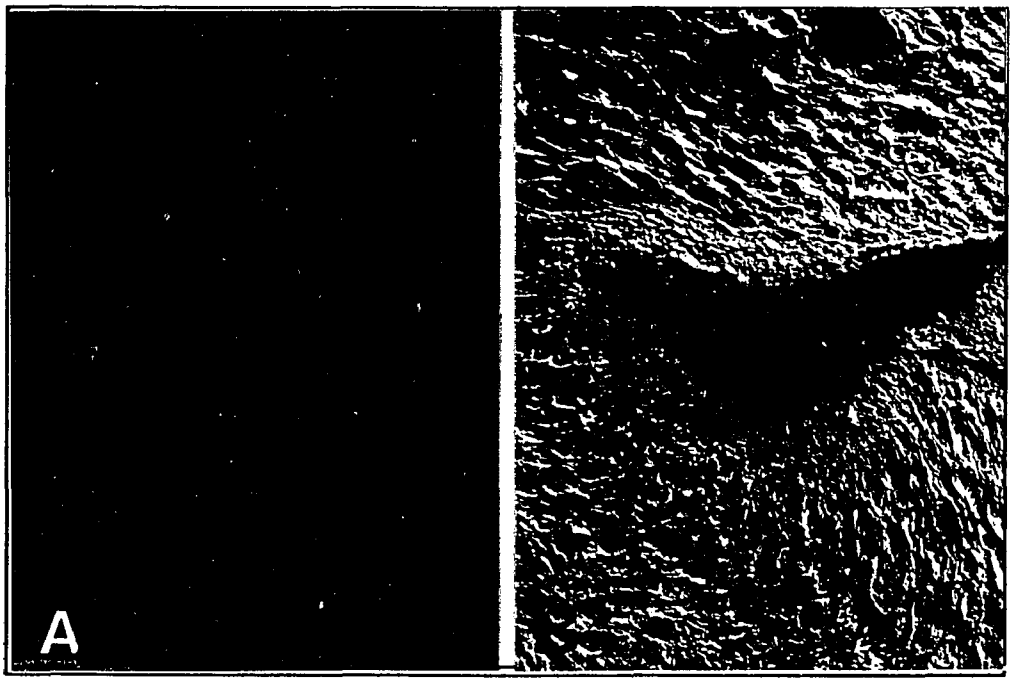


E6 chick embryo, fourth ventricle and ependyma, 80X. **A**: standard exposure; **B**: Nomarski image.

**Figure 15**. Control, chicken skeletal muscle.

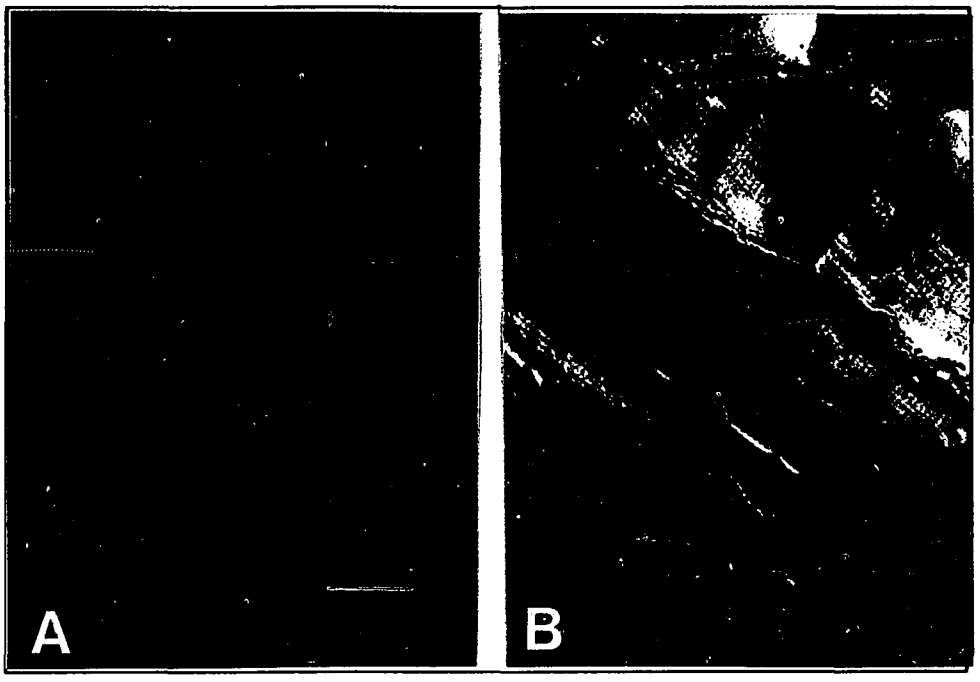


Adult chicken, pectoral muscle, 320X. **A**: standard exposure; **B**: Nomarski image.

The negative controls were consistently unlabelled. In both controls and regular sections, some cells were pale yellow. This yellow tint represents formaldehyde-induced fluorescence (FIF) of endogenous catecholamines (Partanen, 1975; Eränkö, 1967). FIF is caused by the closure of the catecholamine side chain by formaldehyde to form a fluorescent derivative of isoquinoline. This reaction has no connection with immunofluorescent labelling, nonspecific or otherwise. The mild yellow tint of these cells does not interfere with fluorescein or rhodamine emission, and cannot be misidentified.

When examining embryonic tissues, which in the earliest developmental stages were not expected to express NP185, the problem of false negative reactions became important. To make sure that the incubation conditions were favorable for desired labelling, sections of adult chicken cerebella were always included with the embryonic sections, as positive controls.

# III. RESULTS

## A. DEVELOPMENTAL EXPRESSION OF NP185

To establish cross-reactivity of mAb 8G8 in avian brain tissue, and to determine the onset of expression of NP185 in chick embryo, embryo samples were subjected to Western blot analysis. Figure 16 shows a Western blot of the prepared samples.

**Figure 16**. Western blot of chick embryo samples.

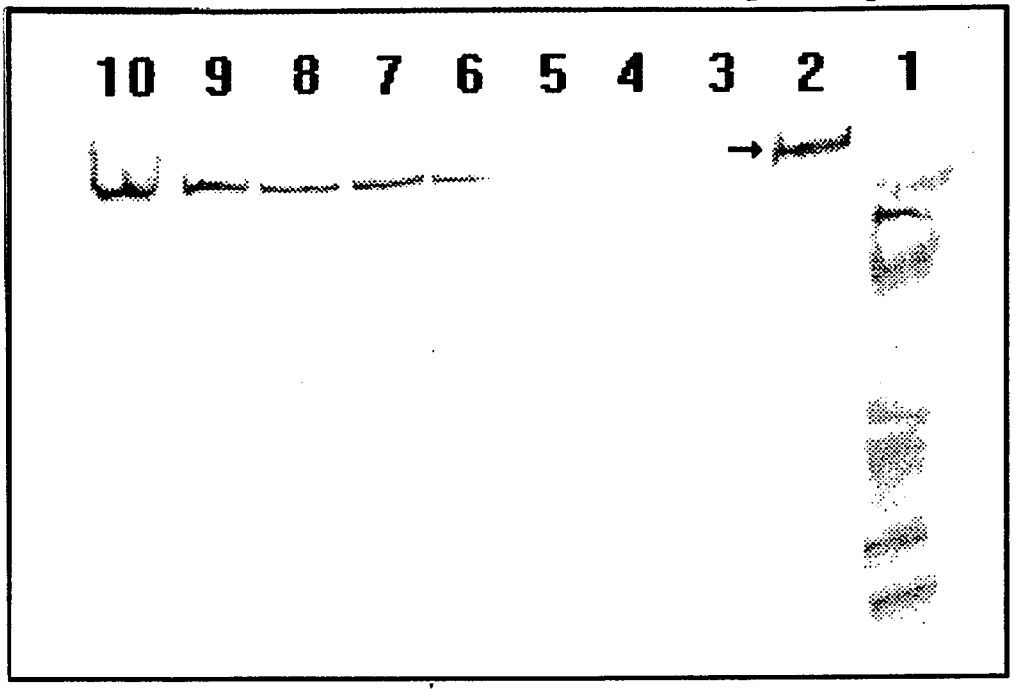


Chick embryos, E9 through E16. **1**: molecular weight standard; **2**: clathrin coated vesicle standard (**arrow**, 180 kD); **3-4**: E9-E10, heads; **5-10**: E11-E16, brains. NP185 reactivity begins to appear at E12, and gets progressively stronger through E16.

Lane 2 presents samples of bovine brain coated vesicles purified by the method of Schook and Puszkin (1985). These are included as positive controls for immunoreactivity. The antibody to NP185 cross-reacts with avian brain tissue, demonstrated by the bands which first appear at E12. Expression levels increase with each embryonic day thereafter, based on the qualitative increase in band density. The total protein content in each sample lane was controlled by proportional pooling of tissue samples, and by equal dilution based on sample weight.

The above result establishes the presence of NP185 in avian brain tissue, and that the onset of expression occurs no later than E12. However, earlier expression of NP185 cannot be ruled out. The sensitivity of Western blot analysis is dependent upon adequate levels of protein in the migrating sample. It is possible that in earlier embryonic days NP185 is present but too low to detect. Immunohistochemistry confirms this, as given in section III.B.1.

## B. IMMUNOLOCALIZATION

### 1. Ontogenic distribution of NP185

The earliest embryonic day of NP185 expression detectable by immunohistochemistry is E10. Within the 24-hr window created by taking embryo samples day-to-day, the onset of this expression is sudden: In four repeated experiments, E9 tissue sections were completely negative

for NP185; E10 sections were strongly positive. A typical labelling pattern is shown in Figure 17.

**Figure 17**. Typical NP185 label in early embryo.


NP185 distribution, chick embryo cerebellum, 128X. **E**: external granular layer; **M**: mantle. Mantle positive for NP185. Reticular labelling surrounds unlabelled cell bodies (**arrow**).

At E10 the cerebellum histologically consists of the external granular layer and the mantle layer (Nelsen, 1953). The external granular layer is the proliferative zone, which produces uncommitted neuroblasts. These cells are pre-neuronal, and therefore the external granular layer has no synapses. The mantle layer is the migratory zone, where neuroblasts migrate and differentiate into neurons. Migration and cell differentiation is influenced by early, indiscriminate synaptic formation (Jacobson, 1978), and the mantle accommodates synapses from its onset. Significantly, immunolabelling of NP185 is strongly and exclusively associated with the mantle. The labelling pattern is reticular, forming a fluorescent network surrounding dark cell bodies (arrow, Figure 17, p. 60). This pattern is identical to that described in the developing rat cerebellum for p65, a synaptic vesicle-associated protein with exclusive synaptic localization (Cambray-Deakin *et al.*, 1987).

At higher magnification, the reticular nature of this labelling pattern is more clearly seen (Figure 18).

**Figure 18**. Reticular immunoreactivity surrounding cell bodies.


NP185 distribution, E10 embryonic chick cerebellum, 320X. **E**: external granular layer; **M**: mantle. Border between external granular layer and mantle. Strongly labelled matrix surrounds the cells contacting the mantle **(asterisk)**. Leading points of the matrix **(arrow)** are intercalated between the premigratory neuroblasts.

This figure is a close-up of the border between the synapse-rich mantle and the nonsynaptic external granular layer, where neuroblasts begin their medial migration. The matrix of the mantle is strongly labelled for NP185; the external granular layer is not. The neuroblasts adjacent to the mantle are surrounded by the labelled matrix, as indicated by the asterisks. Cambray-Deakin *et al.* reported an identical distribution pattern with synaptic vesicle-associated p65 (1987). Significantly, the uncommitted neuroblasts, which in the external granular layer have no protosynaptic neurites, are negative for NP185; such was also found for p65.

As the cerebellum matures, synaptic distribution becomes more organized and regionally distinct. Figure 19 gives a panoramic view of a single folium at E14, labelled for NP185.

**Figure 19**. Distribution of NP185 at E14.

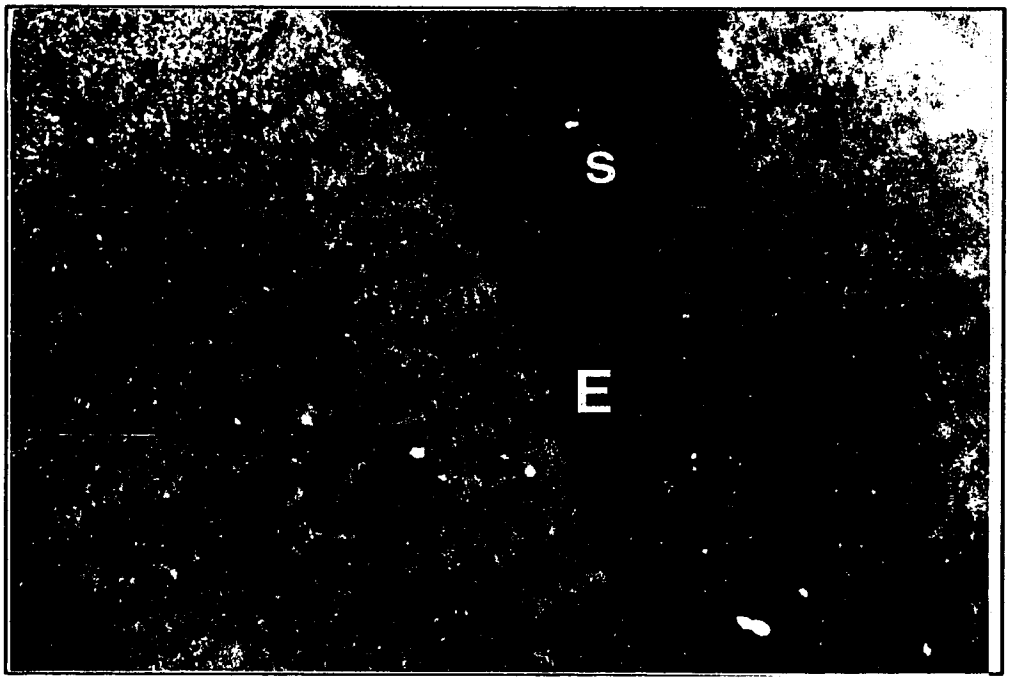


E14 chick embryo cerebellum, panoramic view of folium, 32X. **S**: interfolial space; **E**: external granular layer; **I**: intermediate layer of mantle; **V**: ventricular layer of mantle. Mantle positive for NP185. Note denser, stronger labelling in intermediate layer and reticular labelling in ventricular layer.

The labelling pattern manifestly follows synaptic distribution: The early mantle, which arises at E4 (Fujita, 1969), divides into the superficial mantle and deep mantle zones as early as E6 (Hanaway, 1967). By E12, these zones are more distinct, and have been referred to as the intermediate and ventricular layers (Chuong *et al.*, 1987). The superficial mantle zone, nearest to the external granular layer, becomes enriched with abundant synaptic connections, as the parallel fibers begin to synapse with the dendritic spines of Purkinje cells (Fults *et al.*, 1985; Gray, 1961). As synaptic density and organization continue to develop, NP185 labelling in this region also becomes more dense.

In contrast, the deep mantle zone is rich in neuronal cell bodies, caused by the migration of immature neurons from the external granular layer (Fujita, 1969) and from the ependyma (Miale and Sidman, 1961). Synapses, which are not as extensive as in the superficial mantle zone, are displaced by nerve soma. This results in a synaptic distribution pattern that is characteristically reticular--a net with holes, giving the appearance of a sectioned sponge (Figure 17, page 60).

The major contributing factor to this synaptic distribution is the strong adhesion of the granule cells (Mugnaini, 1969). The clumping of the granule cell bodies encourages focal organization of the synapses around

protoglomeruli. The synaptic terminals of the mossy fibers, which are so large that they have been referred to as "synaptic bags" (Gray, 1961) and "synaptic vesicle-filled varicosities" (Burgoyne and Cambray-Deakin, 1988), surround the clusters of granule cells. The mossy fiber terminals synapse with granule cell dendrites, which are close to their originating somas, but separated by astrocyte processes (Mugnaini and Forstrønen, 1967). This establishes a synapse-dense neuropil with a nonsynaptic core--the glomerulus of the granular layer. Labelling of any synapse-specific protein in this structure will yield halos of fluorescence surrounding dark cores, exactly the pattern seen in labelling of NP185 (Figure 20).

**Figure 20**. Early neuropil labelling for NP185.

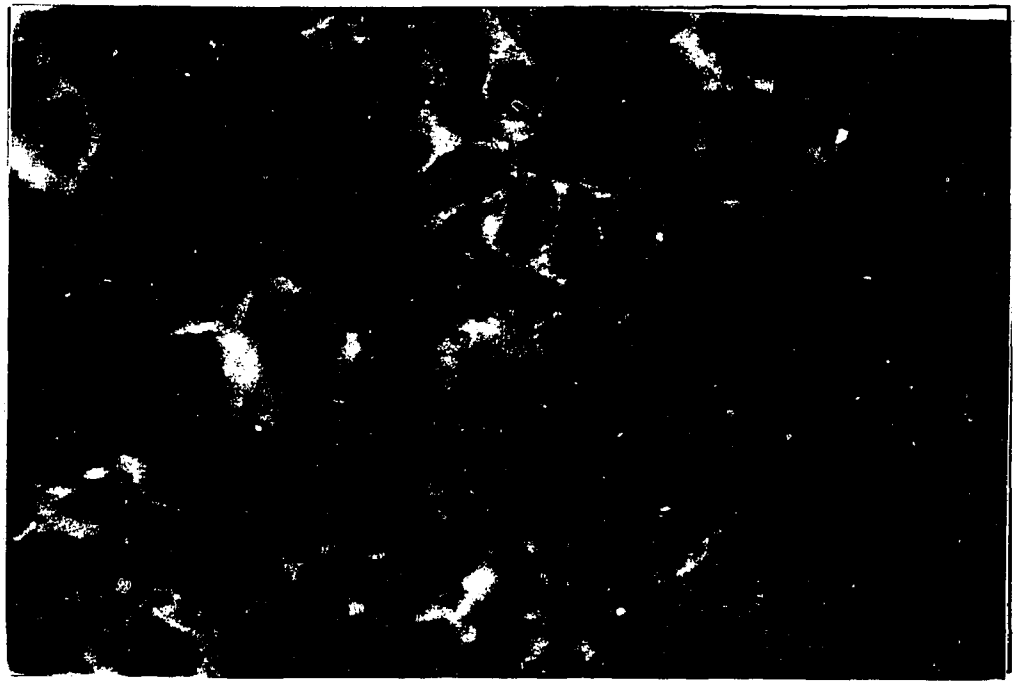

NP185 distribution, E15 chick embryo cerebellum, mantle, 320X. A cluster of immature granule cells (**asterisk**) adjacent to a synapse-rich neuropil (**arrow**).

This pattern is carried into maturity: The internal granular layer, which arises from the mantle (Fults *et al.*, 1985), maintains this reticular synaptic architecture.

Throughout cerebellar development, the external granular layer remains negative for NP185. At E13, the granule cells of the external granular layer begin migrating down Bergmann glial fibers to form the internal granular layer (Chuong *et al.*, 1987; Palacios-Prü *et al.*, 1981; Rakic, 1971). As these cells become situated, they are enveloped by mossy fiber rosettes to form glomeruli. In Figure 21, the granule cells are surrounded by intense fluorescent labelling of NP185, while the premigratory granule cells remain negative.

**Figure 21**. NP185 distribution at E15.

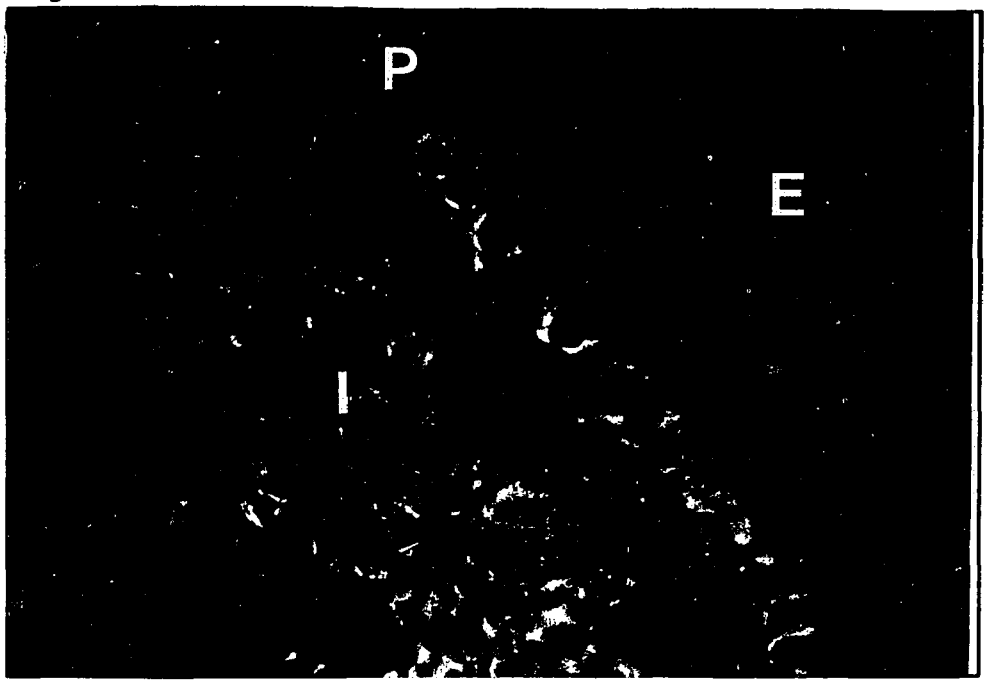


E15 chick cerebellum, 128X. **E**: external granular layer; **P**: Purkinje layer; **I**: internal granular layer; **arrowhead**: labelled protoglomerulus; **arrow**: perimembranous labelling of Purkinje cell.

The focal synaptic organization in the internal granular layer is now well established (arrowhead). Climbing and mossy fibers, granule cell dendrites, and early Golgi cells contribute to the synaptic organization in this region (Fults *et al.*, 1985; Altman, 1972c).

E15 marks the appearance of a monolayer of Purkinje cells, which constitutes the nascent Purkinje layer (P, Figure 21, p. 69; Foelix and Oppenheim, 1974). The Purkinje cells have intense areolate labelling of NP185 (arrow). At E15, Purkinje cell bodies are studded with spiny processes, or pseudopodia. These serve as anchoring sites for climbing fibers and basket cell axons, with which they form extensive axo-somatic synapses (Altman, 1972b; Mungnaini, 1969). As the axons form baskets around the Purkinje cells--hence the name--the pseudopodia retract. Significantly, NP185 is localized to the perimembranous space corresponding to the site of extensive, transient axo-somatic synapses, creating intensely fluorescent halos around the cells (Figure 22).

**Figure 22.** Labelling of young Purkinje cells for NP185.

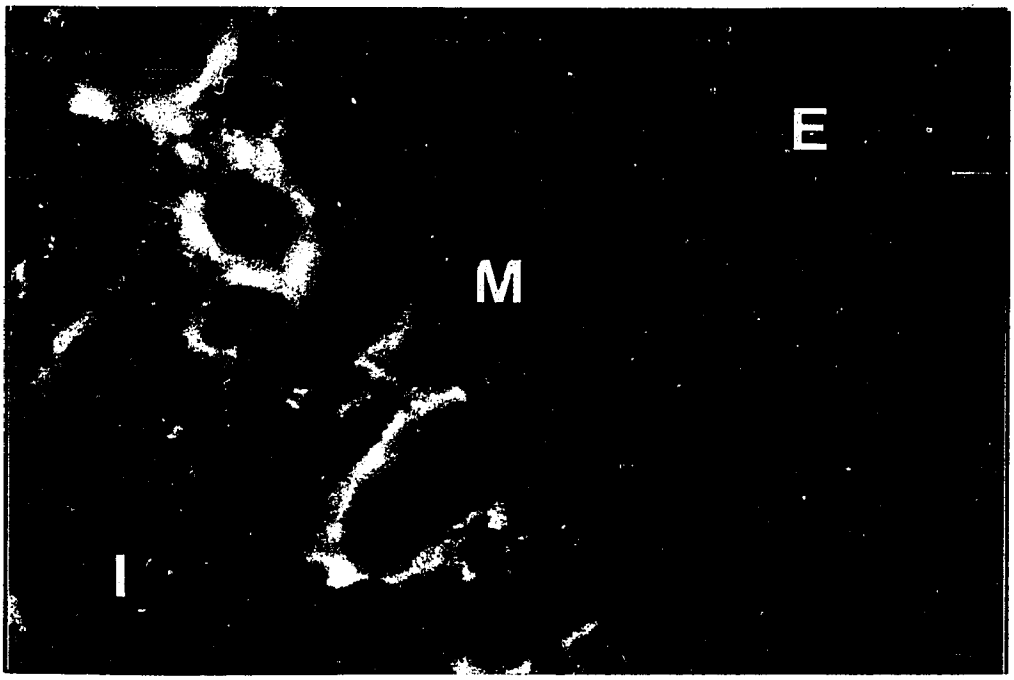


NP185 distribution in incipient Purkinje layer, E15 chick embryo cerebellum, 320X. **E**: external granular layer; **M**: early molecular layer; **I**: internal granular layer; **P**: Purkinje cell labelled for NP185; **G**: putative migrating granule cell (based on smaller size).

By E15, many of the Purkinje cells have developed apical cones and early dendritic projections (Palacios-Prü, 1981). These make direct contact with parallel fibers to form shaft junctions (Landis, 1987). Shaft junctions are specialized, transient synapses present only during neuronal development. They serve as precursors of mature synaptic organization, perhaps through target recognition. By electron microscopy, Landis observed coated vesicles associated with these structures. In Figure 23, an apical cone is visualized. It is strongly labelled for NP185.

**Figure 23**. Apical cone of Purkinje cell, labelled for NP185.


NP185 distribution at the mantle/external granular layer border, E15 chick embryo cerebellum, 320X. **E**: external granular layer; **M**: molecular layer; **P**: Purkinje cell. A strong fluorescent stain designates the apical cone (**arrow**). Note the light flocculate labelling in the nascent molecular layer.

Figure 24 provides a side-by-side example of the different patterns of NP185 distribution in the developing chick cerebellar cortex.

**Figure 24.** NP185 distribution in embryonic cerebellar cortex.

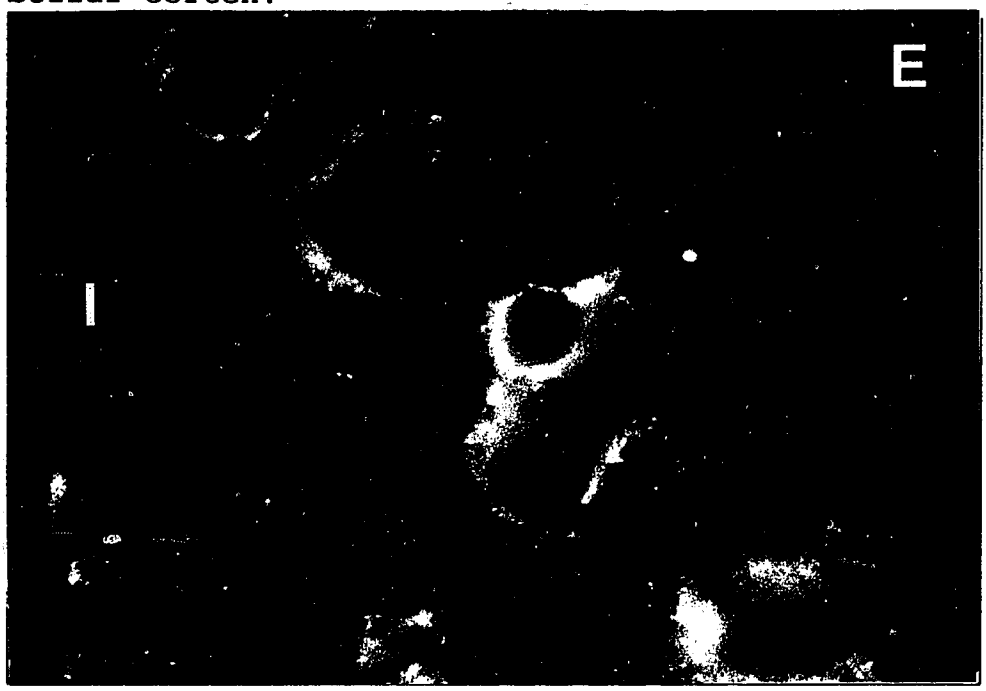


Labelling for NP185 in E15 chick embryo cerebellum, 320X. **E**: external granular layer; **M**: molecular layer; **I**: internal granular layer. No staining in the external granular layer; flocculate staining in the molecular layer; strong perimembranous staining in the Purkinje layer; reticular staining in the internal granular layer. **P**: Purkinje cell; **G**: migrating granule cell; **arrow**: protoglomerulus.

NP185 is not found in the external granular layer, where synaptic connections are entirely absent.

The early molecular layer is labelled for NP185 in a grainy pattern. In the molecular layer, synaptogenesis and cellular maturation begin at the Purkinje layer, and progress outwardly towards the pia mater (Altman, 1972b). Inwardly migrating granule cells lay down trailing axons which lengthen and align in parallel arrays, as their name implies. As younger granule cells migrate, their axons are deposited on top of the existing parallel fibers. While this is taking place, immature Purkinje cells produce apical cones, which wend into the molecular layer. The apical cones evolve into dendrites, and establish synapses with parallel fibers (Landis, 1987). Dendritic arborization progresses outwardly as the parallel fibers continue to stratify. This results in directional synaptogenesis, beginning at the Purkinje layer and moving externally, towards the pia mater. In Figure 24, page 75, the early molecular layer, adjacent to the Purkinje layer, is labelled for NP185 in a grainy manner. This labelling pattern is consistent with the progression of synaptogenesis (Woodward *et al.*, 1969): The label is always strongest in the deep molecular layer (nearest the Purkinje layer), and progressively diminishes towards the superficial molecular layer (nearest the pia mater).

The Purkinje layer in Figure 24, page 75 is labelled for NP185 in the same manner as in Figure 22, page 71. The areolate labelling of the Purkinje cells is apparent in the cell marked **P**. This is characteristic of early Purkinje cell labelling for NP185. The staining is clearly not confined to the cell body membrane. At E15 (the developmental stage of the tissue in this figure), Purkinje cell somata are studded with spiny processes (Foelix and Oppenheim, 1974). These processes serve as synaptic anchors for the climbing fibers (Altman, 1972b) and basket cell axons (Mugnaini, 1969). The fuzzy, intense staining seen here conforms to the synaptic arrangement on the perisomatic processes. Notably, these transient spiny processes begin to retract at E16 and disappear by E20. The mature Purkinje cell soma is covered with a glial sheath, and possesses significantly fewer axo-somatic synapses. In like manner, the Purkinje cell label for NP185 diminishes from a bright, fuzzy halo at E15 to a well defined perimembranous ring at maturity. (Compare Figure 24, page 75 with Figure 27, page 84.) As in the developing molecular layer, NP185 distribution appears to follow synaptic distribution.

Finally, Figure 24 (p. 75) shows the lattice structure of the early internal granular layer. A protoglomerulus is well visualized (arrow). Individual unlabelled granule cell bodies can be seen clumped together to form the glo-

merular core, which is covered by a glial sheath. Mossy fiber synaptic bags and granule cell dendrites contribute to the synapse-dense neuropil. Consistent with the labelling patterns of the molecular and Purkinje layers, NP185 distribution closely adheres to synaptic distribution in the internal granular layer.

These findings all suggest a synaptic distribution of NP185, even in the immature and transient synapses of developing neural tissue.

Granule cells arise from the external granular layer and migrate through the mantle to reside in what will become the internal granular layer (Fults *et al.*, 1985). Figure 25 captures an immature granule cell (arrow) during this migration.

**Figure 25**. Migrating granule cell, labelled for NP185.

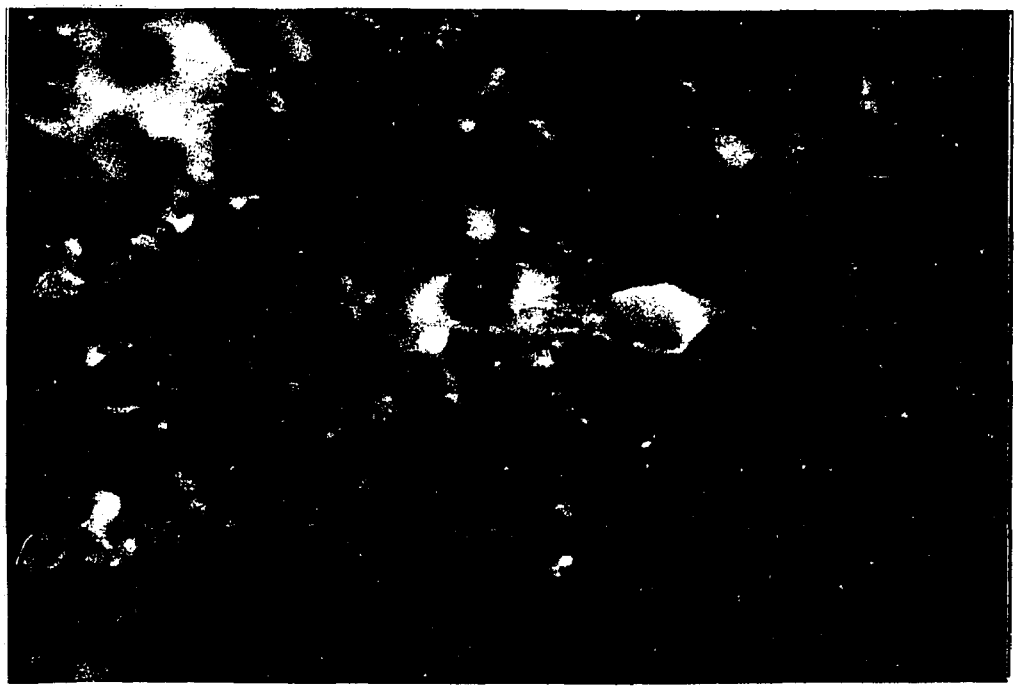

NP185 distribution, E15 chick embryo cerebellum, 320X. **Arrow**: migrating granule cell, medially directed; trailing axon (parallel fiber) with studded labelling (**arrowhead**); **G**: glomerulus.

As granule cells migrate, they assume a spindle shape, and leave trailing axons that eventually become the parallel fibers of the molecular layer (Quesada and Genis-Galvez, 1983; Altman, 1972a). In Figure 25, page 79, both of these characteristics are well visualized by the NP185 label. The migrating granule cell is followed by its axon, which is decorated with punctate fluorescence (arrowhead), imparting a beads-on-a-string appearance. The fusiform granule cell body is wider at the axonal base, which is characteristic of this cell (Mugnaini and Forstrønen, 1967). As soon as granule cells enter the matrix of the mantle layer, they initiate dendritic development (Quesada and Genis-Galvez, 1983), and establish axo-dendritic synapses with immature Purkinje cells (Landis, 1987; Kim, 1975; Miale and Sidman, 1961). With this in mind, the appearance of NP185 around the migrating granule cell body and immature parallel fiber in Figure 25, page 79 is significant, and again suggests a synaptic distribution of this protein.

**2. NP185 distribution in mature cerebellum**

A low magnification photomicrograph gives a multilayered view of NP185 distribution in the cerebellar cortex at maturity (Figure 26).

**Figure 26**. NP185 distribution in mature cerebellar cortex.

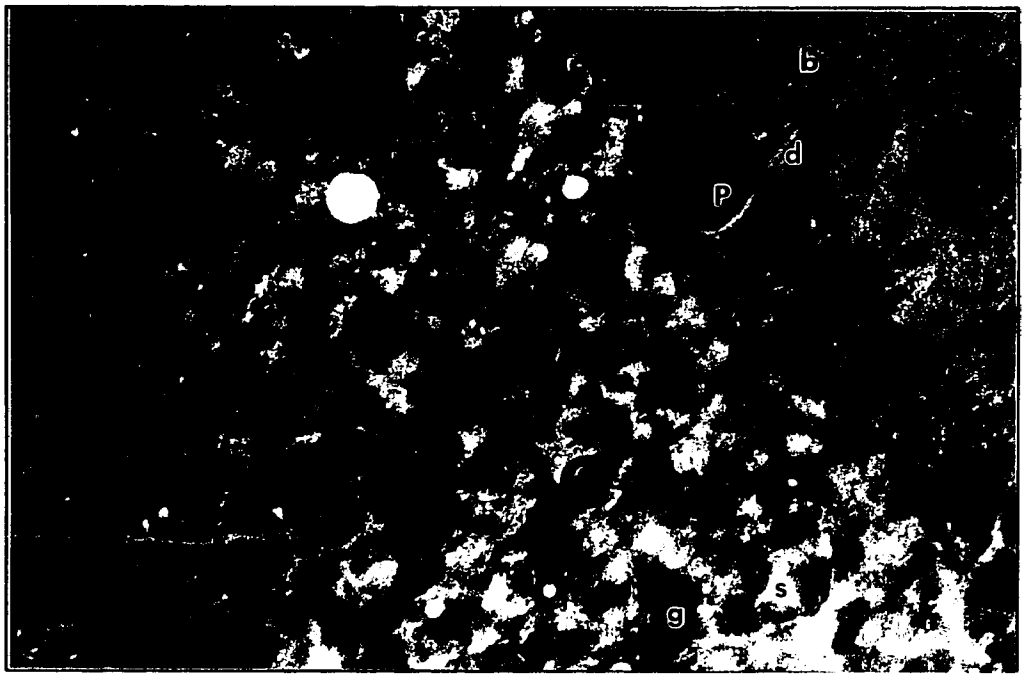


Immunofluorescent labelling of NP185, adult mouse cerebellum, 128X. **M**: molecular layer; **b**: basket cell; **P**: Purkinje cell; **d**: dendritic trunk; **G**: granular layer; **g**: glomerulus; **S**: mossy fiber synaptic bag.

In keeping with its high synaptic density, the molecular layer is densely labelled for NP185. The labelling in this layer is uniform, with the exception of dark holes (one of which is identified by **b**) that represent basket cell somata (Obata and Fujita, 1984), and perhaps a fortuitous cross-section of a dendritic trunk traversing out of plane. Turning back to Figure 23, page 73, it can be seen that the NP185 label in the nascent molecular layer is composed of innumerable fluorescent grains. In the mature, synapse-dense molecular layer (Figure 26, page 81), this grainy labelling is so extensive that it almost gives a pointillistic illusion of a solid, continuous stain.

In order to map the synaptic distribution in chick cerebellum, Howe *et al.* (1977) generated antisera against subcellular fractions enriched in synaptic vesicles and synaptic plasma membrane. Their immunofluorescent data are in excellent agreement with the distribution of NP185 reported here. In their study, the molecular layer is intensely labelled with dense, grainy fluorescence. This pattern is characteristic of synaptic labelling, as reported in other investigations of synapse-specific proteins (Leclerc *et al.*, 1989; Cambray-Deakin *et al.*, 1987; Wiedenmann and Franke, 1985; de Camilli *et al.*, 1983).

The Purkinje layer has discrete, perimembranous staining around the Purkinje cell bodies (P) and dendritic trunks (D). Gone is the areolate pattern seen at E15

(Figure 24, page 75). This is because the transient perisomatic processes, which are so abundant in synaptogenesis, have all retracted. The mature Purkinje cell body is left with axo-somatic synapses provided by basket cell axons (Uchizono, 1969). These connections are less numerous and more spatially confined. This transformation is demonstrated in two Purkinje cells shown in closeup in Figure 27.

**Figure 27.** Perimembranous labelling of Purkinje cells for NP185.

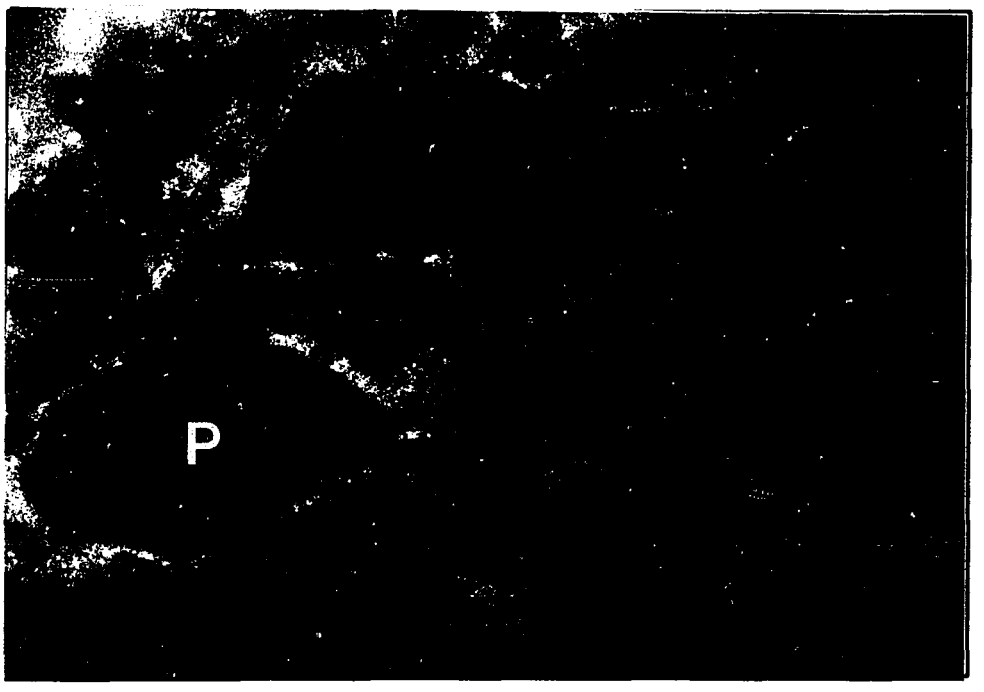


NP185 localization, Purkinje cells, adult mouse cerebellum, 320X. **P**: Purkinje cell soma; perimembranous labelling with occasional punctate concentration (**arrow**).

The discrete localization of NP185 at the perimembranous region of the Purkinje cell body is well displayed in this figure. The Purkinje cell cytoplasm is entirely unlabelled. Punctate concentrations (arrow) of fluorescent label may signify sites of axo-somatic synapses that happen to be precisely in the focal plane. An identical label pattern for the Purkinje cell was observed by Howe *et al.* (1977) in their synaptic mapping study of the cerebellum. Further corroboration of the synaptic nature of this labelling pattern is provided by others: Baumert *et al.* mapped the distribution of neuronal membrane protein p29, and compared its distribution to that of the synapse-specific, integral protein synaptophysin (1990). The somata of brain stem neurons, known to have well established axo-somatic synapses, were labelled in a pattern identical to that seen in Figure 27. In a study of cerebellar pathology, Goto *et al.* observed the distribution of synaptophysin in the normal cerebellum, including Purkinje cells (1989). Their findings on synaptophysin labelling of the Purkinje cell body are identical to the above findings. De Camilli *et al.* examined the general distribution of synapsin I in rat cerebellum, with identical findings as above (1983).

Figure 26, page 81, also provides a good perspective of the granular layer. This layer is referred to *in ovo* as the internal granular layer, to distinguish it from its

germinal namesake, the external granular layer, which disappears shortly after hatching. Once established by the protoglomeruli, the overall synaptic architecture (at the tissue level) in the granular layer remains in a reticular, or net-like, formation. Dark, unlabelled glomeruli (g) reside next to bright, intensely labelled mossy fiber synaptic bags (S). Figure 28 shows glomeruli at high magnification.

**Figure 28**. Glomerular distribution of NP185.

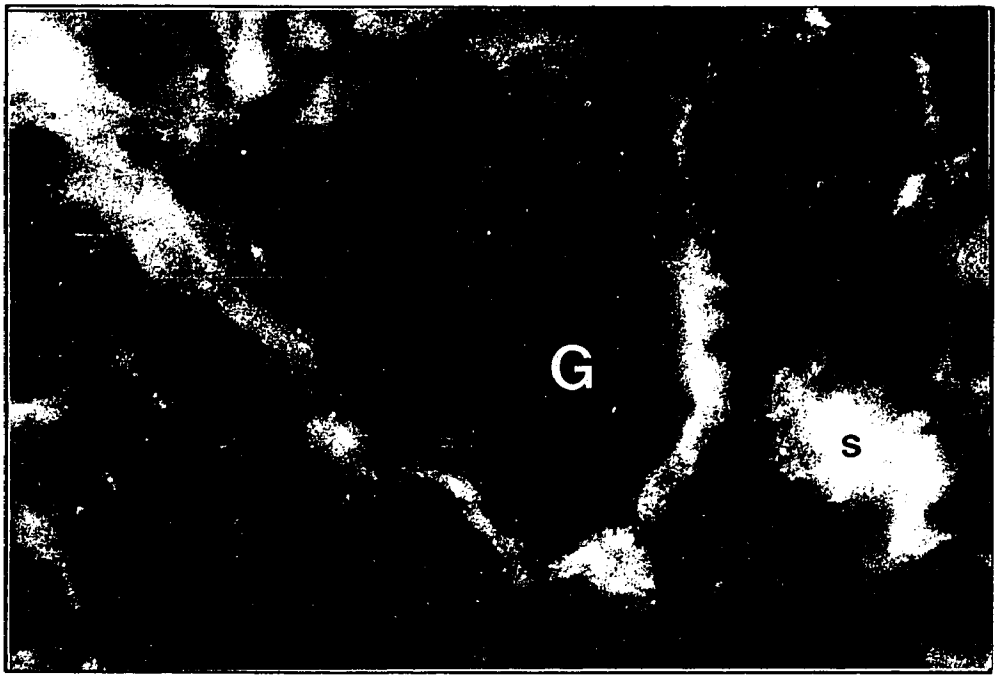


Immunolabelling for NP185, adult mouse cerebellum, granular layer, 320X. **G**: glomerulus; **S**: synaptic bag of mossy fiber.

A glomerulus (G) is outlined with immunofluorescent label. This is the vicinity of synapsis between Golgi cell axons, mossy fibers, and granule cell dendrites (Jacobson, 1978). A mossy fiber synaptic bag (S), is intensely labelled for NP185.

As in the molecular and Purkinje layers, this label pattern is identical to that reported by Howe *et al.* (1977).

In summary, NP185 expression *in embryo* conforms with synaptogenesis, including the appearance of transient protosynapses. The localization of NP185 waxes with early synaptic proliferation, and wanes with synaptic retrenchment, as seen in developing Purkinje cells. In mature cerebellum, NP185 distributes according to established synaptic organization. Conversely, NP185 is not found in those places where synapses do not exist. For example, NP185 is not present in neuronal somata, even those of Purkinje cells, in which the cytoplasm is easily visualized. These findings strongly suggest that NP185 is synapse-specific.

**3. Comparative distributions of neuronal proteins**

To confirm that NP185 is confined to the synapse, I compared its distribution with that of two neuronal proteins, synaptophysin and NF68. In neurons, synaptophysin is synapse-specific (Wiedenmann and Franke, 1985); NF68 is predominantly axonal (Liem *et al.*, 1978).

a. Synaptophysin

Synaptophysin is an integral protein (Jahn *et al.*, 1985) found in presynaptic membrane (Wiedenmann and Franke, 1985). It is also found in the neuromuscular junction (Torri-Tarelli *et al.*, 1990). It is a hexamer that is very similar to other channel-forming proteins (Thomas *et al.*, 1988). It has four transmembrane domains (Südhof *et al.*, 1987), and binds to calcium (Burgoyne, 1990). It probably plays a central role in membrane retrieval (Valtorta *et al.*, 1989).

Synaptophysin has been used by others as a comparative synaptic marker when mapping the distribution of other proteins (Cabalka *et al.*, 1990; Goto *et al.*, 1989; Reynolds and Wilkin, 1988). Synaptophysin expression correlates well with synaptogenesis (Knaus *et al.*, 1986). All of these features makes synaptophysin a useful comparative marker in the present study.

The monoclonal antibody SY38 does not cross-react with chicken brain or chick embryo. Therefore a comparative study of synaptophysin distribution with NP185 distribution was limited to adult murine brain. The cerebella of the chicken and mouse agree very well in cytoarchitecture and neurogenesis (Fujita, 1969), although much of the maturation of the murine cerebellum occurs postnatally.

Figure 29 shows the distribution of immunoreactivity for synaptophysin in adult mouse cerebellum.

**Figure 29.** Synaptophysin distribution in murine cerebellum.

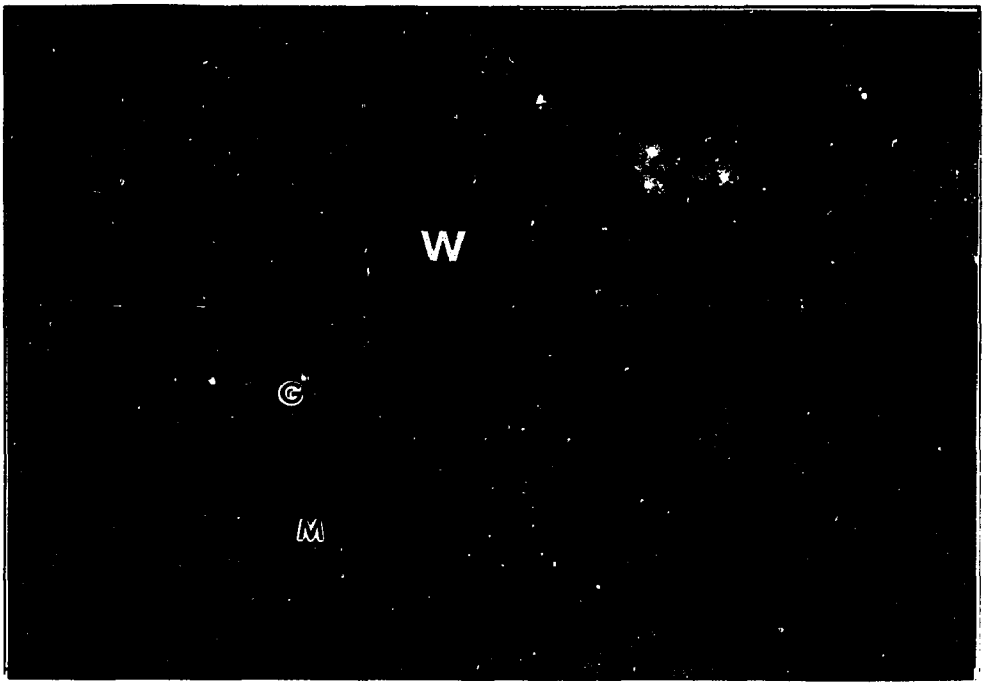


Adult mouse cerebellum, 32X. **W**: white matter; **G**: granular layer; **M**: molecular layer.

The distribution pattern seen here is identical with that reported by others (Leclerc *et al.*, 1989; Goto *et al.*, 1989; Reynolds and Wilkin, 1988). The molecular layer is intensely labelled in a dense, continuous arrangement, consistent with the high density of parallel fiber-Purkinje cell dendrite synapses. The granular layer has a flocculent pattern of immunoreactivity, which reflects the tufted formation of the synaptic glomeruli. The white matter, which essentially is a large bundle of axons, is completely negative for stain. Figure 30 provides a more magnified view of the labelling patterns in the different cerebellar layers.

**Figure 30.** Differential distribution of synaptophysin.

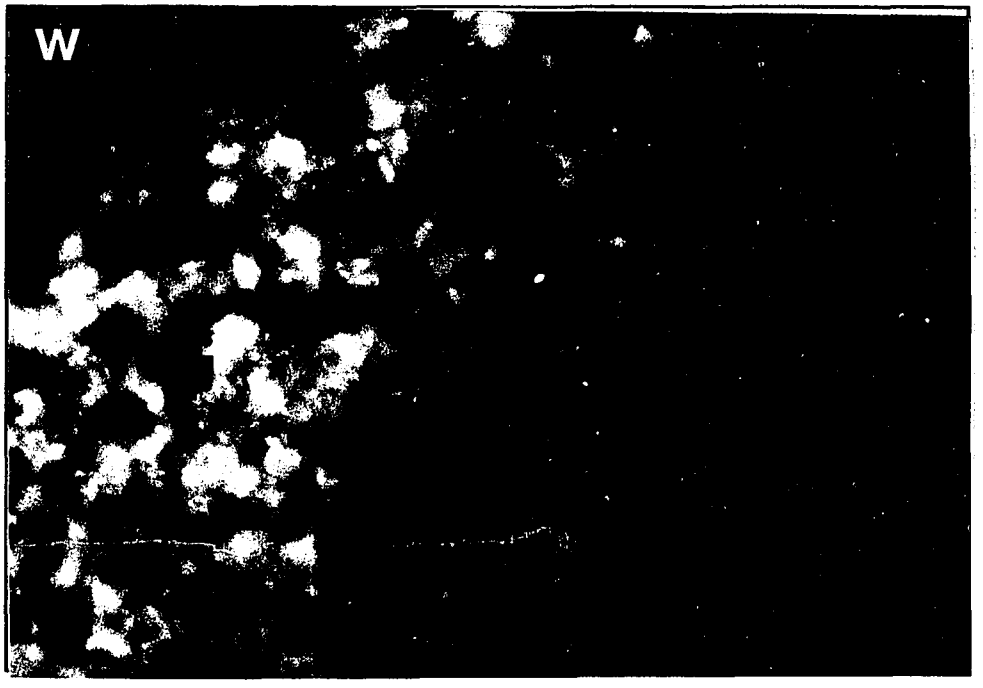


Immunolabelling of synaptophysin, adult mouse cerebellum, 80X. **M**: molecular layer; **G**: granular layer; **W**: white matter.

At the higher magnification seen in this figure, the reticular labelling pattern in the granular layer is more apparent. The label in the molecular layer is dense and grainy. The distribution of NP185 is virtually the same, as can be seen by comparing this figure with Figure 26, page 81.

The distribution of synaptophysin, known to be synapse-specific in the cerebellum, agrees with the distribution of NP185. This supports the argument that NP185 is localized to synapses.

b. Neurofilament NF68

Neurofilaments are a class of intermediate filaments that are neuron-specific (Romand *et al.*, 1988). They comprise a triplet of proteins with molecular weights of 68, 160, and 200 kD (Liem *et al.*, 1978). They are distributed in most neurons of the central nervous system (Trojanowski *et al.*, 1986), primarily in axons (Hoffman and Lasek, 1975). As such, they are useful neuronal markers (Luthman *et al.*, 1988; Osborn, 1983), especially for axonal histochemistry (Hoffman and Cleveland, 1988). The 68 kD neurofilament (NF68) undergoes self-assembly and participates in the organization of the axonal cytoskeleton (Geisler and Weber, 1981). I chose this protein as a nonsynaptic neuronal marker.

I examined chick embryos beginning with embryonic day E2. Although Tapscott *et al.* reported that neurofilaments

are expressed in the chick embryo as early as E3 (1981), I did not detect expression of NF68 in the cerebellar plate until E6. This is the period during which the external granular layer and mantle are forming (Fujita, 1969). This is also when nascent Purkinje cells arise from neuroblasts in the ventricular (ependymal) layer (Miale and Sidman, 1961).

In the E6 embryo, immunolabelling for NF68 appears as a ring surrounding the outer border of the ependyma around the fourth ventricle. This is shown in Figure 31.

**Figure 31**. Earliest expression of NF68.

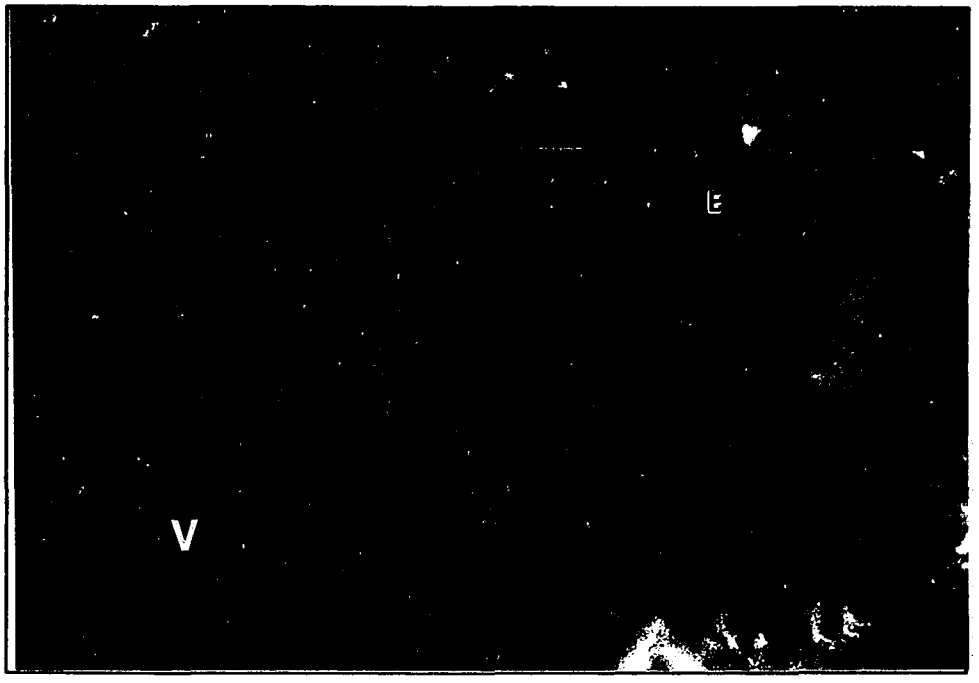


Immunolabelling for NF68, ependymal layer, E6 chick embryo, 80X. **V**: fourth ventricle; **E**: ependyma. The outer perimeter of the ependymal layer is labelled for NF68.

By E7, the distribution is more extensive, covering more than half of the ependymal layer (Figure 32).

**Figure 32.** Distribution of NF68 in E7 embryo.

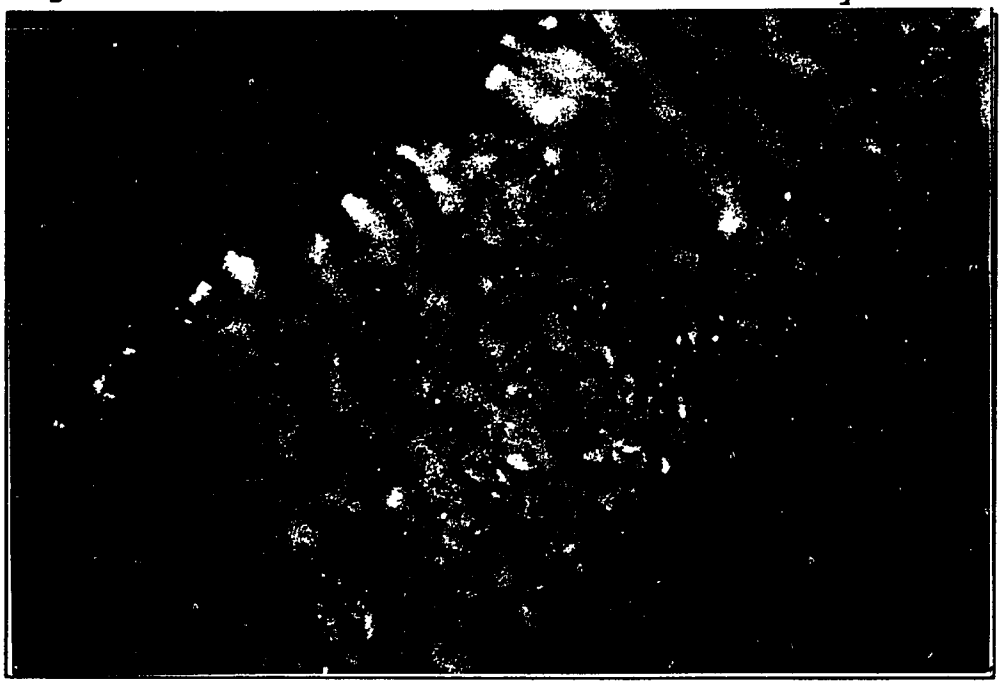

NF68 distribution in ependymal layer, E7 chick embryo, 128X. Labelled area covers outer half of ependyma, organized into parallel bands.

The organization has increased; the labelled area is comprised of an array of parallel bands. (These bands are not to be confused with the thin, distinct radial fibers discussed in section III.B.4., page 110.)

In contrast to these findings, NP185 does not appear until E10. The ependyma, like the external granular layer, remains negative for NP185.

By E18, NF68 is concentrated in the cytoplasm and axons of Purkinje cells (Figure 33).

**Figure 33**. Labelling of Purkinje cells for NF68.

E18 chick embryo, Purkinje layer, 80X. **Arrow**: nucleus of Purkinje cell; **arrowhead**: axon of Purkinje cell. Both the cytoplasm and axons of Purkinje cells are positive for NP185; the nuclei are negative.

Here NF68 is found exclusively in the Purkinje cells. The cytoplasm is strongly labelled, allowing visualization of the dendritic hillock up to the first bifurcation. The nucleus (arrow) is unlabelled, and stands out in strong contrast to the perikaryal stain. The axon (arrowhead) is well labelled. The axons can be easily seen projecting all the way to the white matter (not shown in Figure 33).

At higher magnification, the perikaryal stain is seen to be punctate and concentrated in a region corresponding to the endoplasmic reticulum (Figure 34).

**Figure 34**. Perikaryal labelling of NF68.

Purkinje cells, cerebellum, E19 chick embryo, 320X.
**Arrow**: punctate labelling around nucleus.

This finding exactly agrees with that of Langley *et al.* (1988), who confirmed this subcellular distribution by electron microscopy. They noted that in the cytoplasm, the neurofilaments remain in a granular, nonfilamentous form. The perikaryal concentration of granular neurofilaments is transient, and disappears by maturity (Bignami *et al.*, 1985). It probably reflects intense production for axonal expansion (Sinicropi and McIlwain, 1983).

At this stage of cerebellar development, the differences in distribution between NF68 and NP185 are marked. NP185 is extensively distributed throughout the cerebellar cortex in a grainy or flocculent pattern. It never is seen in any filamentous type of distribution. In contrast, at E18-E19, NF68 is exclusively confined to the cytoplasm and axons of Purkinje cells, as well as axons of other neurons. This is the expected distribution of an axonal, nonsynaptic neuronal protein.

In the immature Purkinje cell, such as the E15 Purkinje cell seen in Figure 24, page 75, some cytoplasmic staining for NP185 is apparent. This can signify the buildup phase of NP185 production, analogous to that speculated for NF68. Yet more significant is the much more intense areolate staining <u>outside</u> of the Purkinje cell body, where early synaptogenesis is taking place. This pattern is never seen with NF68.

A remarkable shift in NF68 distribution occurs by the time Purkinje cells reach maturity: The Purkinje cells become entirely negative for NF68; concomitantly, basket cell axons become intensely labelled for NF68, and remain so throughout maturity. Basket cell axons are readily identified by their distribution. They run along the Purkinje/molecular layer border, perpendicular to the longitudinal axis of the Purkinje cells (Altman, 1972a). These axons then descend into the Purkinje layer to embrace the Purkinje cell body by forming their characteristic basket of pinceaux (Langley *et al.*, 1988; Uchizono, 1969). An example of this basket arrangement is given in Figure 35.

**Figure 35.** NF68 distribution in mature cerebellum.

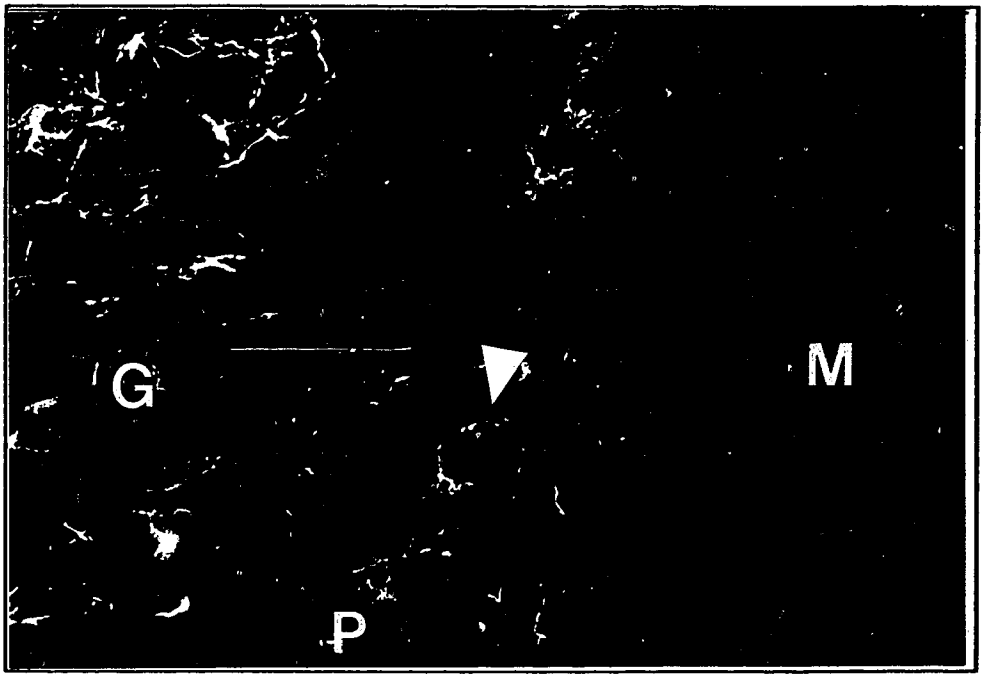


Immunolabelling for NF68, adult chicken, cerebellar cortex, 80X. **M**: molecular layer; **P**: Purkinje layer; **G**: granular layer; **arrow**: Purkinje cell. Unlabelled Purkinje cells are surrounded by labelled basket cell axons.

Here the Purkinje cells are completely unlabelled. Their presence is only indicated by the highly stained baskets which surround them. This result is identical to that published by Sternberger *et al.* (1982) and McKay and Hockfield (1982). These baskets are of course formed by the axons of their namesakes. The filamentous labelling seen in the granular layer probably represents axons of mossy fibers and Purkinje cells (Langley *et al.*, 1988). Figure 36 gives a closeup of the Purkinje layer.

**Figure 36**. NF68 distribution in the mature Purkinje layer.


NF68 distribution in basket cell axons, Purkinje layer, adult chicken cerebellum, 128X. **P**: Purkinje cell. Labelled basket cell axons surround unlabelled Purkinje cells.

The labelling seen here is so different than that seen in Figure 33, page 99, that at first it is hard to imagine that the same monoclonal antibody has been used. In superficial appearance, NF68 seems to redistribute from the cytoplasm and axons of the Purkinje cells to the axons of basket cells. This startling change is best appreciated by comparing Figure 34, page 101, with Figure 37.

**Figure 37.** NF68 confinement to basket cell pinceau.


Adult chicken cerebellum, Purkinje layer, 320X. **P**: Purkinje cell; **arrow**: basket cell axon.

In this figure, an individual Purkinje cell is outlined by immunofluorescent pinceaux of basket cells. The Purkinje cell, which is so clearly labelled in Figure 34, appears absent!

This seemingly paradoxical result was first noticed by Bignami *et al.* (1985), who obtained exactly the same results presented here. They noted that the cytoplasm of the immature Purkinje cells, while immunochemically positive for neurofilament proteins, was devoid of actual filaments. From this they surmised that in the cytoplasm of these immature cells, the neurofilaments must reside in a nonpolymerized form. This "granular" form of neurofilament proteins probably represents the early synthesis of the nonpolymerized subunits, which are being produced in abundance to meet the needs of the growing cell. The subcellular localization of NF68 in the endoplasmic reticulum by Langley *et al.* (1988) supports this hypothesis.

The apparent redistribution of NF68 from the immature Purkinje cell to the mature basket cell axon is caused by the conversion of NF68 from its early, nonpolymerized form to its mature, polymerized state. In the immature neuron, the neurofilaments are rapidly expressed and processed within the cell body; as the cell matures, the proteins are transported to their natural destination away from the cell body, where they are concentrated. This redistribution is probably regulated by phosphorylation (Langley,

1988). Viewed in this light, it is not surprising to observe NF68 leaving the cytoplasm of one cell even as it collects in the axon of a different cell, if both cells are undergoing maturation. This is the case for the basket and Purkinje cells.

As a further comparison of the distributions of NP185 and NF68 in the mature Purkinje layer, Figure 27 (page 84) may be contrasted with Figure 36. The basket cell axons make synaptic connections to the Purkinje cell somata (Landis and Reese, 1974), although not as extensively as in immaturity. The axonal pattern of distribution in Figure 36 is entirely different than that seen in Figure 27, which has no filamentous label. NP185 stain is limited to the membrane region of the Purkinje cell; NF68 stain loosely surrounds the cell. The punctate labelling around the Purkinje cell, seen with NP185 stain, is absent with NF68 stain. These results further confirm the synaptic--as opposed to axonal--distribution of NP185.

**4. Comparative distributions of nonneuronal proteins**

To determine whether NP185 is truly neuron-specific, as opposed to nervous tissue-specific, I mapped the distribution of two intermediate filaments, glial fibrillary acidic protein (GFAP) and vimentin. In the cerebellum, both proteins are exclusively located in glial cells (Graeber *et al.*, 1988; Schiffer *et al.*, 1986). I compared the distributions of these proteins with that of NP185.

a. Glial fibrillary acidic protein

GFAP is an intermediate filament found in astrocytes (Pelc *et al.*, 1986; Bovolenta *et al.*, 1984). It is distributed in the granular, Purkinje, and molecular layers of the cerebellum (Ghandour *et al.*, 1980). As such, this protein is a good marker of cerebellar glial cells.

Chick embryo cerebella were examined from E8, which is the day of onset of glial differentiation in the avian cerebellum (Fujita, 1969). Expression of GFAP was first detected at E16, long after initial glial differentiation. The late onset of GFAP expression relative to glial development in the mouse was reported by Schnitzer *et al.* in 1981.

The distribution of immunofluorescent labelling shown in Figure 38 gives an example of the labelling pattern in the molecular layer.

**Figure 38**. Immunolabelling for GFAP.

GFAP localization, molecular layer, E17 chick embryo cerebellum, 457X. Bergmann fibers are exclusively labelled.

The Bergmann glia are strongly and exclusively labelled. This finding is identical published results (Wilkin and Levi, 1986; Sommer *et al.*, 1981; Bignami and Dahl, 1973). Bergmann glia are readily identified by their linear, parallel organization in the molecular layer, sometimes referred to as palisade architecture (de Blas, 1984). The fibers of the Bergmann glia radiate--hence their common name, the radial fibers--out towards the pial surface of the cerebellar cortex. During migration, the granule cell is in direct contact with these fibers (Burgoyne and Cambray-Deakin, 1988). These glial processes serve as guiding pathways for medial migration of the nascent granule cell from the external granular layer to the internal granular layer (Grovas and O'Shea, 1984; Rakic, 1971). In Figure 38 (page 112) there is a complete absence of neuronal staining. The distribution of the immunofluorescent label in the molecular layer is entirely unlike that seen for NP185 (Figure 26, page 81).

b. Vimentin

Vimentin is an intermediate filament formed by cells of mesenchymal origin (Franke *et al.*, 1978), including microglia (Graeber *et al.*, 1988). It is also found in astrocytes and ependymal cells (Schnitzer *et al.*, 1981). Like GFAP, it is a useful marker of non-neuronal cells in the cerebellum.

Chick embryo brains were examined from E2 (the cerebellar plate from E4) up through hatching. Vimentin expression is first detected in the cerebellum at E7. The expression of this glial protein precedes that of GFAP by 9 embryonic days, a considerable span in the 21-day developmental period of the chick embryo. This marked difference in onset between vimentin and GFAP was noted by Schnitzer *et al.* (1981).

In the cerebellar cortex, labelling occurred exclusively in the radial fibers of the Bergmann glia in the molecular layer. At earliest expression, E7, these fibers were short, sparse, unaligned, and deep within the mantle. By E10, these fibers had established their terminal pods at the pial surface. The fibers were still sparse, but more aligned. By E16, the day of onset of GFAP expression, the radial fibers were well aligned in an orderly array--the palisade arrangement of de Blas (1984). An example is given in Figure 39.

**Figure 39.** Localization of vimentin in Bergmann glial fibers.

Labelling for vimentin, E16 chick embryo cerebellum, molecular layer. **Arrow**: terminal foot of radial fiber at pial surface. Parallel lines are individual fibers of Bergmann glia.

Although the expression of GFAP lagged behind that of vimentin by 9 embryonic days, once they both are expressed, the distributions of these proteins are identical in Bergmann fibers. Others noted this in previous comparative studies (Bovolenta *et al.*, 1984; Schnitzer *et al.*, 1981). As was seen with GFAP distribution presented in section III.B.4.a, page 111, the labelling was non-neuronal, and followed a distribution entirely different than that of NP185.

To summarize, the labelling patterns of the non-neuronal proteins GFAP and vimentin are entirely different than that of NP185. This is true throughout all developmental stages after the proteins first appear. Vimentin is earliest in expression, commencing at E7; NP185 follows next at E10; GFAP is last at E16. NP185 does not co-distribute with either glial protein, which are reliable markers for non-neuronal cerebellar cells (Schnitzer, 1981). This evidence strongly suggests that NP185 is neuron-specific.

**5. Localization of NP185 in the neuromuscular junction**

Based on the above findings, which strongly suggest that NP185 is synapse-specific, it seemed reasonable to look for NP185 in a peripheral synapse. If NP185 is synapse-specific, one could predict that it is also localized in the neuromuscular junction. From the earliest days of coated vesicle research, CVs were observed in the

neuromuscular junction (Heuser and Reese, 1973). Clathrin-coated plaques (0.5–1 μm), pits (0.1–0.15 μm), and vesicles are all found in neuromuscular junctions, even embryonic ones (Bloch and Pumplin, 1988). Coated pits and vesicles participate in membrane insertion and removal of acetylcholine receptors. Bursztajn demonstrated that coated vesicles internalize acetylcholine receptors (Bursztajn and Fischbach, 1984), and are involved in AchR transport (Bursztajn *et al.*, 1987). These observations make it appropriate to look for NP185 in the neuromuscular junction.

a. Establishing NP185 localization

The immunolabelling shown in Figure 40 establishes the presence of NP185 in chicken skeletal muscle.

**Figure 40.** Presence of NP185 in chicken skeletal muscle.

Immunofluorescent labelling of NP185. Longitudinal section, neck skeletal muscle, P34 chicken, 672X. NP185 is localized in a discrete region, with punctate concentrations.

The distribution of NP185 is confined to an area 60 μm diameter, with distinct concentrated points. This distribution pattern is consistent with the morphology of the neuromuscular junction (Purves and Lichtman, 1985). The motor nerve terminal is often referred to as a single synapse, but in fact it is a collection of many synaptic boutons. The boutons are polymorphic sacs that extend into the complementary troughs of the postsynaptic endplate (Carry and Morita, 1984). The general arrangement is illustrated in Figure 41.

**Figure 41.** Gross morphology of neuromuscular junction.

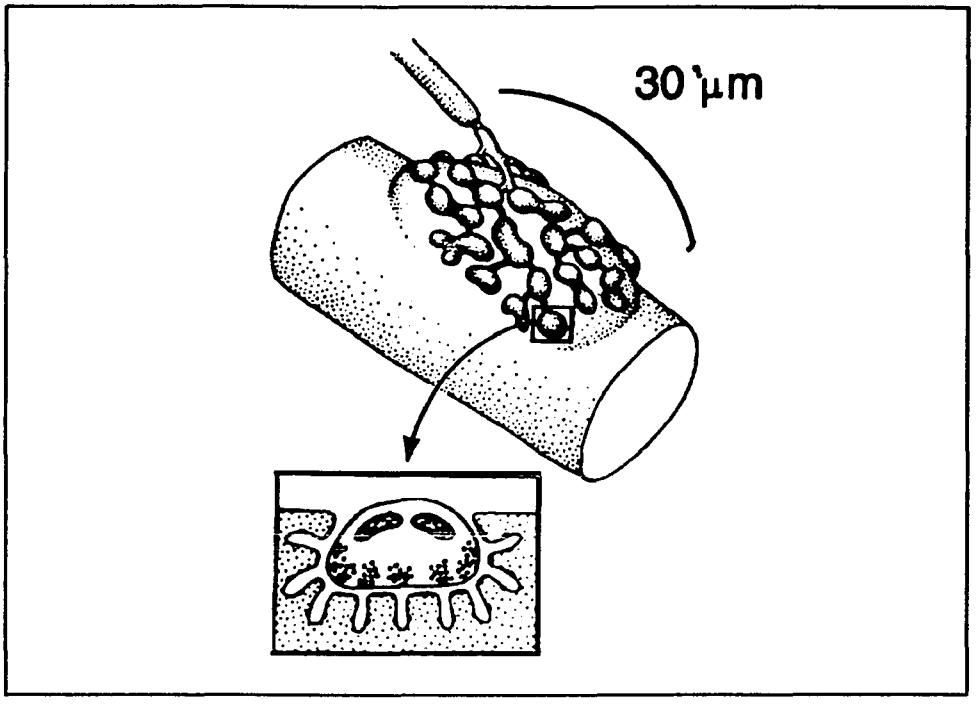


Stylized drawing of a muscle fiber with a single neuromuscular junction. Terminal boutons ramify over the muscle fiber surface. **Closeup**: cross-section of a single terminal bouton, with its apposite postsynaptic endplate. (Adapted from Purves and Lichtman, 1985.)

The saccular structure of the terminal bouton constitutes a pocket; the presynaptic material is localized in these pockets and cannot be evenly distributed over the general area associated with the neuromuscular junction (Scott *et al.*, 1988). In immunohistochemical tagging of a presynaptic protein, this limitation is manifested as an archipelago of irregular immunolabelling when the neuromuscular junction is viewed from above. This is exactly what is seen in Figure 40, page 118, and in Figure 42.

**Figure 42**. Localization of NP185 in chick skeletal muscle.

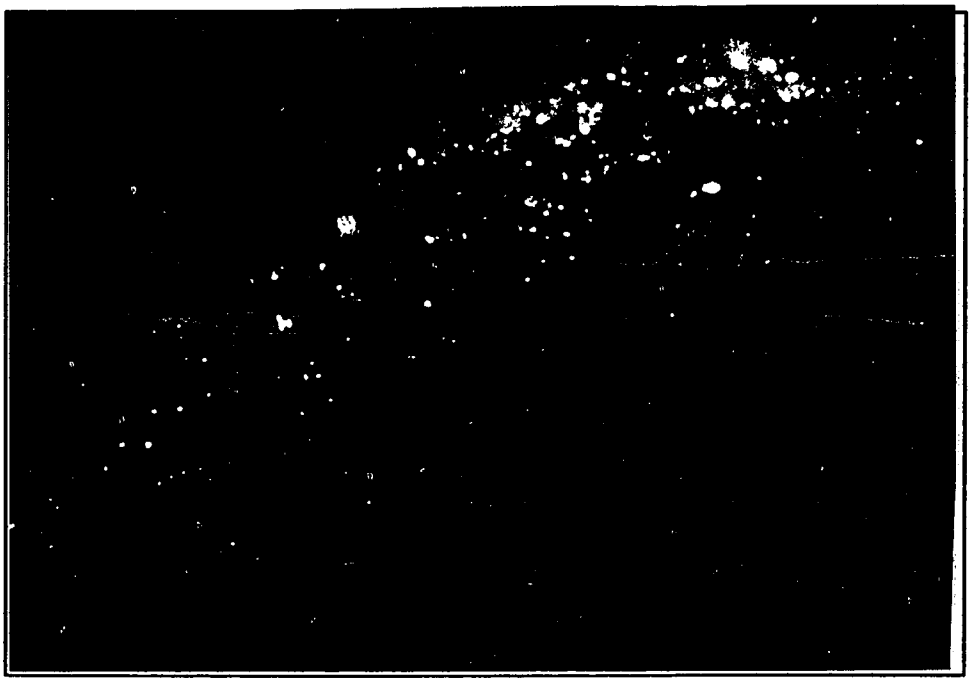

Longitudinal section, neck skeletal muscle, P34 chicken, 320X. NP185 is localized to discrete points within a limited region, creating an immuno-fluorescent archipelago. **Arrow**: short queue of speckles.

In Figure 42, the labelled area follows the longitudinal axis of the underlying muscle fiber (not apparent in this photomicrograph). The speckled labelling is very loosely organized, occasionally following a short linear array (**arrow**), and having highest concentration in a centralized region.

The organization of the fluorescent points varied. Often the speckles were seemingly randomly distributed within the labelled area, as seen in Figure 40, page 118. The speckles were sometimes queued, as shown in Figure 42. Figure 43, gives a more magnified view of NP185 localization in skeletal muscle.

**Figure 43**. Close-up of NP185 localization.

Immunolabelling of NP185, longitudinal section, neck skeletal muscle, P28 chicken, 457X. Speckling occasionally seems to follow a curvilinear array (**arrow**).

The punctate labelling is well distributed over the labelled region. The points occasionally seem to form small constellations of curves or loops (**arrow**). This looping is reminiscent of the endplate visualized by Gunther and Letinsky using zinc-iodide/osmium tetroxide staining (1982), but there is no evidence that this pattern reflects underlying structure.

When the skeletal muscle was viewed in cross-section, labelling of NP185 occurred along the muscle fiber perimeter. An example is shown in Figure 44.

**Figure 44**. NP185 distribution in muscle cross-section.

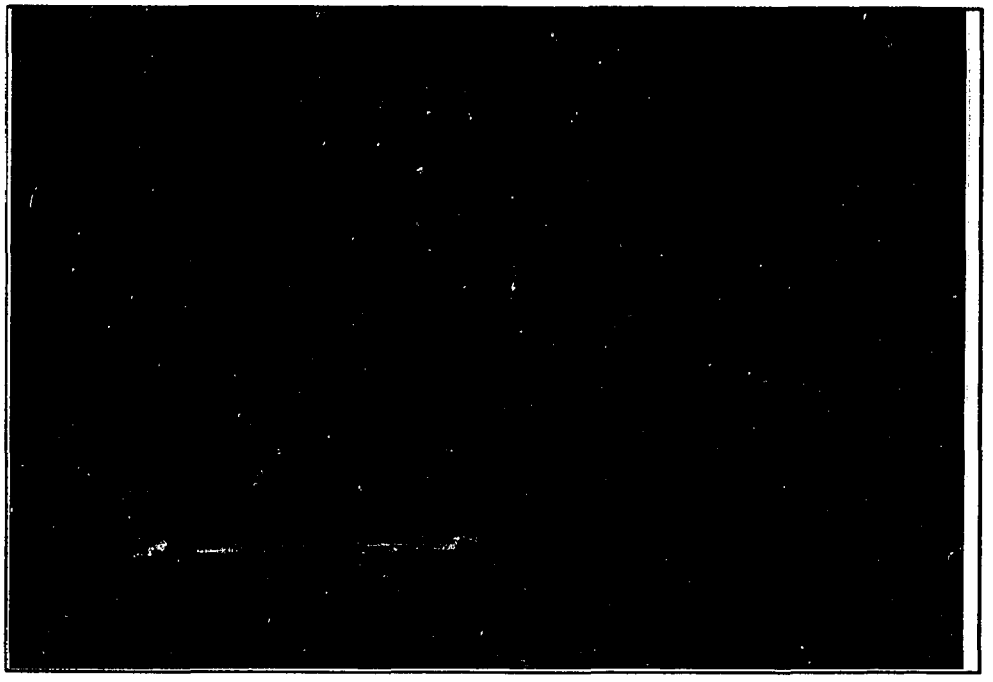

Cross-section, neck skeletal muscle, P28 chicken, 320X. The label runs along the perimeter of a muscle fiber.

Note that the label is continuous, not punctate. The absence of punctation is likely when the neuromuscular junction is viewed laterally, rather than from above. The label configuration seen here is identical to published results of neuromuscular junction labelling taken in cross-section (Fontaine *et al.*, 1988; Bender *et al.*, 1976).

Occasionally the NP185 label was laid out in linear fashion, which seemed to follow the linear arrangement of the neuromuscular junction more commonly seen in Amphibia (Silver, 1963; Figure 45).

**Figure 45.** Linear labelling for NP185 in neuromuscular junction.

Longitudinal section, pectoral muscle, P34 chicken, 320X. Linear array of immunofluorescent label for NP185.

These figures represent typical labelling patterns when present. The incidence of positive labelling is presented in Table IV.

**Table IV**. Incidence of positive label of NP185 in the neuromuscular junction.

| Experiment | Sections | Total Area* $mm^2$ | Positive Labels‡ | Label/$mm^2$ |
|---|---|---|---|---|
| 9/24/90 | 3 | 54 | 2 | 0.037 |
| 10/2/90 | 6 | 120 | 9 | 0.075 |
| 10/5/90 | 6 | 102 | 8 | 0.078 |

* Summed trapezoidal approximations; ‡ fluorescence. *Label/$mm^2$* reflects the efficiency of labelling for NP185.

The dimensions of these labelled areas agree with the findings of others who visualized the avian neuromuscular junction by histochemical methods (Scott *et al.*, 1988; Silver, 1963; Cole, 1955).

b. Double-labelling of NP185 and AchR

The above results confirm the presence of NP185 in skeletal muscle tissue, and suggest that NP185 is sequestered in a particular region of the muscle fiber. However, these results cannot establish *ipso facto* the localization of NP185 at the neuromuscular junction. For this reason, I carried out double-labelling experiments. To label the neuromuscular junction, I used a fluorescein conjugate of α-bungarotoxin (αBT-F). This snake venom derivative is known to bind selectively and irreversibly to acetylcholine receptors (AchR) in the postsynaptic endplate of the neuromuscular junction (Chang and Lee, 1963). It can bind to the receptors both intracellularly and on the cell surface (Bursztajn *et al.*, 1987). Rhodamine-conjugated IgG (IgG-R) was used as the probe for mAb 8G8.

Figure 46 gives an example of the double labelling of AchR and NP185.

**Figure 46**. Double label of AchR and NP185.

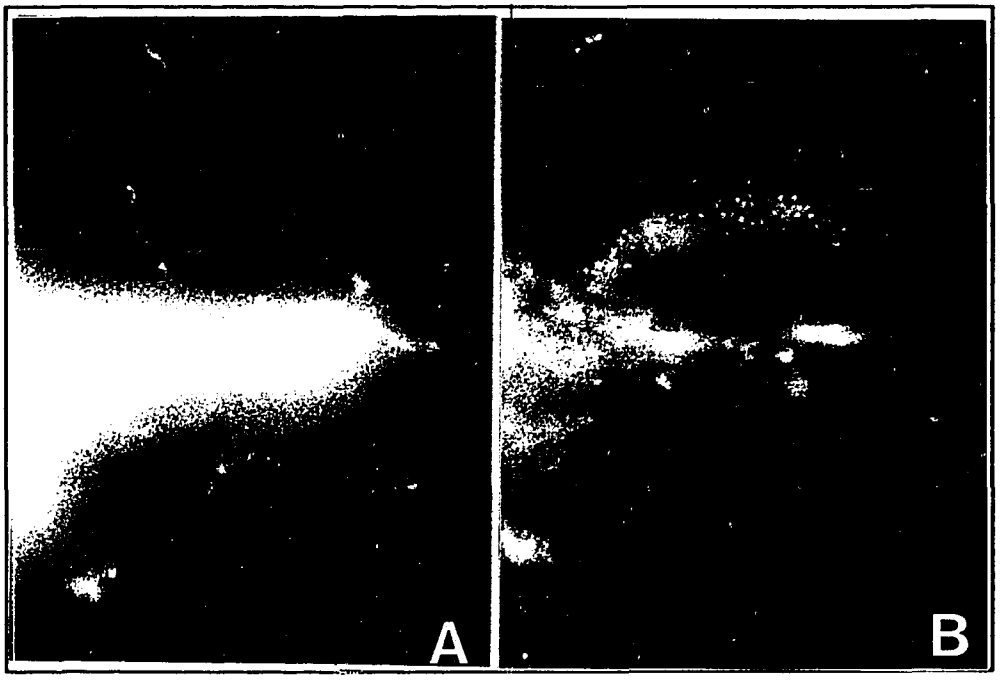


Longitudinal section, neck skeletal muscle, P49 chicken, 320X. **A**: labelling of AchR; **B**: labelling of NP185; **arrow** emphasizes speckling.

The fluorescent label for AchR is continuous; in contrast, the label for NP185 is punctate. This pattern is especially apparent in the area accented by the arrow. This area appears as a loop which does not correspond to the AchR label. Except for this region, the labelling is generally coextensive, with the NP185 label tending to be more discrete than continuous.

In Figure 47, we see another example of AchR and NP185 codistribution.

**Figure 47**. Codistribution of AchR and NP185.

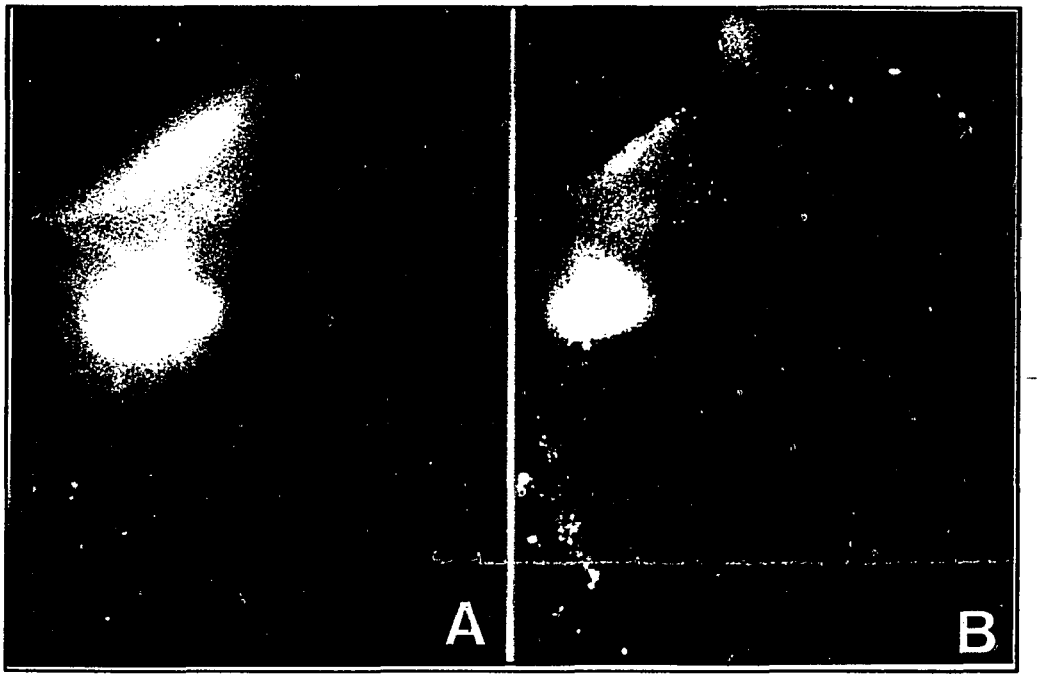


Labelling for AchR and NP185, neck skeletal muscle, P49 chicken, 320X. **A**: AchR distribution; **B**: NP185 distribution; **arrow**: speckling of label.

Once again, the label for NP185 is speckled (arrow).

There is also a speckled label for AchR, but not to the same degree as for NP185. In chick myotubes, AchRs are commonly aggregated in patches in the sarcolemma (Cohen and Pumplin, 1979). This pattern is readily visible under epifluorescent light microscopy. Clustering of AchR is induced by innervation (Bloch and Pumplin, 1988; Anderson *et al.*, 1977). This distribution is caused by cytoskeletal anchoring of the receptors (Pumplin and Bloch, 1987). In Figure 47, page 134, the AchR clusters seen in Panel A correspond point-for-point with the NP185 clusters seen in Panel B. However, as was always the case, NP185 has a much more punctate distribution, with many points that have no correspondence with any AchR clusters. Yet it is important to note that the labelling of NP185 is coextensive with the labelling of AchR, covering the same tissue area.

Figure 48 presents further evidence that NP185 is localized in the neuromuscular junction.

**Figure 48.** Co-localization of AchR and NP185 in a neuromuscular junction.

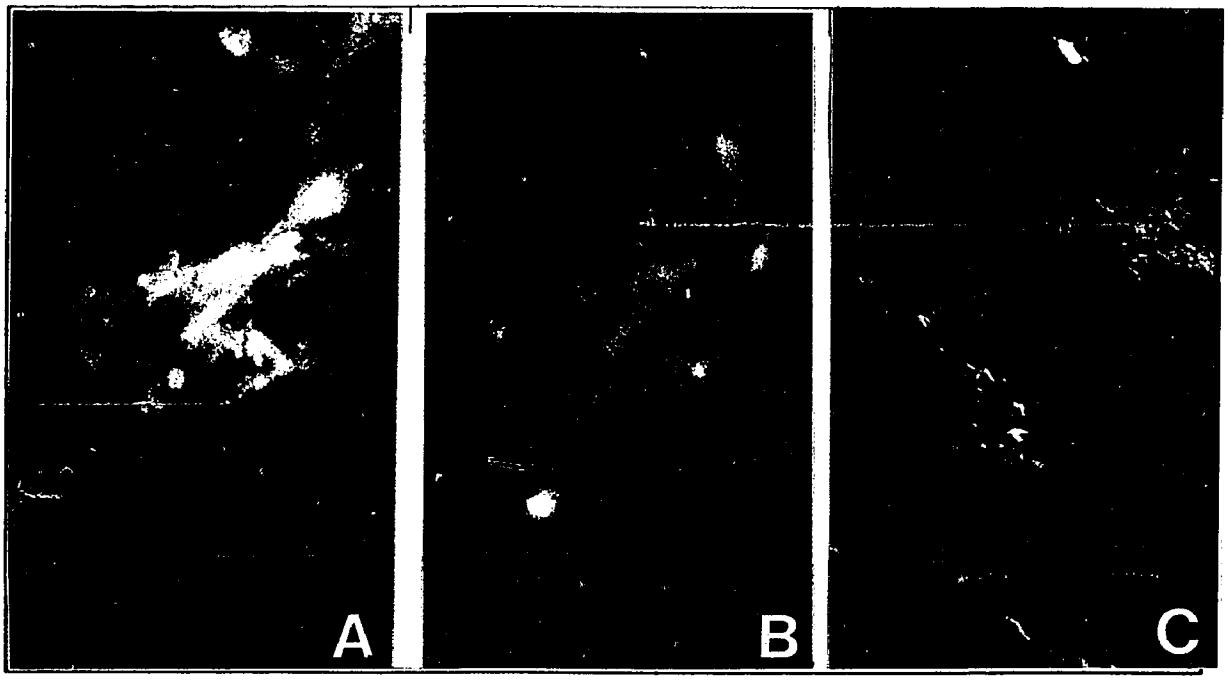


Longitudinal section, neck skeletal muscle, P54 chicken, 304X. **A**: Localization of AchR; **B**: localization of NP185; **C**: Nomarski image of underlying structure.

Here the distribution of AchR and NP185 is virtually identical. The labelled area is 50 μm across. In Panel C, Nomarski optics reveal a structure on the surface of a muscle fiber that has the characteristics of an avian neuromuscular junction. In fowl, the neuromuscular junction is broad and extends across the muscle fiber (Silver, 1963). Whole chicken muscle sections depict neuromuscular junctions traversing muscle fibers perpendicular to the fiber longitudinal axis, overlapping to such an extent that they appear continuous (Wenger and Wenger, 1978; Atsumi, 1971). (This overlapping appearance is not seen in most publications dealing with neuromuscular junction research, because these studies most often employ myotubes or individual muscle fibers, rarely whole tissue sections.) Each large junction deploys saccular terminal boutons, which are loosely arrayed and ramify over the surface of the muscle fiber (Cole, 1955). The Nomarski image of the neuromuscular junction in Panel C is in good agreement with Hoffman images published by Gunther and Letinsky (1982).

The incidence of labelling in these double-labelling experiments is summarized in Table V.

**Table V.** Incidence of double-labelling in the neuromuscular junction.

| Experiment | Sections | Total Area,* mm² | Positive,‡ AchR only | Positive, NP185 only | Positive, both | Colabel ratio§ |
|---|---|---|---|---|---|---|
| 10/9/90 | 12 | 288 | 21 | 0 | 5 | 0.19 |
| 10/18/90 | 6 | 32 | 6 | 1 | 2 | 0.22 |
| 10/19/90 | 6 | 60 | 7 | 1 | 2 | 0.20 |
| 10/23/90 | 12 | 96 | 14 | 0 | 6 | 0.30 |
| 11/13/90 | 6 | 192 | 3 | 0 | 1 | 0.25 |

* Summed trapezoidal approximations; ‡ fluorescence; § colabel ratio = both / (AchR + NP185 + both).

In all experiments, the incidence of AchR labelling is 3 to 5-fold greater than that of NP185 labelling. This may reflect the net binding efficiency of α-bungarotoxin relative to that of mAb 8G8. The net binding efficiency is influenced by such factors as intrinsic receptor-ligand affinity and epitope availability. This difference in labelling capacity is not surprising: *Bungarus multicinctus* depends on its venom to paralyze its prey. Therefore, α-bungarotoxin is designed by nature, as it were, to quickly and overwhelmingly bind with and deactivate AchR. This binding occurs with the receptors which are exposed at the membrane surface, but can also occur intracellularly (Bursztajn *et al.*, 1987). In contrast, mAb 8G8 must make its way into the cell to find an available epitope on NP185, which presumably is fixed *in situ* to its natural surroundings. In other words, the binding site of NP185 is inherently cryptic compared to the naturally exposed binding site of AchR.

On the other hand, when NP185 labelling <u>is</u> present, AchR colabelling occurs in almost every instance. Referring to Table V, of the 18 instances of positive NP185 label, all but 2 also had AchR colabel. This is a double-label "success rate" of 89%.

In summary, NP185 colocalizes with AchR in a distribution consistent with the dimensions and structure of neuromuscular junctions. Nomarski optics can visualize

neuromuscular junctions that are coextensive with these double-labels. The evidence clearly implies that NP185 is localized in the neuromuscular junction. Synaptophysin, which in the neuron is synapse-specific, has also been localized in the neuromuscular junction (Torri-Tarelli *et al.*, 1990). The localization of NP185 in the neuromuscular junction corroborates the conclusion, based on the findings presented in the previous sections, that NP185 is synapse-specific.

# IV. DISCUSSION

NP185 first becomes detectable in the avian cerebellum at E10, which corresponds to important neurogenic events:

1) Although early protosynapses are formed between E7 and E9, the first appearance of morphologically mature synapses in the cerebellar cortex occurs at E10 (Foelix and Oppenheim, 1974). These synapses are characterized by increased membrane thickening and a marked increase in synaptic vesicles.

2) Within the mantle, the nascent molecular and Purkinje layers begin to develop at this stage (Foelix and Oppenheim, 1974). There is abundant synaptogenesis in this region as the Purkinje cells migrate to their final position and climbing fibers establish synaptic contact with Purkinje cell bodies (Shimono *et al.*, 1976).

Purkinje cell development offers an example of the close association of NP185 expression with synaptic distribution. In maturity, only one climbing fiber contacts each Purkinje cell (Mariani and Changeux, 1981), but during early development of these neurons, each Purkinje cell body is in synaptic connection with many climbing fibers. These synapses subsequently undergo retrenchment. By maturity, one climbing fiber forms synapses with the dendrites of one Purkinje cell. The Purkinje cell body itself now only has minor axosomatic synapses with basket cell axons. The distribution

of NP185 in the Purkinje layer reflects these developmental changes: the early Purkinje cell soma, covered with terminal boutons of several climbing fibers, has an intense areolate label; the mature Purkinje cell soma has only a perimembranous label with a few punctate concentrations.

Coated vesicles play a pivotal role in synaptogenesis (Altman, 1971). They are concentrated at incipient synaptic sites, especially at future postsynaptic membranes. They may provide prospective synapses with the material necessary to form early adhesion plaques, through direct insertion of electron-dense membrane. Stelzner *et al.* (1973) found that coated vesicles congregated at newly formed synaptic junctions. This group postulated that coated vesicles could contribute to synapse formation by releasing adhesion mediators into the extracellular space (exocytosis), or alternatively, by incorporating recognition factors into the cell (endocytosis). Eckenhoff and Pysh (1979) found that coated vesicles internalize apposed membrane in neurons undergoing synaptogenesis. This internalization probably allows the transfer of morphogenetic material essential for early neurite growth and for later synaptic remodelling. Coated vesicles are also common in the developing neuromuscular junction (Bloch and Pumplin, 1988).

Coated vesicles are implicated in more than early synaptogenesis. They are a general feature of the postsynaptic membrane of mature synapses (Waxman and Pappas, 1969). Based

on their ubiquity, they are undoubtedly vital in maintaining mature synaptic function as well as forming new synaptic sites.

Given the close connection of coated vesicles and synapses, and the association of NP185 with CCVs, it is not surprising that NP185 has a synapse-specific distribution. The synaptic association of NP185 and CCVs is supported by the work of Cheng *et al.* (1980). They raised a polyclonal antibody against clathrin HC, and studied its distribution in rodent cerebellum by immunohistochemistry. The distribution pattern is identical to that seen for NP185: dense, grainy labelling in the molecular layer; reticulate labelling in the granular layer; distinct, perimembranous labelling of Purkinje cells, with punctate concentrations. From this distribution, the authors inferred that clathrin HC is highly concentrated in synaptic terminals.

In themselves, the results in chick embryo and adult chicken strongly suggest that NP185 is localized in the synapse. The further work in this study corroborates this finding. Using antibodies to other proteins for comparative immunohistochemistry is useful in tracking a protein at the light microscopic level. This technique has been successfully used by others (Baumert *et al.*, 1990; Goto *et al.*, 1989; Reynolds and Wilkin, 1988; Eriksdotter-Nilsson *et al.*, 1987; Pelc *et al.*, 1986; Schiffer *et al.*, 1986). NP185 distribution is identical to that of synaptophysin, which in

the central nervous system is neuronal and synapse-specific. In contrast, NF68, which is neuronal and axon-specific (i.e., nonsynaptic), has an entirely different distribution. Both of the nonneuronal proteins, GFAP and vimentin, have distributions completely unlike that of NP185. Therefore, NP185 is both neuron-specific and synapse-specific.

The distribution of NP185 in the neuromuscular junction is the final evidence of synapse-specificity. Coated vesicles are on the postsynaptic side of the neuromuscular junction, distributed in AchR clusters in domains nearby but separate from the AchR domains (Pumplin, 1989). Coated vesicles are present from the very beginning of contact formation between the neurites of ciliary neurons and chick embryo myotubes (Bursztajn, 1984). This contact is regarded as a good in vitro model of a developing neuromuscular junction. As the growth cone comes in contact with the myotube, it extends numerous filopodia along the myotube surface. This multiple contact may be necessary for proper neuromuscular development, perhaps by preparing the myotube for mature association with a functional motor neuron. Eventually a single neuronal process gains dominance, and the developing myotube loses most of the other neurite contacts. This loss is analogous to synaptic retrenchment after initial abundant proliferation, the final step in synaptogenesis. Throughout the course of neurite-myotube association, coated vesicles are observed to be in close apposition

to contact sites. As the dominant neuronal process matures, this association remains. Bursztajn *et al.* demonstrated that coated vesicles internalize acetylcholine receptors (1987). Chloroquine, which blocks lysosomal fusion, produces accumulation of acetylcholine receptors in postsynaptic coated vesicles (Bursztajn and Libby, 1981).

The contact and adhesion model of Bloch and Pumplin (1988) assigns to clathrin-coated plaques and vesicles a role in neuromuscular synaptogenesis. AchR clustering in the postsynaptic membrane of the neuromuscular junction occurs in response to innervation of young muscle fibers. Three membrane domains are constructed in the process of receptor clustering: (1) First, nerve and muscle membranes contact each other. (2) Adhesion molecules, perhaps such as neural cell adhesion molecule (N-CAM), strengthen this contact. (3) Microfilaments are attached to the cytoplasmic side of the membrane at points of innervation, where nerve and muscle membranes adhere. It is likely that talin and vinculin, interacting with the membrane-associated receptors of the adhesion molecules, establish an anchor on the cytoplasmic surface which allows further cytoskeletal organization. (4) Clathrin-coated plaques form next to the contact domains. (5) Clathrin-coated vesicles insert acetylcholine receptors in the postsynaptic membrane. (6) The insertion of acetylcholine receptors triggers the formation of a spectrin-actin network. (7) This network grows to create

domains rich in acetylcholine receptors. This model probably applies to synaptogenesis in the central nervous system.

NP185 is synapse specific. In brain, it is closely associated with clathrin-coated vesicles (Kohtz and Puszkin, 1988). Since clathrin-coated plaques and vesicles are crucial in synaptogenesis, NP185 undoubtedly plays an important part in synaptic function. NP185 has phosphorylation-modulated binding affinity for clathrin LCs (Su *et al.*, 1991), and also binds to tubulin in a casein kinase II-regulated manner (Kohtz and Puszkin, 1989). These characteristics are reminiscent of synapsin I, a neuronal protein associated with synaptic vesicles on their cytoplasmic surface (Ueda and Greengard, 1977). Its binding affinity to SVs is decreased 5-fold when it is phosphorylated (Schiebler *et al.*, 1986). Phosphorylation is catalyzed by $Ca^{++}$/calmodulin-dependent protein kinase II (Huttner *et al.*, 1981). Synapsin I binds with neurofilaments (Goldenring *et al.*, 1986) and microtubules (Baines and Bennett, 1986). When in the unphosphorylated state, it promotes cross-linking of synaptic vesicles at the presynaptic membrane (Steiner *et al.*, 1987). Like other neuronal proteins, it is found in the neuromuscular junction (Valtorta *et al.*, 1988). Lastly, it shares the same cerebellar distribution as NP185 (de Camilli *et al.*, 1983).

Considering these properties, it is tempting to speculate that NP185 may serve as a cytoskeletal docking protein for

CCVs, in a manner analogous to that of synapsin I for SVs (Valtorta *et al.*, 1989).

# V. APPENDIX: Abbreviations used in text

| | |
|---|---|
| ab: | antibody |
| AchR: | acetylcholine receptor |
| En: | embryonic day n |
| DHS: | donor horse serum |
| FCS: | fetal calf serum |
| FIF: | formaldehyde-induced fluorescence |
| FITC: | fluorescein isothiocyanate |
| FS: | full strength |
| GFAP: | glial fibrillary acidic protein |
| GLU: | 0.1% glutaraldehyde/PFA/PBS 7.4 |
| mAb: | monoclonal antibody |
| MES: | 2-(*N*-morpholino)-ethanesulfonic acid, pH 6.5 (unless otherwise stated) |
| NGF: | neural growth factor |
| NGS: | normal goat serum |
| o.n.: | overnight |
| OCT: | optimum cutting temperature compound: 10% polyvinyl alcohol, 5% carbowax |
| PBS: | phosphate buffered saline: 19 mM $NaH_2PO_4$, 81 mM $Na_2HPO_4$, 150 mM NaCl, pH 7.4 unless otherwise stated) |
| PFA: | 4% paraformaldehyde/PBS 7.4 |
| Pn: | posthatch day n |
| RT: | room temperature |
| SCa, SCb: | slow component a or b of slow axonal transport |
| SDS-PAGE: | sodium dodecyl sulfate-polyacrylamide gel electrophoresis |
| stg: | stage |
| TBS/BSA: | 0.1% bovine serum albumin/TBS pH 7.5 |
| TBS/Tween: | 0.1% Tween-20/TBS pH 7.4 |
| TBS: | Tris buffered saline: 50 mM Tris, 150 mM NaCl, pH 7.4 |

# VI. BIBLIOGRAPHY

Ahle, S, Mann, A, Eichelsbacher, U, and Ungewickell, E (1988). Structural relationships between clathrin assembly proteins from the Golgi and the plasma membrane. *EMBO J* **7**:919-929

Altman, J (1971). Coated vesicles and synaptogenesis. A developmental study in the cerebellar cortex of the rat. *Brain Res* **30**:311-322

Altman, J (1972a). Postnatal development of the cerebellar cortex in the rat. I. The external germinal layer and the transitional molecular layer. *J Compar Neurol* **145**:353-398

Altman, J (1972b). Postnatal development of the cerebellar cortex in the rat. II. Phases in the maturation of Purkinje cells and of the molecular layer. *J Compar Neurol* **145**:399-464

Altman, J (1972c). Postnatal development of the cerebellar cortex in the rat. III. Maturation of the components of the granular layer. *J Compar Neurol* **145**:465-514

Anderson, MJ, and Cohen, MW (1977). Nerve-induced and spontaneous redistribution of acetylcholine receptors on cultured muscle cells. *J Physiol* **268**:757-773

Anderson, MJ, Cohen, MW, and Zorychta, E (1977). Effects of innervation on the distribution of acetylcholine receptors on cultured muscle cells. *J Physiol* **268**:731-756

Atsumi, S (1971). The histogenesis of motor neurons with special reference to the correlation of their endplate formation. *Acta Anat* **80**:161-182

Baines, AJ, and Bennett, V (1986). Synapsin I is a microtubule-bundling protein. *Nature* **319**:145-147

Bannerman, PGC, Mirsky, R, Jessen, KR, Timpl, R, and Duance, VC (1986). Light microscopic immunolocalization of laminin, type IV collagen, nidogen, heparan sulphate proteoglycan and fibronectin in the enteric nervous system of rat and guinea pig. *J Neurocytol* **15**:733-743

Bar-Zvi, D, and Branton, D (1985). Casein kinase II like protein kinase in calf brain coated vesicles phosphorylates clathrin β light chain. *J Cell Biol* **101**:48a (abstract)

Baumert, M, Takei, K, Hartinger, J, Burger, PM, von Mollard, GF, Maycox, PR, de Camilli, P, and Jahn, R (1990). P29: a novel tyrosine-phosphorylated membrane protein present in small clear vesicles of neurons and endocrine cells. *J Cell Biol* **110**:1285-1294

Bender, AN, Ringel, SP, and Engel, WK (1976). The acetylcholine receptor in normal and pathologic states. *Neurol* **26**:477-483

Benson, RJJ, Porter-Jordan, K, Buoniconti, P, and Fine, RE (1985). Biochemical and cytochemical evidence indicates that coated vesicles in chick embryo myotubes contain newly synthesized acetylcholinesterase. *J Cell Biol* **101**:1930-1940

Bignami, A, and Dahl, D (1973). Differentiation of astrocytes in the cerebellar cortex and the pyramidal tracts of the newborn rat, an immunofluorescence study with antibodies to a protein specific to astrocytes. *Brain Res* **49**:393-402

Bignami, A, Grossi, M, and Dahl, D (1985). Transient expression of neurofilament protein without filament formation in Purkinje cell development. *Int J Devl Neuroscience* **3**:365-377

Birkett, CR, Foster, KE, Johnson, L, and Gull, K (1985). Use of monoclonal antibodies to analyse the expression of a multi-tubulin family. *FEBS Lett* **187**:211-218

de Blas, AL (1984). Monoclonal antibodies to specific astroglial and neuronal antigens reveal the cytoarchitecture of the Bergmann glia fibers in the cerebellum. *J Neurosci* **4**:265-273

Bleil, JD, and Bretscher, MS (1982). Transferrin receptor and its recycling in HeLa cells. *EMBO J* **1**:351-355

Blitz, AL, Fine, RE, and Toselli, PA (1977). Evidence that coated vesicles isolated from brain are calcium-sequestering organelles resembling sarcoplasmic reticulum. *J Cell Biol* **75**:135-147

Bloch, RJ, and Pumplin, DW (1988). Molecular events in synaptogenesis: nerve-muscle adhesion and postsynaptic differentiation. *Am J Physiol* **254**:C345-C364

Bloom, WS, Fields, KL, Yen, SH, Haver, K, Schook, W, and Puszkin, S (1980a). Brain clathrin: Immunofluorescent patterns in cultured cells and tissues. *Proc Natl Acad Sci USA* **77**:5520-5524

Bloom, WS, Schook, W, Feageson, E, Ores, C, and Puszkin, S (1980b). Brain clathrin: Viscometric and turbidimetric properties of its ultrastructural assemblies. *Biochim Biophys Acta* **598**:447-455

Bovolenta, P, Liem, RKH, and Mason, CA (1984). Development of cerebellar astroglia: transitions in form and cytoskeletal content. *Devel Biol* **102**:248-259

Bretscher, MS, Thomson, JN, and Pearse, BMF (1980). Coated pits act as molecular filters. *Proc Natl Acad Sci USA* **77**:4156-4159

Brodsky, FM, Galloway, CJ, Blank, GS, Jackson, AP, Seow, Heng-F, Drickamer, K, and Parham, P (1987). Localization of clathrin light-chain sequences mediating heavy-chain binding and coated vesicle diversity. *Nature* **326**:203-205

Brown, MS, and Goldstein, JL (1986). A receptor-mediated pathway for cholesterol homeostasis. *Science* **23**:34-47

Buc-Caron, Marie-H, Nystrom, P, and Fischbach, GD (1983). Induction of acetylcholine receptor synthesis and aggregation: partial purification of low-molecular-weight activity. *Devel Biol* **95**:378-386

Burgoyne, RD (1990). Secretory vesicle-associated proteins and their role in exocytosis. *Ann Rev Physiol* **52**:647-659

Burgoyne, RD, and Cambray-Deakin, MA (1988). The cellular neurobiology of neuronal development: the cerebellar granule cell. *Brain Res Rev* **13**:77-101

Bursztajn, S (1984). Coated vesicles are associated with acetylcholine receptors at nerve-muscle contacts. *J Neurocytol* **13**:503-518

Bursztajn, S, and Fischbach, GD (1984). Evidence that coated vesicles transport acetylcholine receptors to the surface membrane of chick myotubes. *J Cell Biol* **98**:498-506

Bursztajn, S, and Libby, P (1981). Morphological changes in cultured myotubes treated with agents that interfere with lysosomal function. *Cell Tissue Res* **220**:573-588

Bursztajn, S, Nudleman, HB, and Berman, SA (1987). Coated and smooth vesicles participate in acetylcholine receptor transport. *Cell Tissue Res* **248**:535-540

Cabalka, LM, Ritchie, TC, and Coulter, JD (1990). Immunolocalization and quantitation of a novel nerve terminal protein in spinal cord development. *J Compar Neurol* **295**:83

Cambray-Deakin, MA, Norman, Kathryn-M, and Burgoyne, RD (1987). Differentiation of the cerebellar granule cell: expression of a synaptic vesicle protein and the microtubule-associated protein MAP1A. *Develop Brain Res* **34**:1-7

de Camilli, P, Cameron, R, and Greengard, P (1983). Synapsin I (protein I), a nerve terminal-specific phosphoprotein. I. Its general distribution in synapses of the central and peripheral nervous system demonstrated by immunofluorescence in frozen and plastic sections. *J Cell Biol* **96**:1337-1354

Carry, MR, and Morita, M. (1984). Structure and morphogenesis of the neuromuscular junction. In The Neuromuscular Junction, Brumback, RA, and Gerst, JW, Eds. (Mt. Kisco NY: Futura Publishing Co.), pp. 25-64

Chang, CC, and Lee, CY (1963). Isolation of neurotoxins from the venom of *Bungarus multicinctus* and their modes of neuromuscular blocking action. *Arch Int Pharmacodyn* **144**:241-257

Chappell, TG, Welch, WJ, Schlossman, DM, Palter, KB, Schlesinger, MJ, and Rothman, JE (1986). Uncoating ATPase is a member of the 70 kilodalton family of stress proteins. *Cell* **45**:3-13

Cheng, TPo-O, Byrd, FI, Whitaker, JN, and Wood, JG (1986). Immunocytochemical localization of coated vesicle protein in rodent nervous system. *J Cell Biol* **86**:624-633

Chuong, C-M, Crossin, KL, and Edelman, GM (1987). Sequential expression and differential function of multiple adhesion molecules during the formation cerebellar cortical layers. *J Cell Biol* **104**:331-342

Cohen, SA, and Pumplin, DW (1979). Clusters of intramembrane particles associated with binding sites for α-bungarotoxin in cultured chick myotubes. *J Cell Biol* **82**:494-516

Cole, WV (1955). Motor endings in the striated muscle of vertebrates. *J Compar Neurol* **102**, 671-715

Crick, FHC (1983). The packing of α-helices: simple coiled-coils. *Acta Cryst* **6**:689-697

Crowther, RA, and Pearse, BMF (1981). Assembly and packing of clathrin into coats. *J Cell Biol* **91**:790-797

Duband, JL, and Thiery, JP (1982). Distribution of fibronectin in the early phase of avian cephalic neural crest cell migration. *Devel Biol* **93**:308-323

Eckenhoff, MF, and Pysh, JJ (1979). Double-walled coated vesicle formation: evidence for massive and transient conjugate internalization of plasma membranes during cerebellar development. *J Neurocytol* **8**:623-638

Eränkö, O (1967). The practical histochemical demonstration of catecholamines by formaldehyde-induced fluorescence. *J Roy Micr Soc* **87**:259-276

Eriksdotter-Nilsson, M, Björklund, H, Dahl, D, Olson, L, and Ingvar, M (1987). Sustained seizures cause circumscribed cerebral changes in glial fibrillary acidic protein, neurofilament and laminin immunofluorescence. *Exp Brain Res* **69**:155-166

Fine, RE (1989). Vesicles without clathrin: intermediates in bulk flow exocytosis. *Cell* **58**:609-610

Foelix, RF, and Oppenheim, R (1974). The development of synapses in the cerebellar cortex of the chick embryo. *J Neurocytol* **3**:277-294

Fontaine, B, Sassoon, D, Buckingham, M, and Changeux, Jean-P (1988). Detection of the nicotinic acetylcholine receptor α-subunit mRNA by *in situ* hybridization at neuromuscular junctions of 15-day-old chick striated muscles. *EMBO J* **7**:603-609

Franke, WW, Schmid, E, Osborn, M, and Weber, K (1978). Different intermediate-sized filaments distinguished by immunofluorescence microscopy. *Proc Natl Acad Sci USA* **75**:5034-5038

Friend, DS, and Farquhar, MG (1967). Functions of coated vesicles during protein absorption in the rat vas deferens. *J Cell Biol* **35**:357-376

Fujita, S. (1969). Autoradiographic studies on histogenesis of the cerebellar cortex. In Neurobiology of Cerebellar Evolution and Development, Llinás, R, Ed. (Chicago: American Medical Association), pp. 743-747

Fults, DW, Towle, AC, Lauder, JM, and Maness, PF (1985). pp60$^{c\text{-}src}$ in the developing cerebellum. *Mol Cell Biol* **5**:27-32

Geisler, N, and Weber, K (1981). Self-assembly *in vitro* of the 68,000 molecular component of the mammalian neurofilament triplet proteins into intermediate-sized filaments. *J Mol Biol* **151**:565-571

Ghandour, MS, Vincendon, G, and Gombos, G (1980). Astrocyte and oligodendrocyte distribution in adult rat cerebellum: an immunohistological study. *J Neurocytol* **9**:637-646

Glickman, JN, Conibear, E, and Pearse, BMF (1989). Specificity of binding of clathrin adaptors to signals on the mannose-6-phosphate/insulin-like growth factor II receptor. *EMBO J* **8**:1041-1047

Goldenring, JR, Lasher, RS, Vallano, ML, Ueda, T, Naito, S, Sternberger, NH, Sternberger, LA, and DeLorenzo, RJ (1986). Association of synapsin I with neuronal cytoskeleton. *J Biol Chem* **261**:8495-8504

Gorden, P, Carpentier, Jean-L, Cohen, S, and Orci, L (1978). Epidermal growth factor: morphological demonstration of binding, internalization, and lysosomal association in human fibroblasts. *Proc Natl Acad Sci USA* **75**:5025-5029

Goto, S, Hirano, A, and Rojas-Corona, RR (1989). A comparative immunocytochemical study of human cerebellar cortex in X-chromosome-linked copper malabsorption (Menkes' kinky hair disease) and granule cell type cerebellar degeneration. *Neuropath App Neurobiol* **15**:419-431

Gower, DJ, and Tytell, M (1987). Axonal transport of clathrin-associated proteins. *Brain Res* **407**:1-8

Gozes, I, and Richter-Landsberg, C (1978). Identification of tubulin associated with rat brain myelin. *FEBS Lett* **95**:169-172

Graeber, MB, Streit, WJ, and Kreutzberg, GW (1988). The microglial cytoskeleton: vimentin is localized within activated cells *in situ*. *J Neurocytol* **17**:573-580

Gray, EG (1961). The granule cells, mossy synapses and Purkinje spine synapses of the cerebellum: light and electron microscope observations. *J Anat* **95**:345-363

Griffiths, G, Pfeiffer, S, Simons, K, and Matlin, K (1985). Exit of newly synthesized membrane proteins from the *trans* cisterna of the Golgi complex to the plasma membrane. *J Cell Biol* **101**:949-964

Grovas, AC, and O'Shea, KS (1984). An SEM examination of granule cell migration in the mouse cerebellum. *J Neurosci Res* **12**:1-14

Gunther, JS, and Letinsky, MS (1982). A preparation for studying dystrophic avian muscle and neuromuscular junctions. *Mus Nerve* **5**:7-13

Haigler, HT, McKanna, JA, and Cohen, S (1979). Direct visualization of the binding and internalization of a ferritin conjugate of epidermal growth factor in human carcinoma cells A-431. *J Cell Biol* **81**:382-395

Hamburger, V, and Hamilton, HL (1951). A series of normal stages in the development of the chick embryo. *J Morph* **88**:49-92

Hanaway, J (1967). Formation and differentiation of the external granular layer of the chick cerebellum. *J Compar Neurol* **131**:1-14

Georgieva-Hanson, V, Schook, WJ, and Puszkin, S (1988). Brain coated vesicle destabilization and phosphorylation of coat proteins. *J Neurochem* **50**:307-315

Hanson, VG, Schook, WJ, and Puszkin, S (1990). Novel regulatory role of phosphorylated clathrin light chain β in bovine brain coated vesicles. *J Neurochem* **54**:46-50

Hantaï, D, Gautron, J, and Labat-Robert, J (1983). Immunolocalization of fibronectin and other macromolecules of the intercellular matrix in the striated muscle fiber of the adult rat. *Collagen Rel Res* **3**:381-391

Helenius, A, Kartenbeck, J, Simons, K, and Fries, E (1980). On the entry of Semliki Forest virus into BHK-21 cells. *J Cell Biol* **84**:404-420

Heuser, JE, and Reese, TS (1973). Evidence for recycling of synaptic vesicle membrane during transmitter release at the frog neuromuscular junction. *J Cell Biol* **57**:315-344

Heuser, J (1980). Three-dimensional visualization of coated vesicle formation in fibroblasts. *J Cell Biol* **84**:560-583

Hill, BL, Drickamer, K, Brodsky, FM, and Parham, P (1988). Identification of the phosphorylation sites of clathrin light chain LCb. *J Biol Chem* **263**:5499-5501

Hoffman, PN, and Cleveland, DW (1988). Neurofilament and tubulin expression recapitulates the developmental program during axonal regeneration: induction of a specific β-tubulin isotype. *Proc Natl Acad Sci USA* **85**:4530-4533

Hoffman, PN, and Lasek, RJ (1975). The slow component of axonal transport. *J Cell Biol* **66**:351-366

Holmes, N, Biermann, JS, Brodsky, FM, Bharucha, D, and Parham, P (1984). Comparison of the primary structures of clathrin light chains from bovine brain and adrenal gland by peptide mapping. *EMBO J* **3**:1621-1627

Howe, PRC, Fenwick, EM, Rostas, JAP, and Livett, BG (1977). Immunochemical comparison of synaptic plasma membrane and synaptic vesicle membrane antigens. *J Neurocytol* **6**:339-352

Huttner, WB, DeGennaro, LJ, and Greengard, P (1981). Differential phosphorylation of multiple sites in purified protein I by cyclic AMP-dependent and calcium-dependent protein kinases. *J Biol Chem* **256**:1482-1488

Hynes, R (1985). Molecular biology of fibronectin. *Ann Rev Cell Biol* **1**:67-90

Hynes, RO, and Yamada, KM (1982). Fibronectins: multifunctional modular glycoproteins. *J Cell Biol* **95**:369-377

Jackson, AP, and Parham, P (1988). Structure of human clathrin light chains. *J Biol Chem* **263**:16688-16695

Jackson, AP, Seow, Heng-F, Holmes, N, Drickamer, K, and Parham, P (1987). Clathrin light chains contain brain-specific insertion sequences and a region of homology with intermediate filaments. *Nature* **326**:154-159

Jacobson, M. (1978). Developmental Neurobiology, 2nd ed. (New York: Plenum Press), p. 78

Jahn, R, Schiebler, W, Ouimet, C, and Greengard, P (1985). A 38,000-dalton membrane protein (p38) present in synaptic vesicles. *Proc Natl Acad Sci USA* **82**:4137-4141

Johnson, GD, and de C Nogueira Araujo, GM (1981). A simple method of reducing the fading of immunofluorescence during microscopy. *J Immun Meth* **43**:349-350

Jongsma, APM, Hijmans, W, and Ploem, JS (1971). Quantitative immunofluorescence. *Histochemie* **25**:329-343

Kanaseki, T, and Kadota, K (1969). The "vesicle in a basket". *J Cell Biol* **42**:202-220

Keen, JH, Willingham, MC, and Pastan, IH (1979). Clathrin-coated vesicles: isolation, dissociation and factor-dependent reassociation of clathrin baskets. *Cell* **16**:303-312

Kim, SU (1975). Formation of unattached spines of Purkinje cell dendrite in organotypic cultures of mouse cerebellum. *Brain Res* **88**:52-58

Kirchhausen, T, and Harrison, SC (1981). Protein organization in clathrin trimers. *Cell* **23**:755-761

Kirchhausen, T, Scarmato, P, Harrison, SC, Monroe, JJ, Chow, EP, Mattaliano, RJ, Ramachandran, KL, Smart, JE, Ahn, AH, and Brosius, J (1987). Clathrin light chains LCA and LCB are similar, polymorphic, and share repeated heptad motifs. *Science* **236**:320-324

Knaus, P, Betz, H, and Rehm, H (1986). Expression of synaptophysin during postnatal development of the mouse brain. *J Neurochem* **47**:1302-1304

Kohtz, DS, and Puszkin, S (1988). A neuronal protein (NP185) associated with clathrin-coated vesicles. *J Biol Chem* **263**:7418-7425

Kohtz, DS, and Puszkin, S (1989). Phosphorylation of tubulin by casein kinase II regulates its binding to a neuronal protein (NP185) associated with brain coated vesicles. *J Neurochem* **52**:285-295

Kohtz, DS, Hanson, VG, Kohtz, JD, Schook, WJ, and Puszkin, S (1987). Mapping two functional domains of clathrin light chains with monoclonal antibodies. *J Cell Biol* **104**:897-903

Krebs, EG, and Beavo, JA (1979). Phosphorylation-dephosphorylation of enzymes. *Ann Rev Biochem* **48**:923-959

Laemmli, UK (1970). Cleavage of structural proteins during the assembly of the head of bacteriophage T4. *Nature* **227**:680-685

Landis, DMD (1987). Initial junctions between developing parallel fibers and Purkinje cells are different from mature synaptic junctions. *J Compar Neurol* **260**:513-525

Landis, DMD, and Reese, TS (1974). Differences in membrane structure between excitatory and inhibitory synapses in the cerebellar cortex. *J Compar Neurol* **155**:93-126

Langley, OK, Sternberger, NH, and Sternberger, LA (1988). Expression of neurofilament proteins by Purkinje cells: ultrastructural immunolocalization with monoclonal antibodies. *Brain Res* **457**:12-20

Larkin, JM, Donzell, WC, and Anderson, RGW (1986). Potassium-dependent assembly of coated pits: new coated pits form as planar clathrin lattices. *J Cell Biol* **103**:2619-2627

Larsell, O. (1967). The Comparative Anatomy and Histology of the Cerebellum from Myxinoids through Birds. (Minneapolis: The University of Minnesota Press). pp. 226-240, 243-245, 262-273

Lasek, RJ, Garner, JA, and Brady, ST (1984). Axonal transport of the cytoplasmic matrix. *J Cell Biol* **99**:212s-221s

Leclerc, N, Beesley, PW, Brown, I, Colonnier, M, Gurd, JW, Paladino, T, and Hawkes, R (1989). Synaptophysin expression during synaptogenesis in the rat cerebellar cortex. *J Compar Neurol* **280**:197-212

Liem, RKH, Yen, Shu-H, Salomon, GD, and Shelanski, ML (1978). Intermediate filaments in nervous tissues. *J Cell Biol* **79**:637-645

Lisanti, MP, Shapiro, LS, Moskowitz, N, Hua, EL, Puszkin, S, and Schook, W (1982). Isolation and preliminary characterization of clathrin-associated proteins. *Eur J Biochem* **125**:463-470

Lisanti, MP, Flanagan, M, and Puszkin, S (1984). Clathrin lattice reorganization: theoretical considerations. *J Theor Biol* **108**:143-157

Lowe, J, Maclennan, KA, Powe, DG, Pound, JD, and Palmer, JB (1989). Microglial cells in human brain have phenotypic characteristics related to possible function as dendritic antigen presenting cells. *J Path* **159**:143-149

Luthman, J, Johansson, O, Ahlström, U, and Kvint, S (1988). Immunohistochemical studies of the neurochemical markers, CGRP, enkephalin, galanin, gamma-MSH, NPY, PHI, proctolin, PTH, somatostatin, SP, VIP, tyrosine hydroxylase and neurofilament in nerves and cells of the human attached gingiva. *Arch Oral Biol* **33**:149-158

Mareš, V; Viklický, V; Geršstein, LM; Dráber, P; Ciesielski-Treska, J (1988). Immunocytochemistry and heterogeneity of rat brain vimentin. *Histochem* **88**, 575-581

Mariani, J, and Changeux, Jean-P (1981). Ontogenesis of olivocerebellar relationships. I. Studies by intracellular recordings of the multiple innervation of Purkinje cells by climbing fibers in the developing rat cerebellum. *J Neurosci* **1**:696-702

Martin, JH (1989). Neuroanatomy, Text and Atlas. (New York: Elsevier). pp. 45-46, 239-266

McComb, RD, and Bigner, DD (1985). Immunolocalization of laminin in neoplasms of the central and peripheral nervous systems. *J Neuropath Exp Neurol* **44**:242-253

McKay, RDG, and Hockfield, SJ (1982). Monoclonal antibodies distinguish antigenically discrete neuronal types in the vertebrate central nervous system. *Proc Natl Acad Sci USA* **79**:6747-6751

McQuarrie, IG, Brady, ST, and Lasek, RJ (1986). Diversity in the axonal transport of structural proteins: major differences between optic and spinal axons in the rat. *J Neurosci* **6**:1593-1605

Miale, IL, and Sidman, RL (1961). An autoradiographic analysis of histogenesis in the mouse cerebellum. *Exper Neurol* **4**:277-296

Moskowitz, N, Schook, W, and Puszkin, S (1982). Comparison of calmodulin binding to brain synaptic and coated vesicles. *Biochim Biophys Acta* **689**:523-530

Mugnaini, E. (1969). Ultrastructural studies on the cerebellar histogenesis. II. Maturation of nerve cell populations and establishment of synaptic connections in the cerebellar cortex of the chick. In Neurobiology of Cerebellar Evolution and Development, Llinás, R, Ed. (Chicago: American Medical Association), pp. 749-782

Mugnaini, E (1970). The relation between cytogenesis and the formation of different types of synaptic contact. *Brain Res* **17**:169-179

Mugnaini, E, and Forstrønen, PF (1967). Ultrastructural studies on the cerebellar histogenesis. I. Differentiation of granule cells and development of *glomeruli* in the chick embryo. *Z Zellforsch* **77**:115-143

Nelsen, OE. (1953). Comparative Embryology of the Vertebrates. (New York: McGraw-Hill), pp. 805-835

Obata, K, and Fujita, SC (1984). Developmental changes of chick cerebellar cortex revealed by monoclonal antibodies. *Neurosci Res* **1**:117-129

Oblinger, MM (1988). Biochemical composition and dynamics of the axonal cytoskeleton in the corticospinal system of the adult hamster. *Metab Brain Dis* **3**:49-65

Ockleford, CD (1976). A three-dimensional reconstruction of the polygonal pattern on placental coated-vesicle membranes. *J Cell Sci* **21**:83-91

Orci, L, Glick, BS, and Rothman, JE (1986). A new type of coated vesicular carrier that appears not to contain clathrin: its possible role in protein transport within the Golgi stack. *Cell* **46**:171-184

Osborn, M (1983). Intermediate filaments as histologic markers: an overview. *J Inves Dermatol* **81**:104s-109s

Osborn, M, and Weber, K. (1982). Immunofluorescence and immunocytochemical procedures with affinity purified antibodies: tubulin-containing structures. In Methods in Cell Biology, vol. 24, Wilson, L, Ed. (New York: Academic Press), pp. 97-132

Partanen, S (1975). Simultaneous fluorescence histochemical demonstration of catecholamines and tryptophyl-peptides in endocrine cells. *Histochem* **43**:295-303

Patten, BM. (1951). Early Embryology of the Chick, 4th ed. (New York: The Blakiston Company), p. 101

Pauloin, A, Bernier, I, and Jollès, P (1982). Presence of cyclic nucleotide-Ca2+ independent protein kinase in bovine brain coated vesicles. *Nature* **298**:574-576

Pauloin, A, and Jollès, P (1986). Presence of a MgATP/ADP-dependent pp50 phosphatase in bovine brain coated vesicles. *J Biol Chem* **261**:12568-12573

Pauloin, A, Thurieau, C, and Jollès, P (1988). Cyclic phosphorylation/dephosphorylation cascade in bovine brain coated vesicles. *Biochim Biophys Acta* **968**:91-95

Payne, GS, and Schekman, R (1985). A test of clathrin function in protein secretion and cell growth. *Science* **230**:1009-1014

Pearse, BMF (1975). Coated vesicles from pig brain: purification and biochemical characterization. *J Mol Biol* **97**:93-98

Pearse, BMF (1976). clathrin: a unique protein associated with intracellular transfer of membrane by coated vesicles. *Proc Natl Acad Sci USA* **73**:1255-1259

Pearse, BMF (1978). On the structural and functional components of coated vesicles. *J Mol Biol* **126**:803-812

Pearse, BMF (1985). Assembly of the mannose-6-phosphate receptor into reconstituted clathrin coats. *EMBO J* **4**:2457-2460

Pearse, BMF (1987). Clathrin and coated vesicles. *EMBO J* **6**:2507-2512

Pearse, BMF (1989). Characterization of coated-vesicle adaptors: their reassembly with clathrin and with recycling receptors. *Meth Cell Biol* **31**:229-243

Pearse, BMF, and Bretscher, MS (1981). Membrane recycling by coated vesicles. *Ann Rev Biochem* **50**:85-101

Pearse, BMF, and Crowther, RA (1981). Packing of clathrin into coats. *Cold Spring Harbor Symp Quant Biol* **46**:703-706

Pearse, BMF, and Crowther, RA (1987). Structure and assembly of coated vesicles. *Ann Rev Biophys Biophys Chem* **16**:49-68

Pearse, BMF, and Robinson, MS (1984). Purification and properties of 100-kd proteins from coated vesicles and their reconstitution with clathrin. *EMBO J* **3**:1951-1957

Pelc, S, Fondu, P, and Gompel, C (1986). Immunohistochemical distribution of glial fibrillary acidic protein, neurofilament polypeptides and neuronal specific enolase in the human cerebellum. *J Neuro Sci* **73**:289-297

Perry, DG, Hanson, V, and Puszkin, S (1990). Immunolocalization of NP185; Developmental expression. *Trans Am Soc Neurochem* **21**:262

Pfeffer, SR, and Kelly, RB (1985). The subpopulation of brain coated vesicles that carries synaptic vesicle proteins contains two unique polypeptides. *Cell* **40**:949-957

Polak, M. (1965). Morphological and functional characteristics of the central and peripheral neuroglia. In Biology of Neuroglia, 1st ed., vol. 15, de Robertis, EDP, and Carrea, R, Eds. (New York: Elsevier Publishing Co.), pp. 12-34

Pollard, TD (1986). Actin and actin-binding proteins. A critical evaluation of mechanisms and functions. *Ann Rev Biochem* **55**:987-1035

Porter, ME, and Johnson, KA (1989). Dynein structure and function. *Ann Rev Cell Biol* **5**:119-151

Pratt, MM (1980). The identification of a dynein ATPase in unfertilized sea urchin eggs. *Devel Biol* **74**:364-378

Pretorius, HT, Nandi, PK, Lippoldt, RE, Johnson, ML, Keen, JH, Pastan, I, and Edelhoch, H (1981). Molecular characterization of human clathrin. *Biochem* **20**:2777-2782

Pumplin, DW (1989). Acetylcholine receptor clusters of rat myotubes have at least three domains with distinctive cytoskeletal and membranous components. *J Cell Biol* **109**:739-753

Pumplin, DW, and Bloch, RJ (1987). Disruption and reformation of the acetylcholine receptor clusters of cultured rat myotubes occur in two distinct stages. *J Cell Biol* **104**:97-108

Purves, D, and Lichtman, JW. (1985). Rearrangement of developing neuronal connections. In Principles of Neural Development, (Sunderland MA: Sinauer Associates, Inc.), pp. 271-300

Puszkin, S, Lisanti, M, Haver, K, Hua, EL, Moskowitz, N, Bloom, WS, and Schook, WJ (1982). Brain clathrin complex: II. Immunofluorescent correlation and biochemical affinity for actin. *J Histochem Cytochem* **30**:497-503

Puszkin, S, Andräs, A, Ores, C, Lisanti, MP, and Schook, WJ (1983). Immunocytochemical characterization of clathrin-associated proteins (CAPs). I. Neuronal distribution of CAPs, a component of clathrin-coated vesicles. *Cell Tissue Res* **231**:495-505

Puszkin, S, Kohtz, JD, Schook, WJ, and Kohtz, DS (1989). Clathrin-coated vesicle subtypes in mammalian brain tissue: Detection of polypeptide heterogeneity by immunoprecipitation with monoclonal antibodies. *J Neurochem* **53**:51-63

Quesada, A, and Genis-Galvez, JM (1983). Early development of the granule cell in the cerebellum of the chick embryo. *J Morph* **178**:323-334

Rakic, P (1971). Neuron-glia relationship during granule cell migration in developing cerebellar cortex. A Golgi and electron microscopic study *Macacus rhesus*. *J Compar Neurol* **141**:283-312

Reynolds, R, and Wilkin, GP (1988). Expression of $G_{D3}$ ganglioside by developing rat cerebellar Purkinje cells in situ. *J Neurosci Res* **20**:311-319

Robinson, MS (1987). 100-kD coated vesicle proteins: molecular heterogeneity and intracellular distribution studied with monoclonal antibodies. *J Cell Biol* **104**:887-895

Robinson, MS (1989). Cloning of cDNAs encoding two related 100-kD coated vesicle proteins (α-adaptins). *J Cell Biol* **108**:833-842

Robinson, MS, and Pearse, BMF (1986). Immunofluorescent localization of 100K coated vesicle proteins. *J Cell Biol* **102**:48-54

Romand, R, Hafidi, A, and Despres, G (1988). Immunocytochemical localization of neurofilament protein subunits in the spiral ganglion of the adult rat. *Brain Res* **462**:167-173

Roth, TF, and Porter, KR (1964). Yolk protein uptake in the oocyte of the mosquito *Aaedes aegypti* L. *J Cell Biol* **20**:313-332

Rothman, JE (1986). Life without clathrin. *Nature* **319**:96-97

Rothman, JE, and Fine, RE (1980). Coated vesicles transport newly synthesized membrane glycoproteins from endoplasmic reticulum to plasma membrane in two successive stages. *Proc Natl Acad Sci USA* **77**:780-784

Schiebler, W, Jahn, R, Doucet, Jean-P, Rothlein, J, and Greengard, P (1986). Characterization of synapsin I binding to small synaptic vesicles. *J Biol Chem* **261**:8383-8390

Schiffer, D, Giordana, MT, Migheli, A, Giaccone, G, Pezzotta, S, and Mauro, A (1986). Glial fibrillary acidic protein and vimentin in the experimental glial reaction of the rat brain. *Brain Res* **374**:110-118

Schlessinger, J, Shechter, Y, Willingham, MC, and Pastan, I (1978). Direct visualization of binding, aggregation, and internalization of insulin and epidermal growth factor on living fibroblastic cells. *Proc Natl Acad Sci USA* **75**:2659-2663

Schlossman, DM, Schmid, SL, Braell, WA, and Rothman, JE (1984). An enzyme that removes clathrin coats: purification of an uncoating ATPase. *J Cell Biol* **99**:723-733

Schnitzer, J, Franke, WW, and Schachner, M (1981). Immunocytochemical demonstration of vimentin in astrocytes and ependymal cells of developing and adult mouse nervous system. *J Cell Biol* **90**:435-447

Schook, WJ, and Puszkin, S (1985). Expression of a brain coated vesicle kinase activity which has clathrin light chain 2 as its principal substrate. *J Cell Biol* **101**:49a (abstract)

Schook, W, Puszkin, S, Bloom, W, Ores, C, and Kochwa, S (1979). Mechanochemical properties of brain clathrin: Interactions with actin and α-actinin and polymerization into basketlike structures or filaments. *Proc Natl Acad Sci USA* **76**:116-120

Schook, WJ, and Puszkin, S (1985). Brain clathrin light chain 2 can be phosphorylated by a coated vesicle kinase. *Proc Natl Acad Sci USA* **82**:8039-8043

Scott, LJC, Bacou, F, and Sanes, JR (1988). A synapse-specific carbohydrate at the neuromuscular junction: association with both acetylcholinesterase and a glycolipid. *J Neurosci* **8**:932-944

Shimono, T, Nosaka, S, and Sasaki, K (1976). Electrophysiological study on the postnatal development of neuronal mechanisms in the rat cerebellar cortex. *Brain Res* **108**:279-294

Silver, A (1963). A histochemical investigation of cholinesterases at neuromuscular junctions in mammalian and avian muscle. *J Physiol* **169**:386-393

Sinicropi, DV, and McIlwain, DL (1983). Changes in the amounts of cytoskeletal proteins within the perikarya and axons of regenerating frog motoneurons. *J Cell Biol* **96**:240-247

Sommer, I, Lagenaur, C, and Schachner, M (1981). Recognition of Bergmann glial and ependymal cells in the mouse nervous system by monoclonal antibody. *J Cell Biol* **90**:448-458

Sotelo, C. (1967). Cerebellar Neuroglia: Morphological and Histochemical Aspects. In The Cerebellum, 1st ed., vol. 25, Fox, CA, and Snider, RS, Eds. (New York: Elsevier Publishing Company), pp. 226-250

Steiner, JP, Ling, E, and Bennett, V (1987). Nearest neighbor analysis for brain synapsin I. *J Biol Chem* **262**:905-914

Stelzner, DJ, Martin, AH, and Scott, GL (1973). Early stages of synaptogenesis in the cervical spinal cord of the chick embryo. *Z Zellforsch* **138**:475-488

Stephens, RE (1986). Membrane tubulin. *Biol Cell* **57**:95-110

Sternberger, LA, Harwell, LW, and Sternberger, NH (1982). Neurotypy: regional individuality in rat brain detected by immunocytochemistry with monoclonal antibodies. *Proc Natl Acad Sci USA* **79**:1326-1330

Su, B. (1989). Biochemical and immunological properties of NP185: A brain clathrin coated vesicle associated protein PhD Dissertation. (City University of New York). 69 pp.

Su, B, Perry, D, Hanson, V, and Puszkin, S (1991). Biochemical and immunological properties of the neuronal protein NP185. *J Neurosci Res* (In press)

Sôdhof, TC, Lottspeich, F, Greengard, P, Mehl, E, and Jahn, R (1987). A synaptic vesicle protein with a novel cytoplasmic domain and four transmembrane regions. *Science* **238**:1142-1144

Tapscott, SJ, Bennett, GS, and Holtzer, H (1981). Neuronal precursor cells in the chick neural tube express neurofilament proteins. *Nature* **292**:836-838

Thomas, L, Kartung, K, Langosch, D, Rehm, H, Bamberg, E, Franke, WW, and Betz, H (1988). Identification of synaptophysin as a hexameric channel protein of the synaptic vesicle membrane. *Science* **242**:1050-1053

Torri-Tarelli, F, Villa, A, Valtorta, F, de Camilli, P, Greengard, P, and Ceccarelli, B (1990). Redistribution of synaptophysin and synapsin I during α-latrotoxin-induced release of neurotransmitter at the neuromuscular junction. *J Cell Biol* **110**:449-459

Towbin, H, Staehelin, T, and Gordon, J (1979). Electrophoretic transfer of proteins from polyacrylamide gels to nitrocellulose sheets: Procedure and some applications. *Proc Natl Acad Sci USA* **76**:4350-4354

Trojanowski, JQ, Walkenstein, N, and Lee, VM-Y (1986). Expression of neurofilament subunits in neurons of the central and peripheral nervous system: an immunohistochemical study with monoclonal antibodies. *J Neurosci* **6**:650-660

Uchizono, K. (1969). Synaptic organization of the mammalian cerebellum. In Neurobiology of Cerebellar Evolution and Development, 1st ed., Llinás, R, Ed. (Chicago: American Medical Association), pp. 549-583

Ueda, T, and Greengard, P (1977). Adenosine 3′:5′-monophosphate-regulated phosphoprotein system of neuronal membranes. *J Biol Chem* **252**:5155-5163

Unanue, ER, Ungewickell, E, and Branton, D (1981). The binding of clathrin triskelions to membranes from coated vesicles. *Cell* **26**:439-446

Ungewickell, E, and Branton, D (1981). Assembly units of clathrin coats. *Nature* **289**:420-422

Ungewickell, E, and Branton, D (1982). Triskelions: the building blocks of clathrin coats. *TIBS* **7**:358-360

Ungewickell, E, Unanue, ER, and Branton, D (1981). Functional and structural studies on clathrin triskelions and baskets. *Cold Spring Harbor Symp Quant Biol* **46**:723-732

Usami, M, Takahashi, A, Kadota, T, and Katoda, K (1985). Phosphorylation of a clathrin light chain of coated vesicles in the presence of histones. *J Biochem* **97**:1819-1822

Vale, RD (1987). Intracellular transport using microtubule-based motors. *Ann Rev Cell Biol* **3**:347-378

Valtorta, F, Torri-Tarelli, F, Campanati, L, Villa, A, and Greengard, P (1989). Synaptophysin and synapsin I as tools for the study of the exo-endocytotic cycle. *Cell Biol Int Rep* **13**:1023-1038

Vigers, GPA, Crowther, RA, and Pearse, BMF (1986). Three-dimensional structure of clathrin cages in ice. *EMBO J* **5**:529-534

de Waegh, S, and Brady, ST (1989). Axonal transport of a clathrin uncoating ATPase (HSC70): a role for HSC70 in the modulation of coated vesicle assembly in vivo. *J Neurosci Res* **23**:433-440

Wall, DA, Wilson, G, and Hubbard, AL (1980). The galactose-specific recognition system of mammalian liver: the route of ligand internalization in rat hepatocytes. *Cell* **21**:79-93

Waxman, SG, and Pappas, GD (1969). Pinocytosis at postsynaptic membranes: electron microscopic evidence. *Brain Res* **14**:240-244

Wenger, E, and Wenger, BS (1978). A histochemical method for gross demonstration of motor end plates. *Stain Technol* **53**:279-282

Wiedenmann, B, and Franke, WW (1985). Identification and localization of synaptophysin, an integral membrane glycoprotein of $M_r$ 38,000 characteristic of presynaptic vesicles. *Cell* **41**:1017-1028

Wilkin, GP, and Levi, G. (1986). Cerebellar Astrocytes. In Astrocytes, 1st ed., vol. 1, Fedoroff, S, and Vernadakis, A, Eds. (New York: Academic Press), pp. 245-268

Willingham, MC, Maxfield, FR, and Pastan, IH (1979). $\alpha_2$Macroglobulin binding to the plasma membrane of cultured fibroblasts. *J Cell Biol* **82**:614-625

Woodward, DJ, Hoffer, BJ, and Lapham, LW. (1969). Correlative survey of electrophysiological, neuropharmacological, and histochemical aspects of cerebellar maturation in rat. In Neurobiology of Cerebellar Evolution and Development, Llinás, R, Ed. (Chicago: American Medical Association), pp. 725-741

Zamboni, L, and de Martino, C (1967). Buffered picric acid-formaldehyde: A new, rapid fixative for electron microscopy. *J Cell Biol* **35**:148A (Abstract)

Zaremba, S, and Keen, JH (1983). Assembly polypeptides from coated vesicles mediate reassembly of unique clathrin coats. *J Cell Biol* **97**:1339-1347